Fall 2010

The coordinated control of autonomous agents

Ryan Orlin Abel
University of Iowa

THE COORDINATED CONTROL OF AUTONOMOUS AGENTS

by

Ryan Orlin Abel

An Abstract

A thesis submitted in partial fulfillment
of the requirements for the Doctor of
Philosophy degree in Electrical and
Computer Engineering in the Graduate
College of The University of Iowa

December 2010

Thesis Supervisors: Professor Soura Dasgupta
Professor Jon G. Kuhl

ABSTRACT

This thesis considers the coordinated control of autonomous agents. The agents are modeled as double integrators, one for each Cartesian dimension. The goal is to force the agents to converge to a formation specified by their desired relative positions. To this end a pair of one-step-ahead optimization based control laws are developed.

The control algorithms produce a communication topology that mirrors the geometric formation topology due to the careful choice of the minimized cost functions. Through this equivalence a natural understanding of the relationship between the geometric formation topology and the communication infrastructure is gained. It is shown that the control laws are stable and guarantee convergence for all viable formation topologies. Additionally, velocity constraints can be added to allow the formation to follow fixed or arbitrary time dependent velocities.

Both control algorithms only require local information exchange. As additional agents attach to the formation, only those agents that share position constraints with the joining agents need to adjust their control laws. When redundancy is incorporated into the formation topology, it is possible for the system to survive loss of agents or communication channels. In the event that an agent drops out of the formation, only the agents with position interdependence on the lost agent need to adjust their control laws. Finally, if a communication channel is lost, only the agents that share that communication channel must adjust their control laws.

The first control law falls into the category of distributed control, since it requires either the global information exchange to compute the formation size or an *a priori* knowledge of the largest possible formation. The algorithm uses the network size to penalize the control input for each formation. When using *a priori* knowledge, it is shown that additional redundancy not only adds robustness to loss of agents

or communication channels, but it also decreases the settling times to the desired formation. Conversely, the overall control strategy suffers from sluggish response when the network is small with respect to the largest possible network. If global information exchange is used, scalability suffers.

The second control law was developed to address the negative aspects of the first. It is a fully decentralized controller, as it does not require global information exchange or any *a priori* knowledge.

Abstract Approved: _____
Thesis Supervisor

_____
Title and Department

_____
Date

_____
Thesis Supervisor

_____
Title and Department

_____
Date

THE COORDINATED CONTROL OF AUTONOMOUS AGENTS

by

Ryan Orlin Abel

A thesis submitted in partial fulfillment
of the requirements for the Doctor of
Philosophy degree in Electrical and
Computer Engineering in the Graduate
College of The University of Iowa

December 2010

Thesis Supervisors: Professor Soura Dasgupta
Professor Jon G. Kuhl

Graduate College
The University of Iowa
Iowa City, Iowa

CERTIFICATE OF APPROVAL

PH.D. THESIS

This is to certify that the Ph.D. thesis of

Ryan Orlin Abel

has been approved by the Examining Committee for the thesis requirement for the Doctor of Philosophy degree in Electrical and Computer Engineering at the December 2010 graduation.

Thesis Committee:

Soura Dasgupta, Thesis Supervisor

Jon G. Kuhl, Thesis Supervisor

Er-Wei Bai

Mark S. Andersland

Jasbir S. Arora

To Dorothy and William Jones

ACKNOWLEDGMENTS

I would like to thank my parents, who taught me that all things are possible and raised me with the drive and determination to achieve them. To Jon and Soura, it would be impossible to enumerate the lessons learned in the space afforded me, you have become so much more to me than advisors. To my Grandma, whose endless support and kind words helped me through this growing process. Finally, to Autumn, whose love and patience allowed me to complete the task.

ABSTRACT

This thesis considers the coordinated control of autonomous agents. The agents are modeled as double integrators, one for each Cartesian dimension. The goal is to force the agents to converge to a formation specified by their desired relative positions. To this end a pair of one-step-ahead optimization based control laws are developed.

The control algorithms produce a communication topology that mirrors the geometric formation topology due to the careful choice of the minimized cost functions. Through this equivalence a natural understanding of the relationship between the geometric formation topology and the communication infrastructure is gained. It is shown that the control laws are stable and guarantee convergence for all viable formation topologies. Additionally, velocity constraints can be added to allow the formation to follow fixed or arbitrary time dependent velocities.

Both control algorithms only require local information exchange. As additional agents attach to the formation, only those agents that share position constraints with the joining agents need to adjust their control laws. When redundancy is incorporated into the formation topology, it is possible for the system to survive loss of agents or communication channels. In the event that an agent drops out of the formation, only the agents with position interdependence on the lost agent need to adjust their control laws. Finally, if a communication channel is lost, only the agents that share that communication channel must adjust their control laws.

The first control law falls into the category of distributed control, since it requires either the global information exchange to compute the formation size or an *a priori* knowledge of the largest possible formation. The algorithm uses the network size to penalize the control input for each formation. When using *a priori* knowledge, it is shown that additional redundancy not only adds robustness to loss of agents

or communication channels, but it also decreases the settling times to the desired formation. Conversely, the overall control strategy suffers from sluggish response when the network is small with respect to the largest possible network. If global information exchange is used, scalability suffers.

The second control law was developed to address the negative aspects of the first. It is a fully decentralized controller, as it does not require global information exchange or any *a priori* knowledge.

TABLE OF CONTENTS

LIST OF FIGURES viii

CHAPTER

1 INTRODUCTION 1

1.1 Motivation 1
1.2 History of the Problem - A Literature Review 3
1.2.1 Behavior Based Formation Control 6
1.2.2 String Stability and the Vehicle Following Problem 7
1.2.3 The Consensus Problem 11
1.3 Contributions and Areas of Interest 14
1.4 Organization 16

2 THE COORDINATED CONTROL OF AUTONOMOUS AGENTS . 19

2.1 Problem Description 20
2.2 The Formation Topology 21
2.3 Viability 23

3 FORMATION CONTROL WITH LIMITED SCALABILITY 27

3.1 Basic Control 27
3.2 Proof of Stability 30
3.3 Simulation Results 33
3.4 Conclusion 35

4 TRAJECTORY FOLLOWING 37

4.1 Control Law and Communication Topology 38
4.2 Proof of Stability 39
4.3 Simulation Results 44
4.4 Conclusion 46

5 THE EFFECT OF REDUNDANCY UPON THE RATE OF CONVERGANCE 48

5.1 A Kalman Decomposition 48
5.2 Rates of Convergence 53
5.3 Simulation Results 56
5.4 Conclusion 57

6 FORMATION CONTROL WITH ENHANCED SCALABILITY . . . 59

6.1 Basic Control 59
6.2 Control Law and Communication Topology 60
6.3 Proof of Stability 63
6.4 Simulation Results 67
6.5 Conclusion 69

7 THE IMPACT OF DYNAMIC CHANGES TO THE COMMUNICATION TOPOLOGY 72

7.1 A Periodic Sequence of Dynamic Communication Changes 72
7.2 Observations for the Limited Scalability Approach 74
7.3 Observations for the Enhanced Scalability Approach 75
7.4 Conclusion 76

8 CONCLUSION 78

APPENDIX

A SELECTED PROOFS - LIMITED SCALABILITY 82

A.1 Basic Control: Proof of Lemma 3.2.1 82

B SELECTED PROOFS - ENHANCED SCALABILITY 91

B.1 Proof of Lemma 6.3.1 91

REFERENCES 100

LIST OF FIGURES

Figure

1.1 Look-Ahead Interconnected System 10

1.2 Agent Formation Topology with no Redundancy 15

1.3 Agent Formation Topology with Redundancy 16

3.1 Agent Formation with no Redundancy 34

3.2 Agent Formation with Redundancy and the Loss of Agent 4 at Time $k = 5$ 35

4.1 Non-Redundant Vehicle Trajectories 44

4.2 Non-Redundant x-Direction Velocity Error 45

4.3 Non-Redundant y-Direction Velocity Error 46

4.4 Redundant Vehicle Trajectories with Agent 3 Dropped at Time 22 . . 47

5.1 Non-Redundant Vehicle Trajectory 56

5.2 Fully Connected Vehicle Trajectory 57

5.3 Convergence Rates 58

6.1 10 Agent Formation Topology with no Redundancy 67

6.2 Synchronization of α and ϵ 68

6.3 Comparison of Convergence Rates 69

6.4 Trajectory of the Limited Scalability Approach 70

6.5 Trajectory of the Enhanced Scalability Approach 71

7.1 Formation Topology 1 (minimal system) 74

7.2 Formation Topology 2 (Minimal System Plus One Link) 75

7.3 Formation Topology 3 (Maximal System) 75

CHAPTER 1
INTRODUCTION

The coordinated control of autonomous agents has become an important area of research over the past few years. The increased activity in this area is largely due to significant advances in wireless communications, networking, and rapidly expanding application domains. The agents can achieve and maintain formations, perform collision and obstacle avoidance, harvest data, and perform collective tasks. Cooperation between the agents is achieved through sensed information and/or the active communication of data between agents.

1.1 Motivation

People have long been fascinated with phenomena that occur in nature. An area of interest has been the cooperative behavior of animals toward achieving a common goal. Examples include the swarming, flocking and schooling behavior, and animals scavenging for food. These types of behavior either protect the members of the group from predators or allow them to better achieve tasks that would not be easily achievable by individual members working alone. In an attempt to better understand these animal coordination behaviors scientists have created simulations and models which attempt to replicate and examine the behavior.

Whether by independent thought, or as a direct result of observations made in nature, scientists began to research and explore the benefits of coordinated control. Groups of agents working together to explore terrain can be more efficient then a single agent. An array of antennas can provide the reception capabilities of a single large antenna with the added reward of signal attenuation in all but the desired direction. Separate optical telescopes acting together, such as the Very Large Telescope (VLT) project, can behave as a single large telescope with a reduced manufacturing cost. Vehicles traveling in tight formation will experience reduced aerodynamic drag.

In a military environment, a fleet of small stealth aircraft can transport the same payload as a single large aircraft, but with a smaller radar footprint. Additionally, if a craft is lost, it would not be as detrimental to the mission as the loss of a single large craft. Further applications include air traffic control, sensor networks, station keeping, satellite clusters, and automated highway systems.

Clearly the realization of these benefits requires some level of coordination between the agents. The coordination can come in the form of preplanning, centralized control, or decentralized control. Each approach has its own benefits and consequences. Preplanning can be the most cost effective approach since there is no requirement for a communication infrastructure. However, preplanning is unable to adapt to dynamically changing environments which can lead perturbation of the desired behavior.

Centralized control typically involves a powerful master controller with communication channels to each agent. The centralized controller monitors all agents and dictates their control through the communication channels. Advantages of a centralized controller typically include faster convergence and enhanced stability. These benefits come with a greater monetary cost due to the required processing and communications resources needed by the master controller. Unfortunately the centralized controller is a single point of failure in these architectures. Additionally, architectures involving a master controller typically do not work well for large systems due to limited communication range and limited processing power of the master agent.

Decentralized control can be further subdivided into two categories: distributed control and fully decentralized control. With distributed control, each agent will process some globally shared information along with a local set of data obtained either through sensing or active communication. The agent will process the information using its internal controller and act in a semi-autonomous fashion. This approach typically has a smaller monetary cost and works better for larger systems than a

centralized controller. The global information required can include information about a formation leader or simply a global clock used for synchronization of actions. The latter is not typically required to achieve the objective, but it does aid in the analysis of the system. The global exchange of data does tend to limit the size of the system, when compared to a fully decentralized controller, but can decrease the time required to achieve the system objective. Fully decentralized control is distributed control without the global information exchange. Of the control schemes described, it works best for large systems; however, the approach can result in reduced stability and slower convergence.

It is certainly advantageous if the coordination has a scalable nature. Scalability imposes a strong requirement on the decentralization of the agents' individual control algorithms. As in the natural behavior of schools and flocks, no one agent can be expected to coordinate the actions of a large system of agents.

Other desires include disturbance rejection, robustness to either agent loss or the loss of a communication channel, and provably correct algorithms which provide a theoretical understanding of the problem domain. Intuitively, one would expect a direct correlation between system connectivity and rate of convergence. Some research has shown through counter example that this is not necessarily true, and in some cases convergence may never occur. Therefore, an understanding of how additional connectivity can impact system performance is also important. Finally, intuitive control laws with a natural relationship between the communication infrastructure, robustness and rate of convergence are of practical interest.

1.2 History of the Problem - A Literature Review

Spurred by the development of inexpensive dependable wireless communication systems and a rapidly expanding application domain, research in the area of the coordinated control of autonomous agents has intensified greatly in recent years.

When these systems are compared with agents acting in a singular fashion, coordinated multi-agent systems provide significantly greater efficiency and operational capability. The agents can achieve and maintain formations, perform collision and obstacle avoidance, harvest data and perform collective tasks. Cooperation between the agents is achieved through sensed information and/or the active communication of data between agents.

This section presents a brief history of the problem domain. The ideas of behavior-based formation control are first presented. While results in this area do not typically focus on provably correct algorithms they have provided some intuition of the coordinated behaviors observed in nature especially in the area of zoological and behavioral sciences. Additionally, the results have motivated other researchers to derive provably correct algorithms that provide a theoretical understanding of the observed behavior, serving as a stepping stone into other areas of research.

The concept of string stability and the vehicle following problem is then introduced. As cities expand, without proper planning, traffic congestion becomes a pressing problem. Using this problem as motivation, control schemes which involve a one-dimensional fleet of vehicles traveling as a platoon with minimal inter-vehicle spacing have been investigated to increase highway capacity. Additional benefits include reduced aerodynamic drag and improved fuel economy. In an attempt to achieve a scalable architecture vehicles only use sensed relative position information from the preceding vehicle and in some cases the relative position, velocity and acceleration of the lead vehicle. As a result, all communication architectures in this area use acyclic one-directional information flow. This type of system is often referred to as a "look-ahead" system. String stability can be intuitively understood as the attenuation of disturbances as they propagate from one vehicle to the next.

Consensus algorithms are then presented. The objective is for the group of

agents to reach consensus on a shared data set, either through sensed or communicated information. Consensus algorithms can be used to solve the rendezvous, flocking, and formation control problems. If a set of n agents with limited sensing range is considered, the goal of the rendezvous problem is to have all agents converge to a common point with only information exchange between agents that are within each other's sensing region. Flocking simulations use similar update rules to the rendezvous problem, but the end goal is to have the agents converge to a common velocity. Formation control can be achieved by having the agents converge to an agreement on the formation center while maintaining a predefined offset from that center. Most of the consensus results investigate a communication exchange protocol and then, based on that protocol, determine if convergence can be achieved. In the case of formation control using consensus algorithms, the formation is achieved with the convergence to a common center reference.

This work concerns itself with the ideas surrounding decentralized formation control. Unlike the approach used in consensus algorithms, an optimal one step-ahead control law is presented which ensures that the formation can be reached and maintained. The approach does not depend upon a common center reference for the agents. A natural relationship is shown to exist between the required communication infrastructure and the relative position dependencies of the formation shape. Additionally, robustness to loss of craft and/or communication channels improves with additional redundancy in the communication network. Also, it is shown that the convergence rate improves with the added communication as one would expect. It is important to note that this is not always the case in other formation control schemes.

1.2.1 Behavior Based Formation Control

Behavior Based Formation control was first investigated by Craig Reynolds in the late 80's to address a need for realistic flocking simulations in the computer graphics area. [1]. The simulation of a flock of birds had been a difficult challenge due the complex behavior of the flock. He expanded upon the notion of a particle system to create a behavioral model of a bird through a set of rules. Each bird was modeled to conserve momentum, limit speed and acceleration, maintain a minimum separation distance, and match the velocity and direction of its neighbors. A birds desire to be at the center of the flock was also modeled. The sensing distance of the bird was limited to reduce the computational complexity of the model. A side-effect of the limited sensing distance resulted in a more realistic simulation that allowed flocks to naturally bifurcate about an object.

Later research, [2] investigated a simplified behavioral model of a fixed velocity particle system. The particles' headings were updated using the average of their neighbors. Some interesting observations were made:

(i) With low particle density, the particles tended to form small coherently moving groups.

(ii) With higher particle density the particles tended to move in the same direction and the average velocity of the group approached that of the individual.

Work continued along this vein into formation control. Balch and Arkin conducted formation simulations using four identical non-holonomic robots with unique ID's [3]. The robots used differential GPS for gathering position information. Multiple behaviors were integrated into a behavioral model that allowed the robots to navigate to way-points, avoid obstacles and maintain a formation simultaneously. Simulations were conducted using a leader reference architecture as well as a unit center approach. The work did not provide any convergence, stability, or collision

avoidance proofs.

The concept of Queues and Artificial Potential Function Theory were presented in [4] and [5]. The queues in combination with the artificial potential functions allow the agents to assume specified formation shapes independent of their agent number, that is, agent order within the formation is not guaranteed. The formations are "robust" to agent loss and provide a decentralized approach to achieving the formation. If ideal communication is assumed, for example communication is not subject to multiple access problems, the approach scales well. However, the queue allocation algorithm requires global communication of information from all agents. If multiple access limitations on the communication channels are considered, scalability concerns quickly become apparent. Unfortunately, no theorems or proofs were provided.

1.2.2 String Stability and the Vehicle Following Problem

In the area of formation control, the notion of string stability often presents itself. One of the concentrations for this area of research was vehicle following systems, or vehicle platoons. The California Partners for Advanced Transit and Highways (PATH) and Automated Highway Systems were key focal points in the late 80's and early 90's. In the area of vehicle platoons, vehicles travel in a string with a small distance between each vehicle to reduce aerodynamic drag and increase highway capacity. In such a system, it is critical that tracking errors do not get amplified as they progress from vehicle to vehicle.

1.2.2.1 String Stability With Global Information Exchange

The "string stability of a countably infinite interconnection of a class nonlinear systems" was first introduced in [6] by Swaroop and Hedrick. A basic leader / follower architecture was presented in which each vehicle can sense the relative

distance between itself and the preceding vehicle. Additionally, each vehicle also receives transmitted acceleration, velocity, and position information about the lead vehicle. Their research showed that the interconnected system is globally exponentially string stable if the system is Lipschitz in its arguments with sufficiently small Lipschitz constants. Additional theorems were presented that proved exponentially string stable systems are robust against small singular perturbations.

Later, in [7], Swaroop, Hedrick and Choi expanded upon an earlier conference paper [8]. They presented an adaptive control algorithm to counteract the parametric uncertainties that are associated with the vehicle following problem. The uncertainties that were addressed included variable aerodynamic drag with vehicle spacing and the change of overall vehicle mass with changes in fuel, passengers, and cargo. In order to obtain these results the strict string stability constraint was relaxed to require only that the velocity and spacing errors be uniformly bounded in time.

1.2.2.2 String Stability Without Global Information Exchange

An overview of string stability without global information exchange was presented in [9]. The paper addressed various control schemes used to solve the vehicle following problem. It was shown that without lead vehicle information, at best, the systems have weak sense string stability since the stability polynomials have at least one simple root at $z = 1$. As a result, the systems presented are not robust against signal processing delays or actuator lags. Of particular interest, platoons lacking lead vehicle information using identical controllers are not string stable. It was also shown that systems with no lead vehicle information using non-identical controllers have only weak sense string stablity.

In [10] , Khatir and Davison addressed the problem of string stability of a platoon of identical vehicles where the only information available to the ith vehicle

is the sensed information of its predecessor. The primary focus of the paper was to solve the Robust Servomechanism Problem (RSP) using a constant spacing policy without the global communication of the lead vehicle's velocity. It was shown that identical controllers cannot solve the vehicle following problem without lead vehicle information. Additionally, they presented some simulations which show it may be possible to use non-identical controllers to obtain string stability in the absence of lead vehicle information.

The use of identical controllers to solve the vehicle following problem was considered in [11]. A sufficient condition for string stability was referenced from [12]. It was assumed that the error information of the preceding vehicle is known. Simulations were provided which show a ten vehicle system is robust against un-modeled actuator dynamics and time delay. No proofs were provided to support the simulations.

Finally, in [13], Khatir and Davison provided a solution which uses non-identical controllers with linearly increasing gains. The decentralized controller was the same controller used in the simulation results in [10]. Like in [11], it was assumed that each vehicle has knowledge of spacing error between itself and the preceding vehicle. Bounded stability and eventual string stability was proven when the lead vehicle undergoes a step change in speed.

1.2.2.3 Mesh Stability

Historically, string stability addressed one dimensional "look-ahead" systems in which the ith vehicle only has knowledge the preceding vehicles in the formation. String stability results can be extended into multiple dimensions, a two-dimiensional definition of a look-ahead system follows:

Definition 1.2.1 *An interconnected system, is called look-ahead, if the* (i, j)*th subsystem is connected only to the subsystems* (k, l) *such that* $k \leq i$ *and* $l \leq j$*. For an*

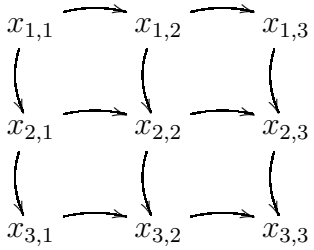

Figure 1.1: Look-Ahead Interconnected System

example of a look-ahead topology see Figure 1.1.

Mesh stability can be intuitively understood as the attenuation of disturbances as they propagate through an interconnected system. Aniruddha *et al.* defined a notion of mesh stability for a class of interconnected nonlinear systems and derived a set of sufficient conditions to guarantee mesh stability for look-ahead interconnected systems in [14]. A theorem was provided which showed that if an interconnected system is globally exponentially mesh stable, it will be robust to singular perturbations provided that some conditions are met. Examples of formation flying in a plane were presented.

In [15], Jin and Murray used mesh stability as a to way quantify disturbance resistance of an acyclic formation. The studied formation is a *look-ahead* system as defined in [14]; however they introduced the concept of a double-graph model, where one graph represents transmitted leader information and the other graph represents sensed vehicle information. A control scheme was presented which weighted the contribution of leader information a scaler α and the contribution of the sensed neighbor information by $1-\alpha$. It was shown that when $\alpha = 1$ the best possible string stability is achieved; however, any loss in communication will cause instability. As α is decreased the fault tolerance improves but there is a negative impact on string stability. Unfortunately, an algorithm which provides the best possible choice of α was not provided.

1.2.3 The Consensus Problem

The consensus problem is a general coordinated control problem in which agents iteratively exchange information with their neighbors to reach a consensus on a shared set of data. Examples of consensus problems include formation control, rendezvous problems, and sensor networks.

1.2.3.1 The Rendezvous Problem

Consider a set of n agents with limited sensing range. Each agent is represented as a node within a graph and an edge connects two nodes if the agents can sense one-another. Starting with a random distribution of agents, the goal of the rendezvous problem is to have all agents converge to a common point.

The rendezvous problem was introduced by Ando *et al.* in [16]. It was assumed that each agent has a limited sensing range of radius r and that an agents "view" may be obstructed by another agent (i.e., two agents within the sensing radius r of one-another may not be able to sense each other if a third agent is between them). The agents alternate between two phases (i) a static phase, in which the agents sense their neighbors and calculate a new position to move to and (ii) a motion phase, in which the agents move to their new locations (no new calculations or changes to the agents destination are allowed during this phase). It was shown that the provided algorithm caused all agents within an initially connected graph to converge to a common point. A theorem was provided to prove the algorithm. However, collision avoidance and view obstruction were not considered.

Later, in [17] and [18], Lin *et al.* extend the work of Ando *et al.* to a larger family of algorithms which include the algorithm presented in [16]. The same basic assumptions of the n agent system were made (i.e., each agent was modeled as a point, such that each agent could not obstruct the view of another agent and problems associated with collision avoidance were ignored). They showed that the

theorem presented in [16] is sufficient but not necessary to obtain convergence. An idea of trapping was considered in which agents not initially connected may also converge to a point.

The results discussed above require synchronization. This is a serious drawback that requires the agents to have a common clock. In [17] and [18] the multi-agent rendezvous problem was addressed once again; however, they solved the problem asynchronously. In the synchronous case it is fairly intuitive to show agents retain their neighbors as the system evolves. This proof is much more involved in the asynchronous case. Nevertheless, Lin, Morse, and Anderson did provide proofs to show their rendezvous algorithm is correct.

Finally, Luc Moreau developed necessary and sufficient conditions to drive agents to a common state in [19]. A simple model with time-dependent communication links was presented. State information was updated using strict convex combination of its state information along with the state information of its neighbors. The approach applies to a large family of problems including formation control, synchronization, and swarming. The stability and convergence proofs were accomplished using set-valued Lyapunov theory which exploited the convex hull of the agent's states as the non-increasing Lyapunov function. An important result was shown through counter example: when considering unidirectional communication, the agents may not converge to a common state even if during each time interval an agent sends its state information to all other agents. It was shown, however, that if the propagation time for information exchange is bounded that convergence will occur.

1.2.3.2 Flocking Behavior

An overview of flocking behavior was presented in Section 1.2.1. Previous work in this area has presented interesting algorithms and behavioral models but did not

offer any stability or convergence proofs. Here we focus on algorithms with provably correct algorithms.

Motivated by the results presented in [1], Tanner *et al.* presented a system of N mobile agents modeled as double integrators. A control scheme was presented using identical agent controllers which allow the agents to achieve desired inter-agent distances, avoid collision and move as a cohesive group with a common velocity. Collision avoidance, and desired inter-agent distances are achieved using an artificial potential function. Convergence to a common velocity results from the static inter-agent separation and from a velocity alignment component in the control law. Neighboring relations were modeled as a graph and can reflect either sensed or communicated information. A theorem was provided which proves convergence and collision avoidance if the starting graph is connected. While it is not stated, we conjecture the theorem is a sufficient but not necessary condition. The concept of trapping presented in [18] should also apply to this result

In [20], Jadbabaie *et al.* presented a theoretical explanation for the behavior observed in [2]. The heading update for the ith agent is an average of the heading of the ith agent and the headings of its neighbors. The definition of neighbors does differ in the two papers. In [2] the ith agent's neighbors were defined as agents which lied within a radius r of agent i. In [20] the neighbors of agent i are defined through a connectivity graph. To model the idea that an agent's neighbors may change over time a switching signal was introduced which indexes through a complete set of connectivity graphs. The switching signals do not take into account heading vectors; therefore the presented is not truly identical to the model presented in [2]. Convergence results were presented for a large set of switching signals and initial heading vectors.

1.2.3.3 Formation Control

Consensus algorithms can be used to achieve and maintain formations. Typically agents reach consensus at the formation center and individually maintain a predefined relative distance to the formation center. In [21], [22] and [23] Fax and Murray developed a formation control scheme to drive N agents formation center reference. The sensing network is modeled as a directional graph. A Nyquist-like stability criterion that exploits the eigenvalues of the Laplacian matrix of the graph was used to analyze the effect that different sensing topologies have on stability. Necessary and sufficient conditions for stability were provided. The goal of the papers was to provide a framework to analyze the effect the communication structure can have on overall stability.

In [24], Glavaski *et al.* extended the results of [21] and [22] to allow for non-fixed frame formations and intermittent sensor data and communication loss. Simulations were presented; however, no stability proofs were provided. In [25], Williams *et al.* extended [21]-[23] to address a hierarchy of formations.

1.3 Contributions and Areas of Interest

Early work in the area of formation control, such as [21] and [23], has first chosen a communications architecture and a formation shape and then performed an analysis to determine if the chosen communication architecture suffices to achieve the desired formation. The work presented in this thesis reverses the approach. First the desired formation shape is chosen and then it is determined what communication architecture is required to achieve and maintain the formation.

The same geometric formation can be described in multiple ways. For instance, if the desired geometry is of that depicted in Figure 1.2, it can be described by specifying the relative positions between agents joined by arrows. In this figure relative positions of the pairs (1, 2), (1, 4), (2, 3) and (4, 5) are specified. One may

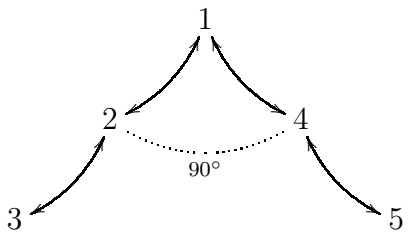

Figure 1.2: Agent Formation Topology with no Redundancy

also specify the same geometry by adding redundant information, as in Figure 1.3, where the additional constraints are added between the pairs (1, 3) and (1, 5). Such a redundant structure adds fault tolerance to the geometric description. Thus, while the loss of agent 4 in Figure 1.2, implies that 5 is isolated, in Figure 1.3, 5 retains its position relative to agent 1 and the new topology remains viable. Therfore additional fault tolerance is achieved in Figure 1.3 by adding redundancies in the geometric configuration such that the loss of an agent still results in an acceptable formation topology.

This will be defined as the *Formation Topology*, as opposed to the *Communication Topology* which defines the state information flow required to implement a cooperative control law.

A pair of one-step-ahead optimization based control laws for autonomous agents are developed. Each agent is modeled as a double integrator. Only the formation topology for the agents is defined, and by correctly choosing the cost function, it is shown that the algorithm produces a communication topology mirroring the geometric topology. This provides the user with a natural understanding of the relationship between the geometric formation dependencies and the communication infrastructure.

The intuitive nature of the relationship between the formation and communication topologies allows the user to easily add redundancy to the formation topology

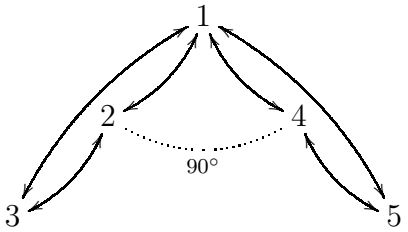

Figure 1.3: Agent Formation Topology with Redundancy

allowing the system to survive loss of agents and/or communication channels. Additionally, by adding redundancy to the formation topology, as in Figure 1.3, not only is the formation more robust to loss of agents, but that the agents converge to the desired formation at a faster rate. Other attractions of the scheme are scalability, the requirement of only local knowledge of the desired formation topology, and ease of reconfiguration in the face of loss of agents and/or communication channels.

The provided control laws not only allow the agents to come into formation, but velocity constraints can be added to allow the formation to follow fixed or arbitrary time dependent velocities.

1.4 Organization

Chapter 2 provides the reader with an introduction to the core mathematical equations and concepts used throughout the thesis. In Section 2.1 a set of equations that will be used to represent our system of agents is intoduced. Section 2.2 introduces the mathematical formulas that will be used to represent the agent formations. Finally, in Section 2.3 a set of conditions is supplied to address the viability of a formation.

Chapter 3 presents a formation control law which has limited scalability. First, in Section 3.1, a one step ahead optimal control law is provided and it is proven that communication topology mirrors the formation topology. Section 3.2 proves that the control law is stable and that all viable formation topologies are attained. Then,

in Section 3.3, a series of simulations is provided which demonstrate some of the characteristics of the control approach.

In Chapter 4, the work presented in Chapter 3 is extended to allow the agents to track arbitrary time varying velocities. In Section 4.1 the control law is defined. The control law is proven to be stable, attain all viable formation topologies and follow the desired trajectory in Section 4.2. Finally, in Section 4.3, simulation results are provided which demonstrate the behavior.

The impact that redundancy has upon the rate of convergence is analyzed in Chapter 5. In Section 5.1 a state transformation is presented to provide a more concise representation of the problem. Section 5.2 proves that the rate of convergence improves with additional redundancy. Finally, the results are demonstrated through simulation in Section 5.3.

Chapter 6 presents an enhanced approach to multi-agent formation control that results in better scalability. In Section 6.1 the problem is presented and some assumptions are defined. In Section 6.2 the one step ahead optimal control law is provided and it is proven that communication topology mirrors the formation topology. It is established that the control law guarantees that a fleet of autonomous agents can attain any fixed velocity viable formation with the additional benefit of enhanced scalability in Section 6.3. Finally, the properties are demonstrated in Section 6.4 and its is shown that in many cases better performance is obtained using this control law when compared to the limited scalability approach.

Finally, in Chapter 7, the influence that dynamic changes to the communication topology can have upon system stability is investigated. A representation for periodic time-varying systems is provided in Section 7.1. In Sections 7.2 and 7.3 periodic sequences which result in instability are presented for the limited scalability approach and the enhanced scalability approach respectively.

The work presented in Chapters 2-6 appears in the following papers: [26], [27],

[28], [29], [30], [31] and [32].

CHAPTER 2
THE COORDINATED CONTROL OF AUTONOMOUS AGENTS

In this chapter we will provide an introduction into the coordinated control of autonomous agents. In Section 2.1 we will provide a mathematical definition for the system of agents. In Sections 2.2 and 2.3 respectively, we will introduce the mathematical representation that will be used to characterize our formations and we will define the conditions required for a formation to be viable.

First let us define the *direct sum* of matrices as we will use this throughout the paper.

Definition 2.0.1 *Consider any two matrices A and B where A is of size $m \times n$ and B is of size $p \times q$. Then the direct sum of A and B is a matrix of size $(m+p) \times (n+q)$ as defined below:*

$$A \oplus B = \begin{bmatrix} A & 0 \\ 0 & B \end{bmatrix} = \begin{bmatrix} a_{11} & \dots & a_{1n} & 0 & \dots & 0 \\ \vdots & \dots & \vdots & \vdots & \dots & \vdots \\ a_{m1} & \dots & a_{mn} & 0 & \dots & 0 \\ 0 & \dots & 0 & b_{11} & \dots & b_{1q} \\ \vdots & \dots & \vdots & \vdots & \dots & \vdots \\ 0 & \dots & 0 & b_{p1} & \dots & b_{pq} \end{bmatrix} \tag{2.1}$$

The direct sum of n matrices $\{A_1, A_2, \dots A_n\}$ can be written

$$\bigoplus_{i=1}^{n} A_i = \ diag\ (A_1, A_2, \dots, A_n) = \begin{bmatrix} A_1 & & & 0 \\ & A_2 & & \\ & & \ddots & \\ 0 & & & A_n \end{bmatrix} \tag{2.2}$$

2.1 Problem Description

Consider the problem of a two dimensional N-agent formation topology. We will partition the global, $4N$ state vector x of the formation as

$$x = \begin{bmatrix} x_p^T & x_v^T \end{bmatrix}^T \tag{2.3}$$

where x_p and x_v contain the positions and velocities respectively. Further partitioning the state vector to show the x and y constraints, where $x_{p,i}$ will be used to denote the i-th element of x_p, we have:

$x_{p,i}$ is the x position of agent i,

$x_{v,i}$ is the x velocity of agent i,

$x_{p,i+N}$ is the y position of agent i, and

$x_{v,i+N}$ is the y velocity of agent i

For convenience we will denote

$$n = 2N. \tag{2.4}$$

Each vehicle will be internally modeled as a double integrator with a sampling interval of 1-second. The system of agents can be represented as:

$$x(k+1) = \Phi x(k) + \Gamma u(k) \tag{2.5}$$

where

$$\Phi = \begin{bmatrix} I_n & I_n \\ 0 & I_n \end{bmatrix}, \tag{2.6}$$

and,

$$\Gamma = \begin{bmatrix} I_n \\ 2I_n \end{bmatrix}. \tag{2.7}$$

Observe the following fact that follows directly from (2.5-2.7).

Fact 2.1.1 *Consider agent i. The corresponding states associated with agent i are $j \in \{i, i+N, i+2N, i+3N\}$. The computation of the j-th element of $\Phi x(k)$ requires only the states associated with agent i.*

2.2 The Formation Topology

There are two views of the formation topology. In graph theory terms, each agent is modeled as a node. An undirected edge exists between agent i and agent j if relative position constraints are specified between them. It is intuitive to think of each arc as a single constraint between two agents.

Now, let us define an algebraic view of the formation topology. We will define the constraints in a similar fashion to the graph theoretic approach. Therefore, if an x-position constraint is specified between a pair of agents, then we assume that a y-position constraint has also been specified and we will consider this pair to be a single constraint. The formation topology will be characterized by a total of $L = L_p + L_v$ constraints.

Observe that the relative positions between two agents, i and j, can be completely specified by the following pair of equations:

$$x_i - x_j = c_{x_{ij}} \qquad\qquad x_{i+N} - x_{j+N} = c_{y_{ij}}. \tag{2.8}$$

Assumption 2.2.1

The L_p position constraints will be characterized by the direct sum of a pair of identical $L_p \times N$ matrices A_{ps} and a $2L_p \times 1$ vector b_p. There are as many rows in A_{ps} as there are arcs in the formation topology, one row for each arc. If an arc exists between agents i and j, then the corresponding row of A_{ps} is a vector, all but the i and j-th elements are zero, the i-th element is 1 and the j-th element is -1.

With

$$A_p = A_{ps} \oplus A_{ps} \tag{2.9}$$

the position constraints can be represented by the $\left[\begin{array}{cc} A_p, & b_p \end{array}\right]$ pair, where $\oplus$ denotes the direct sum as specified in Definition 2.0.1. Thus, using this pair, an arbitary position constrained formation such as in Figure 1.2 or in Figure 1.3 can be specified. Indeed in Figure 1.2, L_p is 4 and in Figure 1.3, L_p is 6.

The velocity constraints will be characterized by a pair of $L_v \times N$ matrices A_{vs}

and a $L_v \times 1$ vector b_v. With

$$A_v = A_{vs} \oplus A_{vs} \tag{2.10}$$

one can add velocity constraints through A_v and b_v. Thus should either of the formations in Figures 1.2 and 1.3 be required to move with a constant velocity, then one can select

$$A_v = \begin{bmatrix} 1 & 0 & \cdots & 0 \end{bmatrix} \oplus \begin{bmatrix} 1 & 0 & \cdots & 0 \end{bmatrix}. \tag{2.11}$$

This would specify a velocity in the x and y directions on agent 1, which together with the relative position constraints, completely defines a formation moving with a constant velocity. One can add redundancy in (2.11) by also specifying the velocity of agent 3, (to guard against the loss of either agent) by choosing

$$A_v = \begin{bmatrix} 1 & 0 & 0 & 0 & 0 \\ 0 & 0 & 1 & 0 & 0 \end{bmatrix} \oplus \begin{bmatrix} 1 & 0 & 0 & 0 & 0 \\ 0 & 0 & 1 & 0 & 0 \end{bmatrix}. \tag{2.12}$$

With

$$A = \begin{bmatrix} A_p & 0 \\ 0 & A_v \end{bmatrix} \qquad \text{and} \qquad b = \begin{bmatrix} b_p \\ b_v \end{bmatrix} \tag{2.13}$$

the topology can be represented by the following equation:

$$Ax = b, \tag{2.14}$$

where x the state vector described in (2.3).

Consider the formation topologies shown in Figure 1.2 and Figure 1.3. The arcs connecting the agents represent a position and/or velocity dependence between the representative agents in the topology. Indeed the following fact connects the existence of an arc in the formation topology with a property of A.

Fact 2.2.1 *Define a_{jl} as the j,l-th element of A. Then an arc exists between agents p and q iff for at least one $i \in \{p, p+N, p+2N, p+3N\}$ and one $j \in \{q, q+N, q+2N, q+3N\}$*

$$a_{li}a_{lj} \neq 0 \text{ for some } l \in \{1, \cdots, 2L\}.$$

In other words there is at least one row of A that contains nonzero entries from columns corresponding to velocities and/or positions of both p and q.

Recall that while Figures 1.2 and 1.3 describe the same geometry the latter represents a formation topology with redundancies. Observe if the formation topologies in Figure 1.2 and Figure 1.3 are respectively defined by the pairs $[A^{(1)}, b^{(1)}]$ and $[A^{(2)}, b^{(2)}]$, then $[A^{(1)}, b^{(1)}]$ is a *sub-matrix* of $[A^{(2)}, b^{(2)}]$. Moreover, should the loss of an agent result in a topology that remains acceptable, for example, the loss of 4 in Figure 1.3, then this new topology characterized by $[A^{(3)}, b^{(3)}]$ obtained by removing the rows corresponding to the constraints featuring 4 and columns corresponding to the states of 4, is itself a sub-matrix of $[A^{(2)}, b^{(2)}]$. The loss of a communication channel, e.g., that between 1 and 5, would involve the use of a new pair obtained by removing rows characterizing the constraint defining this lost arc. This feature forms a core property to be exploited in fault tolerant design. Scalability is likewise incorporated rather easily. Thus if a new agent 6 appears in Figure 1.3 with an arc between it and 5, then the new pair $[A^{(4)}, b^{(4)}]$ characterizing it has $[A^{(2)}, b^{(2)}]$ as a sub-matrix, and involves just the addition of rows and columns, and augmenting rows in $[A^{(2)}, b^{(2)}]$ that feature in $[A^{(4)}, b^{(4)}]$ by zero column entries. In other words with $\times$ denoting arbitrary sub-matrices, one has

$$[A^{(4)}, b^{(4)}] = \begin{bmatrix} A^{(2)} & 0 & b^{(2)} \\ \times & \times & \times \end{bmatrix}. \tag{2.15}$$

Thus the loss of an agent/communication channel requires working with a sub-matrix of the original $\begin{bmatrix} A, & b \end{bmatrix}$, and the addition of an agent requires a super-matrix of $\begin{bmatrix} A, & b \end{bmatrix}$.

2.3 Viability

In this section we explore conditions on $\begin{bmatrix} A, & b \end{bmatrix}$ under (2.13) that ensure the viability of the formation topology (2.14). Before providing a formal definition and analysis of *viability* we first discuss at an intuitive level what it takes for a topology such as this to be both achieved and maintained.

First we make the following assumptions on the pair $\left[\begin{array}{cc} A, & b \end{array}\right]$:

Assumption 2.3.1

(i) The matrix A_{ps} has rank $N-1$.

(ii) Further b is in the range space of A.

It is well known that *(i)* ensures that the formation topology viewed as a graph is connected. Moreover, *(ii)* ensures that it is well defined.

Secondly since x_v is the derivative of x_p and with x defining a target formation, $A_p x_p$ is a constant,

$$A_p x_v = 0.$$

Finally it would be intuitively appealing if, once the formation is attained, it is maintained without any external force. In view of (2.5) this would require that for all nonnegative integers m

$$A\Phi^m x = b. \tag{2.16}$$

In a more formal sense we define a viable topology to be one that can be achieved and maintained by control law that may be centralized and even nonlinear time varying. More precisely:

Definition 2.3.1 *Under (2.5) and (2.13), the formation topology (2.14) is viable if for every $x(0)$ there exists a bounded input sequence $u(k)$ such that.*

$$\lim_{k\to\infty}(Ax(k) - b) = 0. \tag{2.17}$$

The following theorem demonstrates that the intuitive properties we discussed at the outset of this subsection are necessary for viability.

Theorem 2.3.1 *Under (2.13) suppose (2.14) is viable. Then there exists x as in (2.3) such that (2.16) holds for all nonnegative integers m as does (2.18) below.*

$$A_p x_v = 0 \tag{2.18}$$

Proof: If the topology is viable then (2.17) should hold. This implies that there

exists x as in (2.3) and an $\left[\begin{array}{cc} A, & b \end{array}\right]$ as in (2.13) such that

$$A_p x_p = b_p \tag{2.19}$$

and

$$A_v x_v = b_v. \tag{2.20}$$

Also, using the same x as above, under (2.5) and (2.17) there exists an input u such that

$$A\left[\Phi x + \Gamma u\right] = b. \tag{2.21}$$

From (2.6) and (2.7) we have:

$$\left[\begin{array}{cc} A_p & 0 \\ 0 & A_v \end{array}\right] \left[\begin{array}{c} x_p + x_v + u \\ x_v + 2u \end{array}\right] = \left[\begin{array}{c} b_p \\ b_v \end{array}\right] \tag{2.22}$$

It follows that:

$$A_p(x_v + u) = 0 \tag{2.23}$$

and

$$A_v u = 0. \tag{2.24}$$

Now if we define $\hat{x}$ using the same x and u as above

$$\hat{x} = \left[\begin{array}{c} x_p \\ x_v + u \end{array}\right] \tag{2.25}$$

we have

$$A\hat{x} = \left[\begin{array}{cc} A_p & 0 \\ 0 & A_v \end{array}\right] \left[\begin{array}{c} x_p \\ x_v + u \end{array}\right] = \left[\begin{array}{c} b_p \\ b_v \end{array}\right] = b \tag{2.26}$$

since $A_v u = 0$ from (2.24). Also because (2.23) we have

$$A\Phi^m \hat{x} = b \qquad \forall m \in \mathbb{N} \cup \{0\}. \tag{2.27}$$

This can easily be verified since

$$\Phi^m = \left[\begin{array}{cc} I_n & mI_n \\ 0 & I_n \end{array}\right]. \tag{2.28}$$

Therefore (2.27) can be rewritten as

$$\left[\begin{array}{cc} A_p & 0 \\ 0 & A_v \end{array}\right] \left[\begin{array}{c} x_p + m(x_v + u) \\ x_v + u \end{array}\right] = b \quad \forall m \in \mathbb{N} \cup \{0\} \tag{2.29}$$

Finally, since there exists an $\hat{x}$ such that (2.27) holds the input force becomes 0, and

$A_p x_v = 0$ in (2.23). ■

Thus the existence of a control law necessitates the intuitive conditions we stated earlier. Indeed we go on to show that these conditions suffice for the attainment and maintenance of the formation topology and enable these tasks through a communication topology that mirrors the formation topology defining the formation.

CHAPTER 3
FORMATION CONTROL WITH LIMITED SCALABILITY

In this chapter we present a distributed approach to the formation control problem. This approach requires either an *a priori* knowledge of the largest possible formation size or a global information exchange of the current formation size. As such, this approach is not as scalable as some would desire; however, it does have some interesting properties. A one-step-ahead optimal control law which guarantees a fleet of autonomous agents can attain any fixed velocity, viable formation is provided. We show that the formation topology is in fact equivalent to the communication topology and, assuming the use of *a priori* knowledge, only local information exchange. In other words, each agent only requires knowledge of its neighbors, as specified by the formation topology. In the face of a lost agent, only neighbors of the lost agent must adjust their control laws. If a communication channel is lost, only the agents that share the communication channel must adjust their control laws. Finally, the arrival of a new agent only impacts the agents against which the arriving agent's relative position constraints are defined.

3.1 Basic Control

We propose a one step ahead optimization law using the cost function

$$J(k) = [Ax(k+1) - b]^T [Ax(k+1) - b] + u^T(k)Qu(k) \tag{3.1}$$

Where $Q = Q^T > 0$ penalizes the input. The key step in achieving the control law with the desired characteristics described in the introduction is to appropriately select Q.

Since $x(k+1)$ is dependent on $u(k)$ we begin by substituting (2.5) into the cost function defined in (3.1). Taking the partial derivative of the resultant expression with respect to $u(k)$, we obtain:

$$\left[\Gamma^T A^T A\Gamma + Q\right] u(k) = \Gamma^T A^T [b - A\Phi x(k)]$$

Setting:

$$Q = \Lambda - \Gamma^T A^T A \Gamma, \tag{3.2}$$

and choosing:

$$\Lambda = \alpha I \tag{3.3}$$

with α greater than the largest eigenvalue of $\Gamma^T A^T A \Gamma$, Q is invertible and positive definite. Further by making α arbitrarily large one can penalize the input to an aribitrary degree. The resulting control law is shown below.

$$u(k) = \frac{1}{\alpha}\Gamma^T A^T b - \frac{1}{\alpha}\Gamma^T A^T A \Phi x(k) \tag{3.4}$$

Now we will show that the communication topology resulting from (3.4) is identical to the geometric topology and further that only a local knowledge of the formation is required by each agent. Observe that the control inputs to agent i are u_i and u_{i+N}. We will show that if i and j do not have an arc between them in the formation topology, then u_i and u_{i+N} do not depend on $\{\Phi x\}_j, \{\Phi x\}_{j+N}, \{\Phi x\}_{j+2N}$ and $\{\Phi x\}_{j+3N}$. Because of Fact 2.1.1 this in turn implies that u_i and u_{i+N} do not depend on x_j, x_{j+N}, x_{j+2N} and x_{j+3N}, establishing the structure of the communication topology. Observe that (3.4) becomes,

$$u(k) = \frac{A_p^T b_p + 2A_v^T b_v - [A_p^T A_p, 2A_v^T A_v]\Phi x(k)}{\alpha} \tag{3.5}$$

We next present the following lemma.

Lemma 3.1.1 *For any matrix C*

$$\left(C^T C\right)_{ij} \neq 0$$

only if for some l

$$c_{li} c_{lj} \neq 0.$$

Further, the computation of the i-th row of $C^T C$ requires the knowledge of the l-th row of C only if $c_{li} \neq 0$. Finally, for any vector g the computation of the i-th element of $C^T g$ requires the knowledge of the l-th row of C and/or l-th element of g, only if $c_{li} \neq 0$.

Proof: Follows from the fact that

$$\left(C^T C\right)_{ij} = \sum_l c_{li} c_{lj}$$

and

$$\left(C^T g\right)_i = \sum_l c_{li} g_l. \tag{3.6}$$

■

Then we have the following result that establishes the various properties of the communication topology listed in the foregoing.

Theorem 3.1.1 *Consider (3.4) under (2.3), (2.6), (2.7), and (2.13). Then the finding $u_i(k)$ and $u_{i+N}(k)$ requires:*

(i) The states of agent l only if there is an arc between agents l and i in the formation topology.

(ii) The l-th row of A only if for some $j \in \{i, i+N, i+2N, i+3N\}$ $a_{lj} \neq 0$.

(iii) The l-th element of b only if for some $j \in \{i, i+N, i+2N, i+3N\}$ $a_{lj} \neq 0$.

Proof: Consider the determination of u_p, $p \in \{i, i+N\}$. Suppose this requires the knowledge of Φx_q, for some $q \in \{l, l+N\}$. Then from (3.5) $\left(A_p^T A_p\right)_{pq}$ is nonzero. Then because of Lemma 3.1.1 for at least one m the m-th row of A_p must have nonzero entries in both the p-th and the q-th locations. Similarly if the determination of u_p, $p \in \{i, i+N\}$ requires the knowledge of Φx_q, for some $q \in \{l+2N, l+3N\}$, then for at least one m the m-th row of A_v has nonzero entries in both the p-th and the q-th locations. Then Facts 2.1.1 and 2.2.1, together with (2.13) prove *(i)*.

Now, from (3.5), the computation of u_p, $p \in \{i, i+N\}$ requires the computation of the p-th rows of $A_p^T A_p$ and $A_v^T A_v$ and the p-th elements of $A_p^T b_p$ and $A_v^T b_v$. Then from Lemma 3.1.1, for such a p, the computation of the p-th rows of $A_p^T A_p$ and $A_v^T A_v$ require respectively, the knowledge of the l-th rows of A_p and A_v only if the lp-th elements of respectively A_p and A_v are nonzero. Further the p-th elements of $A_p^T b_p$ and $A_v^T b_v$ require the knowledge of l-th rows of A_p and A_v and/or the l-th elements

of b_p and b_v only if the lp-th elements of respectively A_p and A_v are nonzero. Then *(ii)* and *(iii)* follow from (2.13), Fact 2.1.1 and (2.3). ∎

Property *(i)* establishes that the communication topology is the same as the formation topology. Properties *(ii)* and *(iii)* establish that agent i need only know those rows of A and elements of b which define the arcs emanating from it. Thus i must only know its place in the formation topology and therefore, a distributed knowledge of the formation topology suffices.

If, despite the loss of an agent, for example agent 4 in Figure 1.3, the formation topology remains viable, then this modified formation topology is described by a $\left[\begin{array}{cc} A, & b \end{array}\right]$ matrix that is a sub-matrix of its counterpart in the original formation topology, and obtained by removing the rows characterizing the two arcs impacting 4 and the four columns of A corresponding to the states of 4. As the elements of these columns in the rows of the original A matrix defining the arcs of 2 and 3 are zero, the inputs to agents 2 and 3 are unchanged. These agents do not reconfigure their control laws and need not know about the loss. Similarly if communication between 1 and 5 be impaired or lost, then only 1 and 5 must know of this loss and adjust their control law.

Scalability is similarly accommodated. The position of a new arrival can be completely specified by introducing an arc to a single member of the formation. Then because of the relation between the larger $[A, b]$ matrix describing the augmented formation topology, and the old one, see for example (2.15), none of the elements of this new $\left[\begin{array}{cc} A, & b \end{array}\right]$ matrix affect the control laws of the remaining agents.

3.2 Proof of Stability

In this section we prove that the control law in (3.4) asymptotically attains all viable formation topologies, as long as

$$I - \frac{\Gamma^T A^T A \Gamma}{\alpha} > 0. \tag{3.7}$$

To this end observe that with

$$F = \Phi - \frac{\Gamma}{\alpha}\Gamma^T A^T A\Phi, \tag{3.8}$$

and

$$G = \frac{\Gamma}{\alpha}\Gamma^T A^T b, \tag{3.9}$$

the control law (3.4) results in the closed loop

$$x(k+1) = Fx(k) + G. \tag{3.10}$$

Define

$$y(k) = Ax(k) - b. \tag{3.11}$$

We need to find conditions under which $y(k)$ asymptotically approaches zero. To this end we first provide the following lemma.

Lemma 3.2.1 *Under (3.7), with F defined in (3.8), (2.6), (2.7) and A in (2.13), all poles of $A(zI - F)^{-1}$ are inside the unit circle.*

Proof: The detailed proof is in Appendix A.1 and comprises two parts. In the first we show that (3.7) ensures that the poles of F are either at 1 or inside the unit circle. The second part shows that the poles at 1 are unobservable through A. ∎

This brings us to the main result of this section.

Theorem 3.2.1 *Suppose the formation topology is viable and $A_p \neq 0$. Then*

$$\lim_{k\to\infty} Ax(k) = b$$

Proof: We need to show that

$$R(z) = \frac{z-1}{z}\left[A(zI - F)^{-1}x(0) + A(zI - F)^{-1}\frac{Gz}{z-1} - \frac{bz}{z-1}\right]$$

is analytic on or inside the unit circle and

$$\lim_{z\to 1} R(1) = 0.$$

From Lemma 3.2.1, $A(zI - F)^{-1}$ and hence $R(z)$ is analytic on or outside the unit circle. Thus it suffices to show that

$$\lim_{z\to 1}\left[A(zI - F)^{-1}G - b\right] = 0 \tag{3.12}$$

Since the formation topology is viable there exists an x as in (2.3) that satisfies the constraints imposed by Theorem 2.3.1. For such an x and all nonnegative integer l,

from Theorem 2.3.1, we have

$$A\Phi^l \begin{bmatrix} x_v \\ 0 \end{bmatrix} = \begin{bmatrix} A_p & 0 \\ 0 & A_v \end{bmatrix} \begin{bmatrix} I & lI \\ 0 & I \end{bmatrix} \begin{bmatrix} x_v \\ 0 \end{bmatrix} = A_p x_v = 0. \tag{3.13}$$

Further, for such an x and all nonnegative integer m, we have from (3.8) and (3.13) that

$$AF^m \begin{bmatrix} x_v \\ 0 \end{bmatrix} = AF^{m-1} \left[I - \frac{\Gamma\Gamma^T A^T A}{\alpha} \right] \Phi \begin{bmatrix} x_v \\ 0 \end{bmatrix} = AF^{m-1}\Phi \begin{bmatrix} x_v \\ 0 \end{bmatrix}$$

Thus by induction and (3.13) for all nonnegative integer m

$$AF^m \begin{bmatrix} x_v \\ 0 \end{bmatrix} = A\Phi^m \begin{bmatrix} x_v \\ 0 \end{bmatrix} = 0. \tag{3.14}$$

Since $A\Phi^m x = b$ for all nonnegative integer m,

$$\begin{aligned}
&\lim_{z\to 1} A(zI - F)^{-1}G - b \\
&= \lim_{z\to 1} A(zI - F)^{-1}G - Ax \\
&= \lim_{z\to 1} \left[A(zI - F)^{-1} \{G - (zI - F)x\}\right] \\
&= \lim_{z\to 1} \left[A(zI - F)^{-1} \times \right. \\
&\qquad \left. \times \left\{ \tfrac{\Gamma\Gamma^T A^T A}{\alpha} x - x + \Phi x - \tfrac{\Gamma\Gamma^T A^T A \Phi x}{\alpha} \right\}\right] \\
&= \lim_{z\to 1} \left[A(zI - F)^{-1} \{-x + \Phi x\}\right] \\
&= \lim_{z\to 1} \left[A(zI - F)^{-1} \begin{bmatrix} x_v \\ 0 \end{bmatrix} \right].
\end{aligned}$$

We will now show that in fact

$$A(zI - F)^{-1} \begin{bmatrix} x_v \\ 0 \end{bmatrix} = 0$$

almost everywhere. Thus, as it is rational, it is zero every where including at $z = 1$.

Indeed, in the region of convergence of $(zI - F)^{-1}$.

$$\begin{aligned} A(zI-F)^{-1}\begin{bmatrix} x_v \\ 0 \end{bmatrix} &= Az^{-1}(I - z^{-1}F)^{-1}\begin{bmatrix} x_v \\ 0 \end{bmatrix} \\ &= \left[Az^{-1} + z^{-1}\sum_{i=1}^{\infty} z^{-i}AF^i\right]\begin{bmatrix} x_v \\ 0 \end{bmatrix} \\ &= z^{-1}\sum_{i=1}^{\infty} z^{-i}AF^i\begin{bmatrix} x_v \\ 0 \end{bmatrix} \\ &= 0, \end{aligned}$$

where the last equality follows from (3.14). ■

Thus this distributed control law helps attain and maintain all viable formation topologies. Three implications of this result bear reiteration. First, the necessary conditions for viablity given in Theorem 2.3.1 are all that are invoked in the proof of Theorem 3.2.1. Thus these necessary conditions are also sufficient for viability. Second, it is easily seen from the proof of Theorem 3.2.1 that in fact

$$\lim_{k\to\infty} u(k) = 0.$$

In other words once the formation is attained it can be maintained with no control input. Finally, and more compellingly, the class of formation topology under consideration here has the attractive property that a distributed control law for its achievement exists, as long as a centralized law exists. Thus whatever can be done through global action can also be achieved through local action, and as importantly through local knowledge of the overall objective.

3.3 Simulation Results

We assume that there are no velocity constraints, that is, $A_v = 0$. Relative positions are specified using equations of the form in (2.8).

In all the simulations, the initial conditions of the fleet are the same. The starting positions are denoted by an $\times$, the positions at each time step are denoted

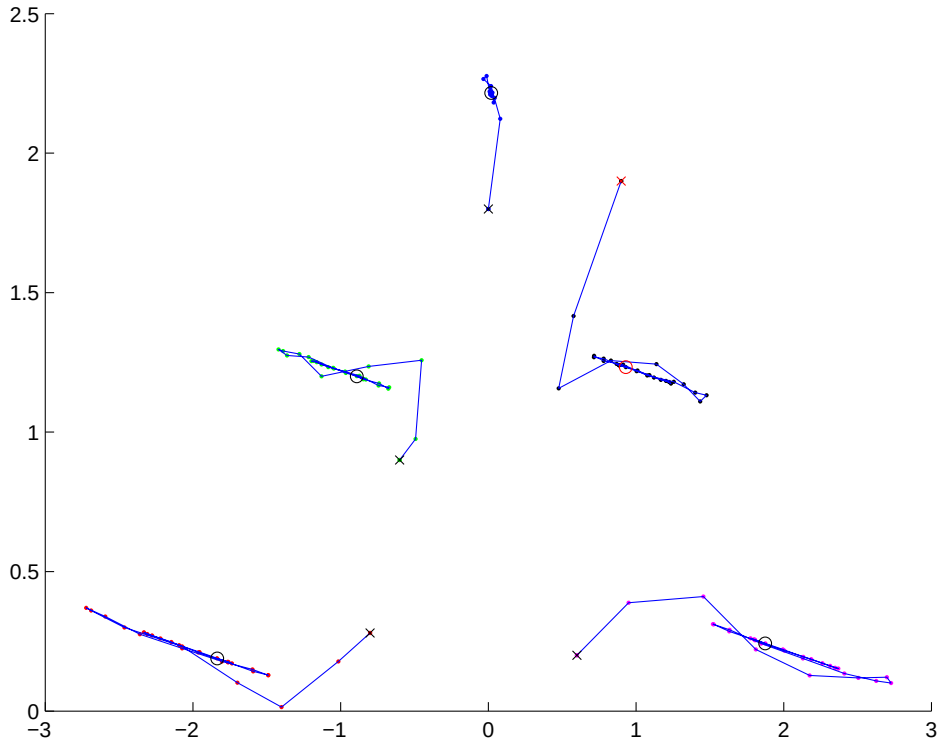

Figure 3.1: Agent Formation with no Redundancy

by a $\cdot$, and the final positions are denoted by a $\circ$. All simulations are run until the desired formation is reached.

Figure 3.1 corresponds to the formation shown in Figure 1.2. Figure 3.2 demonstrates how a formation with additional redundancy is robust to loss of agents. It shows the motion of the fleet with the additional redundancy defined in Figure 1.3, which provides additional relative state information to agents 3 and 5. In this example agent 4 is lost after 4 time steps. The position at which agent 4 is lost is denoted by a red $\circ$ Once a loss has been detected, the rows corresponding to the constraints of the lost agent, and the columns associated with its states are removed.

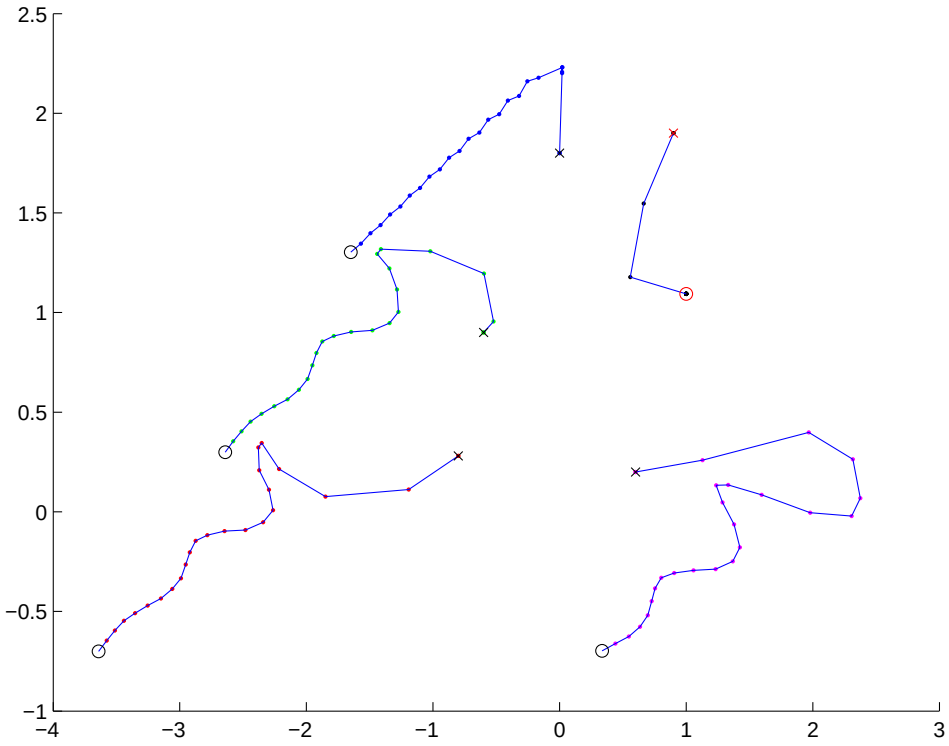

Figure 3.2: Agent Formation with Redundancy and the Loss of Agent 4 at Time $k = 5$

3.4 Conclusion

We have presented a distributed approach to the formation control problem. This approach required either an *a priori* knowledge of the largest possible formation size or the global information exchange of the current formation size. As such, this approach was not as scalable as some would desire; however, it does have some interesting properties which will be presented in Chapter 5. A one-step-ahead optimal control law which guaranteed a fleet of autonomous agents could attain any fixed velocity, viable formation was provided. We showed that the formation topology was in fact equivalent to the communication topology and, assuming the use of *a priori* knowledge, only local information exchange. In other words, each agent only

required knowledge of its neighbors, as specified by the formation topology. In the face of a lost agent, only neighbors of the lost agent were required adjust their control laws. If a communication channel was lost, only the agents that shared the communication channel were required adjust their control laws. Finally, the arrival of a new agent only impacted the agents against which the arriving agent's relative position constraints were defined.

CHAPTER 4
TRAJECTORY FOLLOWING

In in this chapter we extend the work presented in Chapter 3 to allow the agents to track arbitrary velocities. The control law will retain all of the attractive properties presented in Chapter 3, aside from the fact that the agents must apply an input force to maintain their dynamic velocity changes. It is important to note; however, that the input force is not used to maintain the relative positions amongst the agents once the formation is attained.

The formation topology will be characterized by a constant matrix $A_p \in \Re^{2L_p \times n}$, a constant vector $b_p \in \Re^{2L_p \times 1}$, and a $n \times 1$ time varying vector $b_v(k)$. In fact, with

$$A = \begin{bmatrix} A_p & 0 \\ 0 & I_n \end{bmatrix} \text{ and } b(k) = \begin{bmatrix} b_p \\ b_v(k) \end{bmatrix} \tag{4.1}$$

the topology can be represented by the following equation:

$$Ax(k) = b(k), \tag{4.2}$$

where x is the target state vector, and the $\begin{bmatrix} A_p, & b_p \end{bmatrix}$ pair specify the L_p position constraints and the $\begin{bmatrix} I_n, & b_v(k) \end{bmatrix}$ pair specify the n time varying velocity constraints. Observe that we are using the same definition of A specified in (2.13) with $A_v = I_n$.

As in the previous chapter, we make some assumptions. Assumptions 2.2.1 and 2.3.1 define how the relative positions are specified and also ensure that the relative position constraints are compatible. Since our target topology is partly defined by specified relative positions between the agents, the target velocities must be the same for all agents. The first and second N elements of $b_v(k)$ are respectively related, in a manner to be specified later, to the target velocities of each agent in the x and y directions. Thus we have the following assumption.

Assumption 4.0.1 *For some bounded functions $b_x(k)$ and $b_y(k)$, the first N elements of $b_v(k)$ equal $b_x(k)$, and the second N elements equal $b_y(k)$.*

Observe we are requiring that each agent be provided the velocity trajectories that the formation must follow. It is worth asking whether such information can be provided to only one agent. It was shown in Chapter 3 that this is possible if the target formation velocity is a constant. For more arbitrary time varying trajectories, however, this can not be so. Indeed suppose that only agent one in Figure 1.2 knows the trajectory to be followed. Then since in the communication architecture we seek, only its neighbors can sense its states, agents 2 and 4 can react to the current sample velocities of agent 1 only at the next sampling interval, and 3 and 5 at a further interval removed. Thus the formation simply cannot be maintained.

4.1 Control Law and Communication Topology

We propose a one step ahead optimization law using the cost function:

$$J(k) = [Ax(k+1) - b(k)]^T [Ax(k+1) - b(k)] + u^T(k)Qu(k) \tag{4.3}$$

Where $Q = Q^T > 0$ penalizes the input. The key step in achieving the control law with the desired characteristics described in the introduction is to appropriately select Q.

Since $x(k+1)$ is dependent on $u(k)$ we begin by substituting (2.5) into the cost function defined in (4.3). Taking the partial derivative of the resultant expression with respect to $u(k)$, we obtain:

$$\left[\Gamma^T A^T A\Gamma + Q\right] u(k) = \Gamma^T A^T [b(k) - A\Phi x(k)]$$

Setting:

$$Q = \alpha I - \Gamma^T A^T A\Gamma, \tag{4.4}$$

with α greater than the largest eigenvalue of $\Gamma^T A^T A\Gamma$, Q is invertible and positive definite. Further by making α arbitrarily large on can penalize the input to an arbitrary degree. The resulting control law is shown below and requires that $A\Gamma \neq 0$,

that is, at least one amoung A_i is nonzero.

$$u(k) = \frac{1}{\alpha}\Gamma^T A^T b(k) - \frac{1}{\alpha}\Gamma^T A^T A\Phi x(k) \tag{4.5}$$

The results of Theorem 3.1.1 in Chapter 3 apply here as well; however, we substitute equations (4.1) and (4.5) for equations (2.3) and (3.4). Therefore the communication topology is once again the same as the formation topology. Thus agent i must only know its place in the formation topology and therefore, a distributed knowledge of the formation topology suffices.

4.2 Proof of Stability

In this section we prove that the control law in (4.5) asymptotically attains all viable formation topologies, as long as (3.7) is true.

To this end observe that with

$$F = \Phi - \frac{\Gamma}{\alpha}\Gamma^T A^T A\Phi, \tag{4.6}$$

and

$$\bar{G}(k) = \frac{\Gamma}{\alpha}\Gamma^T A^T b(k), \tag{4.7}$$

the control law (4.5) results in the closed loop

$$x(k+1) = Fx(k) + \bar{G}(k). \tag{4.8}$$

This brings us to the first main result of this section, demonstrating that the formation exponentially settles down to its required relative positions.

Theorem 4.2.1 *Suppose Assumptions 2.3.1 and 4.0.1 hold, as does (3.7). Then*

$$\lim_{k\to\infty} A_p x_p(k) = b_p$$

with convergence occurring at an exponential rate.

Proof: Observe

$$A_p x_p(k) - b_p = \begin{bmatrix} A_p & 0 \end{bmatrix} x(k) - b_p \tag{4.9}$$

From (4.8) the Z - transform of (4.9) is

$$\begin{bmatrix} A_p & 0 \end{bmatrix} \left((zI - F)^{-1}x(0) + (zI - F)^{-1}\frac{\Gamma}{\alpha}\Gamma^T A^T \begin{bmatrix} b_p\frac{z}{z-1} \\ B_v(z) \end{bmatrix} \right) - b_p\frac{z}{z-1}$$

Thus we need to show that

$$R(z) = \tfrac{z-1}{z}\left\{ \left[\begin{array}{cc} A_p & 0 \end{array}\right] \left((zI-F)^{-1}x(0) + (zI-F)^{-1}\tfrac{\Gamma}{\alpha}\Gamma^T A^T \left[\begin{array}{c} b_p \frac{z}{z-1} \\ B_v(z) \end{array}\right] \right) - b_p \tfrac{z}{z-1} \right\}$$

is analytic on or inside the unit circle and

$$\lim_{z\to 1} R(1) = 0.$$

From of Lemma 3.2.1, $A(zI-F)^{-1}$ and hence $R(z)$ is analytic on or outside the unit circle. Thus it suffices to show that

$$\lim_{z\to 1}\left\{ \left[\begin{array}{cc} A_p & 0 \end{array}\right] (zI-F)^{-1}\frac{\Gamma}{\alpha}\Gamma^T A^T \left[\begin{array}{c} b_p \\ B_v(z)\frac{z-1}{z} \end{array}\right] - b_p \right\} = 0 \tag{4.10}$$

Because of (2.7), the fact that the vector of all **1**'s is in the null space of A_{ps} and Assumption 4.0.1, $B_v(z)$ is in the null space of A_p. For $B_v(z)$ and all nonnegative integers m we have:

$$A\Phi^m \left[\begin{array}{c} B_v(z) \\ 0 \end{array}\right] = \left[\begin{array}{cc} A_p & 0 \\ 0 & I \end{array}\right] \left[\begin{array}{cc} I & mI \\ 0 & I \end{array}\right] \left[\begin{array}{c} B_v(z) \\ 0 \end{array}\right] = \left[\begin{array}{c} A_p B_v(z) \\ 0 \end{array}\right] = 0 \tag{4.11}$$

Further, for $B_v(z)$ and all nonnegative integers m we have from (4.6) and (4.11) that

$$\begin{aligned} AF^m \left[\begin{array}{c} B_v(z) \\ 0 \end{array}\right] &= AF^{m-1}\left[I - \tfrac{\Gamma}{\alpha}\Gamma^T A^T A\right]\Phi \left[\begin{array}{c} B_v(z) \\ 0 \end{array}\right] \\ &= AF^{m-1}\Phi \left[\begin{array}{c} B_v(z) \\ 0 \end{array}\right] \end{aligned} \tag{4.12}$$

Thus by induction and (4.11) for all nonnegative m

$$AF^m \left[\begin{array}{c} B_v(z) \\ 0 \end{array}\right] = A\Phi^m \left[\begin{array}{c} B_v(z) \\ 0 \end{array}\right] = 0 \tag{4.13}$$

Let us rewrite (4.10) as

$$\begin{aligned} \lim_{z\to 1}\Bigg\{ &\left[\begin{array}{cc} A_p & 0 \end{array}\right] (zI-F)^{-1}\tfrac{\Gamma}{\alpha}\Gamma^T A^T \left[\begin{array}{c} b_p \\ 0 \end{array}\right] - b_p \\ &+ \left[\begin{array}{cc} A_p & 0 \end{array}\right] (zI-F)^{-1}\tfrac{\Gamma}{\alpha}\Gamma^T A^T \left[\begin{array}{c} 0 \\ B_v(z)\frac{z-1}{z} \end{array}\right] \Bigg\} = 0 \end{aligned} \tag{4.14}$$

Since the formation topology is viable there exists an x_p such that for all nonnegative

integers m such that

$$\left[\begin{array}{cc} A_p & 0 \end{array}\right] \Phi^m \left[\begin{array}{c} x_p \\ 0 \end{array}\right] = b_p \tag{4.15}$$

Now lets look at the first part of (4.14)

$$\begin{aligned}
&\lim_{z\to 1} \left[\begin{array}{cc} A_p & 0 \end{array}\right] (zI-F)^{-1} \tfrac{\Gamma}{\alpha}\Gamma^T A^T \left[\begin{array}{c} b_p \\ 0 \end{array}\right] - b_p \\
&= \lim_{z\to 1} \left[\begin{array}{cc} A_p & 0 \end{array}\right] (zI-F)^{-1} \tfrac{\Gamma}{\alpha}\Gamma^T A^T \left[\begin{array}{c} b_p \\ 0 \end{array}\right] - \left[\begin{array}{cc} A_p & 0 \end{array}\right] \left[\begin{array}{c} x_p \\ 0 \end{array}\right] \\
&= \lim_{z\to 1} \left[\begin{array}{cc} A_p & 0 \end{array}\right] (zI-F)^{-1} \left\{ \tfrac{\Gamma}{\alpha}\Gamma^T A^T \left[\begin{array}{c} b_p \\ 0 \end{array}\right] - (zI-F) \left[\begin{array}{c} x_p \\ 0 \end{array}\right] \right\} \\
&= \lim_{z\to 1} \left[\begin{array}{cc} A_p & 0 \end{array}\right] (zI-F)^{-1} \left\{ \tfrac{\Gamma}{\alpha}\Gamma^T A^T \left[\begin{array}{c} b_p \\ 0 \end{array}\right] - \left[\begin{array}{c} x_p \\ 0 \end{array}\right] \right. \\
&\qquad\qquad \left. + \Phi \left[\begin{array}{c} x_p \\ 0 \end{array}\right] - \tfrac{\Gamma}{\alpha}\Gamma^T A^T A \Phi \left[\begin{array}{c} x_p \\ 0 \end{array}\right] \right\} \\
&= \lim_{z\to 1} \left[\begin{array}{cc} A_p & 0 \end{array}\right] (zI-F)^{-1} \left\{ \tfrac{\Gamma}{\alpha}\Gamma^T A^T \left[\begin{array}{c} b_p \\ 0 \end{array}\right] - \tfrac{\Gamma}{\alpha}\Gamma^T A^T \left[\begin{array}{c} A_p x_p \\ 0 \end{array}\right] \right\} = 0
\end{aligned} \tag{4.16}$$

Note that, from (4.1), as $B_v(z)$ is in the null space of A_p,

$$\begin{aligned}
F \left[\begin{array}{c} 0 \\ B_v(z) \end{array}\right] &= \left[I - \tfrac{1}{\alpha}\Gamma\Gamma^T A^T A\right] \Phi \left[\begin{array}{c} 0 \\ B_v(z) \end{array}\right] \\
&= \left[I - \tfrac{1}{\alpha}\Gamma\Gamma^T A^T A\right] \left(\left[\begin{array}{c} B_v(z) \\ 0 \end{array}\right] + \left[\begin{array}{c} 0 \\ B_v(z) \end{array}\right] \right) \\
&= \left[\begin{array}{c} B_v(z) \\ 0 \end{array}\right] + \left(\left[\begin{array}{c} 0 \\ B_v(z) \end{array}\right] - \tfrac{2}{\alpha} \left[\begin{array}{c} B_v(z) \\ 2B_v(z) \end{array}\right] \right) \\
&= \left(1 - \tfrac{2}{\alpha}\right) \left[\begin{array}{c} B_v(z) \\ 0 \end{array}\right] + \left(1 - \tfrac{4}{\alpha}\right) \left[\begin{array}{c} 0 \\ B_v(z) \end{array}\right]
\end{aligned} \tag{4.17}$$

We next assert that in fact for all nonnegative m

$$F^m \begin{bmatrix} 0 \\ B_v(z) \end{bmatrix} = \left(1-\frac{4}{\alpha}\right)^m \begin{bmatrix} 0 \\ B_v(z) \end{bmatrix} + \sum_{i=0}^{m-1} \left(1-\frac{4}{\alpha}\right)^i \left(1-\frac{2}{\alpha}\right) \begin{bmatrix} B_v(z) \\ 0 \end{bmatrix} \tag{4.18}$$

Indeed this holds for $m=0$. Suppose it holds for some $m-1$. Then because of (4.17)

$$\begin{aligned} F^m \begin{bmatrix} 0 \\ B_v(z) \end{bmatrix} &= F^{m-1}\left[I-\tfrac{1}{\alpha}\Gamma\Gamma^T A^T A\right]\Phi \begin{bmatrix} 0 \\ B_v(z) \end{bmatrix} \\ &= F^{m-1}\left(\left(1-\tfrac{2}{\alpha}\right)\begin{bmatrix} B_v(z) \\ 0 \end{bmatrix} + \left(1-\tfrac{4}{\alpha}\right)\begin{bmatrix} 0 \\ B_v(z) \end{bmatrix}\right) \\ &= \left(1-\tfrac{4}{\alpha}\right)^0\left(1-\tfrac{2}{\alpha}\right)\begin{bmatrix} B_v(z) \\ 0 \end{bmatrix} + \left(1-\tfrac{4}{\alpha}\right)F^{m-1}\begin{bmatrix} 0 \\ B_v(z) \end{bmatrix} \\ &= \left(1-\tfrac{4}{\alpha}\right)^m \begin{bmatrix} 0 \\ B_v(z) \end{bmatrix} + \textstyle\sum_{i=0}^{m-1}\left(1-\tfrac{4}{\alpha}\right)^i\left(1-\tfrac{2}{\alpha}\right)\begin{bmatrix} B_v(z) \\ 0 \end{bmatrix} \end{aligned} \tag{4.19}$$

Finally for all nonnegative m

$$\begin{bmatrix} A_p & 0 \end{bmatrix} F^m \begin{bmatrix} 0 \\ B_v(z) \end{bmatrix} = 0 \tag{4.20}$$

Looking at the second part of (4.14), due to (4.13) and (4.20) we have:

$$\begin{aligned} &\lim_{z\to 1}\begin{bmatrix} A_p & 0 \end{bmatrix}(zI-F)^{-1}\tfrac{1}{\alpha}\Gamma\Gamma^T A^T \begin{bmatrix} 0 \\ B_v(z)\frac{z-1}{z} \end{bmatrix} \\ &= \lim_{z\to 1}\begin{bmatrix} A_p & 0 \end{bmatrix} z^{-1}\left(\textstyle\sum_{i=0}^{\infty} z^{-i}F^i\right)\tfrac{2}{\alpha}\begin{bmatrix} I \\ 2I \end{bmatrix} B_v(z)\tfrac{z-1}{z} = 0 \end{aligned} \tag{4.21}$$

Thus because of (4.16) the result holds. ∎

The next theorem concerns the formation velocity.

Theorem 4.2.2 *Suppose Assumptions 2.3.1 and 4.0.1 hold, as does (3.7). Then*

$$|1-2\alpha| < 1. \tag{4.22}$$

Further with $b_v(k)$ defined in Assumption 4.0.1, consider

$$z_x(k+1) = \left(1-\frac{4}{\alpha}\right) z_x(k) + \frac{4}{\alpha} b_x(k). \tag{4.23}$$

and

$$z_y(k+1) = \left(1 - \frac{4}{\alpha}\right) z_y(k) + \frac{4}{\alpha} b_y(k). \tag{4.24}$$

Then with $x_{v,i}$, the ith element of x_v,

$$\lim_{k\to\infty} x_{v,i}(k) = \begin{cases} z_x(k) & \forall\ i \leq N \\ z_y(k) & N < \forall\ i \leq 2N \end{cases} \tag{4.25}$$

Proof: From Theorem 4.2.1 we know:

$$\lim_{k\to\infty} A_p x_p(k) = b_p.$$

Recall the closed loop equation in (4.6) and the fact that $A_p x_v(k) = 0\ \ \forall k$. Thus as k tends to infinity, with $\bar{G}(k)$ defined in (4.7), one has:

$$\begin{aligned} Fx(k) + \bar{G}(k) &= \left(\Phi - \tfrac{1}{\alpha}\Gamma\Gamma^T A^T A\Phi\right) x(k) + \bar{G}(k) \\ &= \Phi x(k) - \tfrac{1}{\alpha}\Gamma\Gamma^T A^T \begin{bmatrix} A_p & 0 \\ 0 & I \end{bmatrix} \begin{bmatrix} x_p(k) + x_v(k) \\ x_v(k) \end{bmatrix} + \bar{G}(k) \\ &= \Phi x(k) - \tfrac{1}{\alpha}\Gamma\Gamma^T A^T \begin{bmatrix} b_p \\ x_v(k) \end{bmatrix} + \tfrac{1}{\alpha}\Gamma\Gamma^T A^T \begin{bmatrix} b_p \\ b_v(k) \end{bmatrix} \\ &= \Phi x(k) - \tfrac{1}{\alpha}\Gamma\Gamma^T A^T \begin{bmatrix} 0 \\ x_v(k) \end{bmatrix} + \tfrac{1}{\alpha}\Gamma\Gamma^T A^T \begin{bmatrix} 0 \\ b_v(k) \end{bmatrix} \\ &= \Phi x(k) - \tfrac{2}{\alpha}\Gamma x_v(k) + \tfrac{2}{\alpha}\Gamma b_v(k) \end{aligned} \tag{4.26}$$

Thus, as k tends to infinity we have:

$$\begin{bmatrix} x_p(k+1) \\ x_v(k+1) \end{bmatrix} = \begin{bmatrix} I & \left(1 - \frac{2}{\alpha}\right) I \\ 0 & \left(1 - \frac{4}{\alpha}\right) I \end{bmatrix} \begin{bmatrix} x_p(k) \\ x_v(k) \end{bmatrix} + \begin{bmatrix} \frac{2}{\alpha} b_v(k) \\ \frac{4}{\alpha} b_v(k) \end{bmatrix} \tag{4.27}$$

The result follows from our definitions of $x_v(k)$ and $b_v(k)$ in Section 2.1 and Assumption 4.0.1, respectively.

■

Thus, this distributed control law ensures that all viable formations are attained and that the input force is only required to maintain the desired trajectory once the position constraints are satisfied. Further (4.23), indicates how to select $b_x(k)$ and $b_y(k)$, given the target x and y-direction velocity trajectories $z_x(k)$ and $z_y(k)$,

respectively: with q the forward shift operator, choose

$$b_x(k) = \left(\frac{\alpha}{4}(q-1)+1\right) z_x(k) \tag{4.28}$$

and

$$b_y(k) = \left(\frac{\alpha}{4}(q-1)+1\right) z_y(k). \tag{4.29}$$

Though the system in (4.28) and (4.29) is non-causal, this poses no practical difficulties because these trajectories are defined offline. If on-line corrections are needed then they can be achieved with a delay of one sample.

4.3 Simulation Results

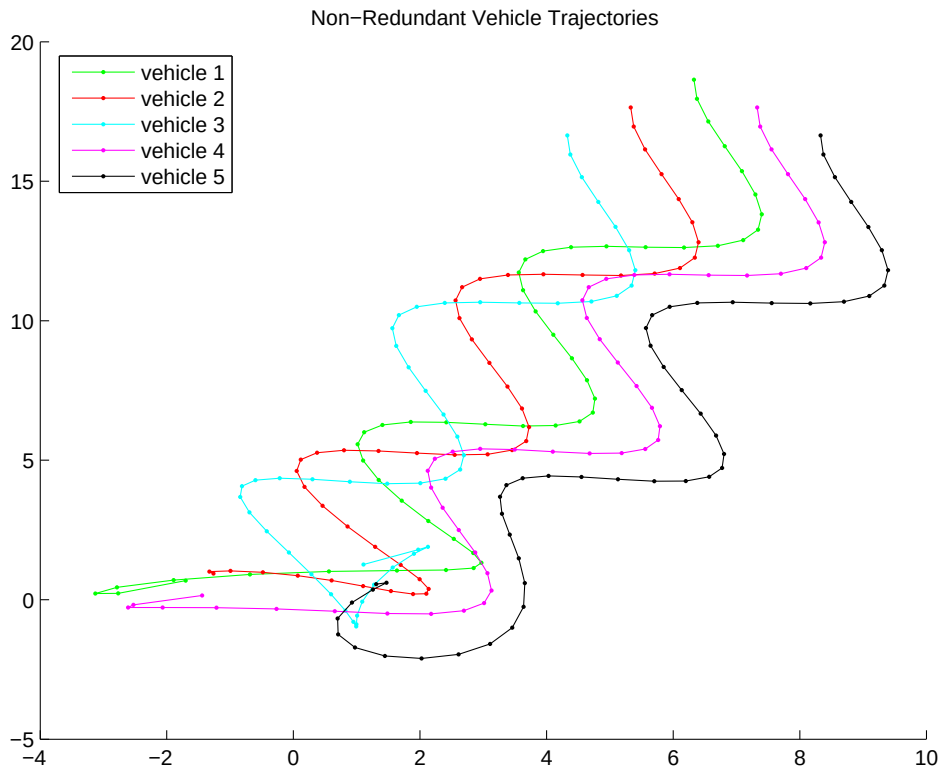

Figure 4.1: Non-Redundant Vehicle Trajectories

We assume a five agent formation with velocities in the x and y directions being

$$\frac{1}{8}\big(1 + 6\sin(\pi k/8)\big) \tag{4.30}$$

and

$$\frac{1}{8}\big(2.5 - 6\sin(\pi k/8)\big) \tag{4.31}$$

respectively.

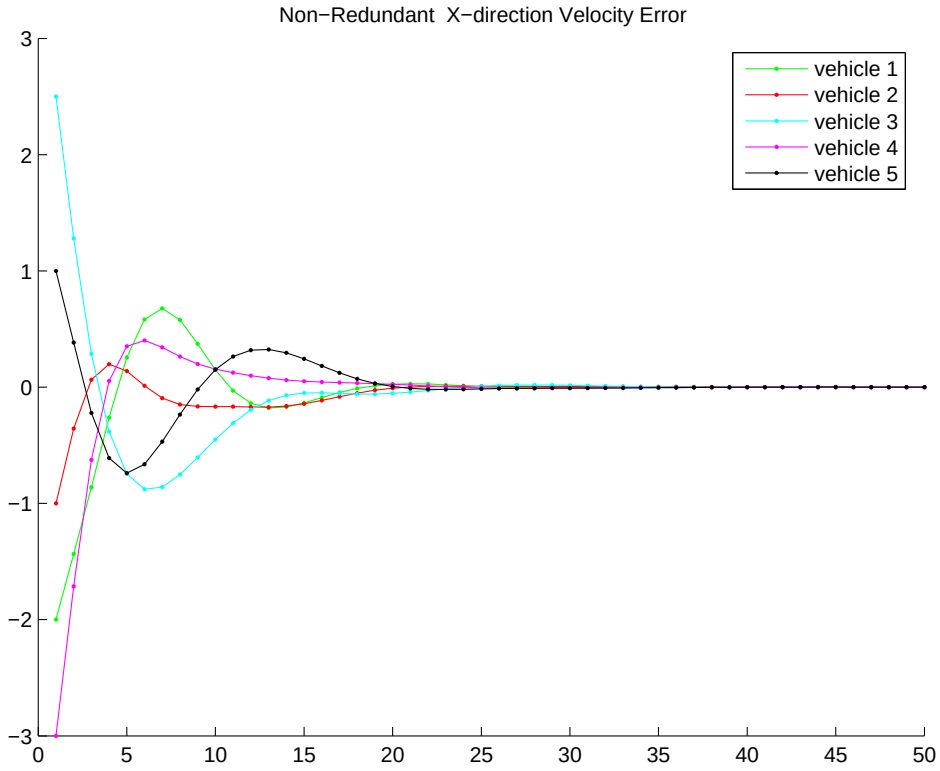

Figure 4.2: Non-Redundant x-Direction Velocity Error

In all the simulations, the initial conditions of the fleet are the same. All simulations are run for 50 samples. Figure 4.1 depicts the trajectory of a formation with the non-redundant formation shown in Figure 1.2.

Figures 4.2 and 4.3 depict the velocity errors in the x and y directions for each agent.

Figure 4.4 depicts the trajectory of a formation with the redundant formation

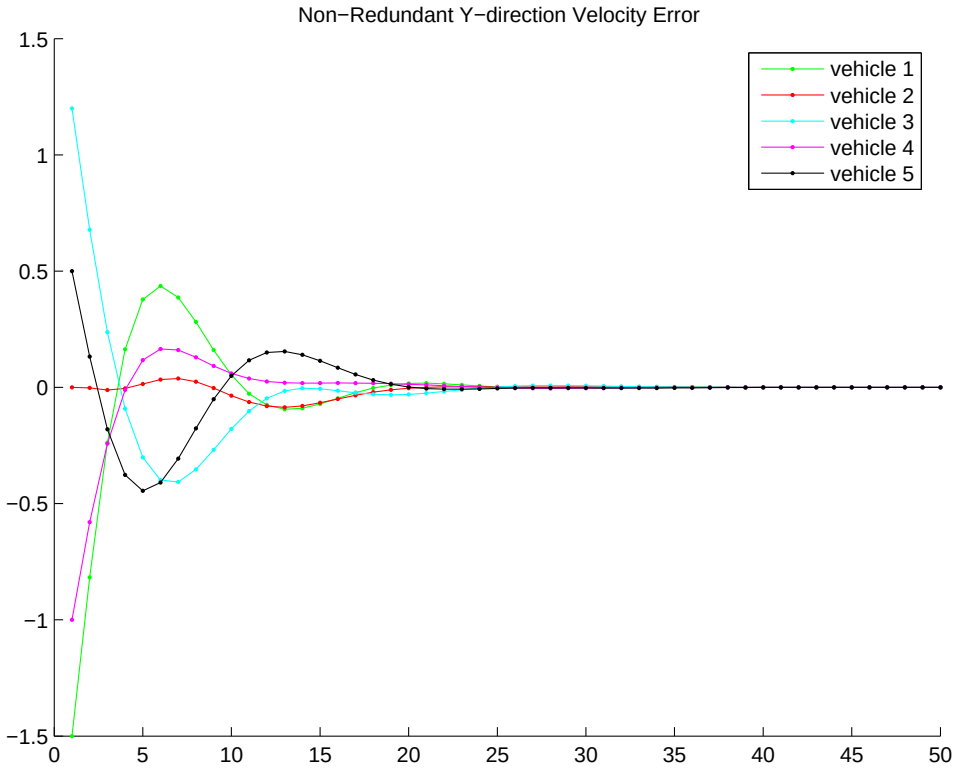

Figure 4.3: Non-Redundant y-Direction Velocity Error

shown in Figure 1.2. Agent 3 drops out of the formation at the 22nd sample. The simulation demonstrates that the formation continues to track despite the loss of the agent.

4.4 Conclusion

In this chapter, we extended the work presented in Chapter 3 to allow the agents to track arbitrary velocities. Using the presented control law, all of the attractive properties presented in Chapter 3 applied, aside from the fact that the agents were required to apply an input force to maintain the dynamic velocity changes. It is important to note; however, that the input force was not used to maintain the relative positions amongst the agents once the formation was attained.

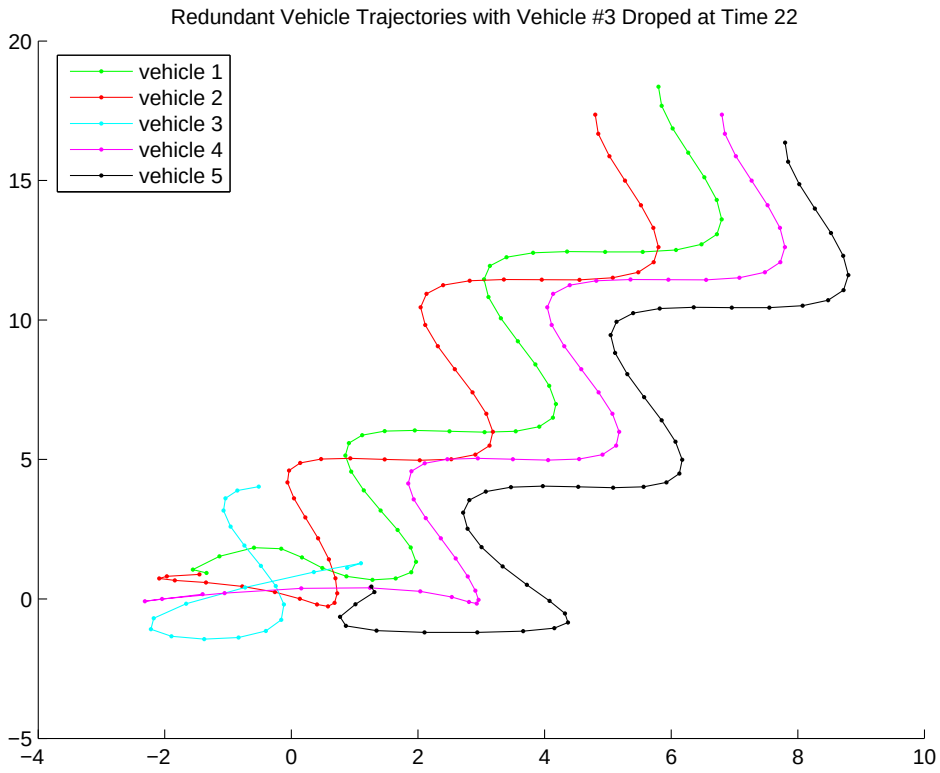

Figure 4.4: Redundant Vehicle Trajectories with Agent 3 Dropped at Time 22

CHAPTER 5
THE EFFECT OF REDUNDANCY UPON THE RATE OF CONVERGANCE

In the previous chapters, a framework was provided that allows for the incorporation of redundancy to allow the network to survive faults caused by loss of agents and/or communication links. In this chapter we will address the impact that redundancy has on the control performance of the control law (3.4) as quantified by the speed with which a desired formation is achieved. It will be shown that when using the control law (3.4), increased redundancy results in better control performance. As mentioned in Section 1.3, this is not always the case with other approaches to formation control. In fact, in some cases increased redundancy can result in instability with other approaches.

In this chapter we will not consider any velocity constraints. This simplifies, slightly, the algebraic representation of the formation topology. Specifically the $\left[\begin{array}{cc} A, & b \end{array}\right]$ pair are simplified as follows:

$$A = \left[\begin{array}{cc} A_p & 0 \end{array}\right] \qquad \text{and} \qquad b = b_p. \tag{5.1}$$

5.1 A Kalman Decomposition

The same cost function (3.1) and resulting control law (3.4) in Section 3.1, with the simplified $\left[\begin{array}{cc} A, & b \end{array}\right]$ pair (5.1) is considered.

A state transformation will be used to allow a more concise presentation of the main result of this chapter. First note that with α chosen to ensure that Q in (3.2) is positive definite, on has that:

$$I - \frac{1}{\alpha}\Gamma^T A^T A \Gamma > 0. \tag{5.2}$$

With

$$F = \Phi - \frac{1}{\alpha}\Gamma\Gamma^T A^T A \Phi \tag{5.3}$$

and

$$G = \frac{1}{\alpha}\Gamma\Gamma^T A^T b \tag{5.4}$$

the closed loop control law becomes

$$x(k+1) = Fx(k) + G. \tag{5.5}$$

Define

$$y(k) = Ax(k) - b. \tag{5.6}$$

Now consider a singular value decomposition (SVD) of A_p:

$$A_p = UDV. \tag{5.7}$$

In view of (2.9) and Assumptions 2.2.1 and 2.3.1, U is a $2L_p \times 2L_p$ unitary matrix, V is a $2N \times 2N$ unitary matrix and D is as defined below:

$$D = \begin{bmatrix} \Delta & 0 \\ 0 & 0 \end{bmatrix}. \tag{5.8}$$

With $n_1 = 2N - 2$, Δ is diagonal, $n_1 \times n_1$ and real positive definite.

Observe that the double integrator dynamics of the agents, coupled with the lack of velocity constraints and the fact that the rank of A is $2N-2$, ensures that four eigenvalues of F are guaranteed to be **1**. The point of the Kalman decomposition developed in this section is to: *(i)* demonstrate that these eigenvalues are not poles of $A(zI - F)^{-1}$, and *(ii)* to isolate the poles that can be made stable. Define

$$S = \begin{bmatrix} V & 0 \\ 0 & V \end{bmatrix} \tag{5.9}$$

Then consider the state transformation described in the lemma below.

Lemma 5.1.1 *With Φ, Γ, A, b, F, G, U, V, D and S defined in (2.6), (2.7), (2.13), (5.3), (5.4), and (5.7 - 5.9) define:*

$$\widehat{A} = \begin{bmatrix} U \begin{bmatrix} \Delta & 0 \\ 0 & 0 \end{bmatrix} & 0 \end{bmatrix} \tag{5.10}$$

$$\widehat{F} = \Phi - \frac{1}{\alpha}\Gamma\Gamma^T \widehat{A}^T \widehat{A}\Phi \tag{5.11}$$

$$\widehat{G} = \frac{1}{\alpha}\Gamma\Gamma^T \widehat{A}^T b \tag{5.12}$$

$$\widehat{x}(k) = Sx(k) \tag{5.13}$$

Then one has that

$$\widehat{x}(k+1) = \widehat{F}\widehat{x}(k) + \widehat{G} \tag{5.14}$$

$$y(k) = \widehat{A}\widehat{x}(k) - b \tag{5.15}$$

and

$$\widehat{A} = AS^{-1}. \tag{5.16}$$

Proof: First note that

$$\begin{aligned} AS^{-1} &= \begin{bmatrix} A_p & 0 \end{bmatrix} \begin{bmatrix} V^H & 0 \\ 0 & V^H \end{bmatrix} \\ &= \begin{bmatrix} A_p V^H & 0 \end{bmatrix} \\ &= \begin{bmatrix} U \begin{bmatrix} \Delta & 0 \\ 0 & 0 \end{bmatrix} & 0 \end{bmatrix} \\ &= \widehat{A} \end{aligned} \tag{5.17}$$

Further in view of (5.9) and (5.17)

$$\begin{aligned} SFS^{-1} &= S\left(I - \tfrac{1}{\alpha}\Gamma\Gamma^T A^T A\right)\Phi S^{-1} \\ &= \widehat{F} \end{aligned} \tag{5.18}$$

and similarly,

$$\begin{aligned} SG &= \tfrac{1}{\alpha} S\Gamma\Gamma^T A^T b \\ &= \widehat{G} \end{aligned} \tag{5.19}$$

■

We next show that a condition comparable to (5.2) holds.

Lemma 5.1.2 *With $\widehat{A}$ as defined in (A.21)*

$$I - \frac{1}{\alpha}\Gamma^T \widehat{A}^T \widehat{A}\Gamma > 0 \tag{5.20}$$

Proof: Follows from (5.17), the fact that

$$\left(V\Lambda^{\frac{1}{2}}\right)\Lambda^{-\frac{1}{2}}V^H = I, \tag{5.21}$$

and

$$V\Lambda^{\frac{1}{2}}\Gamma^T = \Gamma^T S \text{ and that } \Gamma\Lambda^{-\frac{1}{2}}V^H = S^{-1}\Gamma \tag{5.22}$$

■

Denoting 0_p to be the $p \times p$, zero matrix, and I_p to be the $p \times p$, identity matrix, we observe from (5.8) and (A.21) that

$$\begin{aligned}
\widehat{F} &= SFS^{-1} \\
&= S \begin{bmatrix} I - \frac{1}{\alpha} A_p^T A_p & I - \frac{1}{\alpha} A_p^T A_p \\ -\frac{2}{\alpha} A_p^T A_p & I - \frac{2}{\alpha} A_p^T A_p \end{bmatrix} S^{-1} \\
&= \begin{bmatrix} I - \frac{1}{\alpha} V A_p^T A_p V^H & I - \frac{1}{\alpha} V A_p^T A_p V^H \\ -\frac{2}{\alpha} V A_p^T A_p V^H & I - \frac{2}{\alpha} V A_p^T A_p V^H \end{bmatrix} \qquad (5.23) \\
&= \begin{bmatrix} I - \frac{1}{\alpha}\Delta^2 & 0 & I - \frac{1}{\alpha}\Delta^2 & 0 \\ 0 & I_2 & 0 & I_2 \\ -\frac{2}{\alpha}\Delta^2 & 0 & I - \frac{2}{\alpha}\Delta^2 & 0 \\ 0 & 0_2 & 0 & I_2 \end{bmatrix}
\end{aligned}$$

Then the following lemma goes toward a Kalman like decomposition.

Lemma 5.1.3 *Under (5.7-5.15)*

$$\widehat{A}\left(zI - \widehat{F}\right)^{-1} = \begin{bmatrix} H(z) & 0_{2L \times 2(n-n_1)} \end{bmatrix} \qquad (5.24)$$

where

$$H(z) = C\left(zI - \Upsilon\right)^{-1}, \qquad (5.25)$$

$$\Upsilon = \begin{bmatrix} I - \frac{1}{\alpha}\Delta^2 & I - \frac{1}{\alpha}\Delta^2 \\ -\frac{2}{\alpha}\Delta^2 & I - \frac{2}{\alpha}\Delta^2 \end{bmatrix} \qquad (5.26)$$

$$C = \begin{bmatrix} U \begin{bmatrix} \Delta \\ 0 \end{bmatrix} & 0_{2L \times n_1} \end{bmatrix} \qquad (5.27)$$

and

$$\Pi = \begin{bmatrix} I_{n_1} & 0 & 0 & 0 \\ 0 & 0 & I_{n_1} & 0 \\ 0 & I_{n-n_1} & 0 & 0 \\ 0 & 0 & 0 & I_{n-n_1} \end{bmatrix} \tag{5.28}$$

Proof: Note

$$\Pi^T \Pi = I. \tag{5.29}$$

Hence

$$\widehat{A}\left(zI - \widehat{F}\right)^{-1} = \widehat{A}\Pi^T \left[zI - \Pi\widehat{F}\Pi^T\right]^{-1} \Pi. \tag{5.30}$$

Now,

$$\begin{aligned} \widehat{A}\Pi^T &= \begin{bmatrix} U \begin{bmatrix} \Delta \\ 0 \end{bmatrix} & 0_{2L\times n-n_1} & 0_{2L\times n} \end{bmatrix} \begin{bmatrix} I_{n_1} & 0 & 0 & 0 \\ 0 & 0 & I_{n-n_1} & 0 \\ 0 & I_{n_1} & 0 & 0 \\ 0 & 0 & 0 & I_{n-n_1} \end{bmatrix} \\ &= \begin{bmatrix} U \begin{bmatrix} \Delta \\ 0 \end{bmatrix} & 0_{2L\times n_1} & 0_{2L\times 2(n-n_1)} \end{bmatrix} \\ &= \begin{bmatrix} C & 0_{2L\times 2(n-n_1)} \end{bmatrix} \end{aligned} \tag{5.31}$$

Further, from (5.23)

$$\begin{aligned} \Pi\widehat{F}\Pi^T &= \begin{bmatrix} I - \frac{1}{\alpha}\Delta^2 & I - \frac{1}{\alpha}\Delta^2 & 0 & 0 \\ -\frac{2}{\alpha}\Delta^2 & I - \frac{2}{\alpha}\Delta^2 & 0 & 0 \\ 0 & 0 & I_{n-n_1} & I_{n-n_1} \\ 0 & 0 & 0 & I_{n-n_1} \end{bmatrix} \\ &= \begin{bmatrix} \Upsilon & 0 \\ 0 & \begin{bmatrix} I_{n-n_1} & I_{n-n_1} \\ 0 & I_{n-n_1} \end{bmatrix} \end{bmatrix}. \end{aligned} \tag{5.32}$$

Then the result follows. ■

Taken together, the results of this section show that the poles of $A(zI - F)^{-1}$ are in fact the eigenvalues of Υ. The next section shows that *(i)* these can be made stable, and *(ii)* that their magnitudes determine that rate of convergence.

5.2 Rates of Convergence

To ease notation call

$$B = \frac{1}{\alpha}\Delta^2 \tag{5.33}$$

and Note that:

$$0 < \lambda(B) < 1 \tag{5.34}$$

Then:

$$\Upsilon = \begin{bmatrix} I - B & I - B \\ -2B & I - 2B \end{bmatrix} \tag{5.35}$$

Recall that the poles of $A(zI - F)^{-1}$ are in fact the eigenvalues of Υ. Assume for the moment that all of the eigenvalues of Υ are in the open unit disc. Further under Assumption 2.3.1 there exists an x such that

$$Ax = b. \tag{5.36}$$

Thus using (2.6), (2.7), (5.3) and (5.4) and using the fact that

$$\Phi \begin{bmatrix} x \\ 0 \end{bmatrix} = \begin{bmatrix} x \\ 0 \end{bmatrix}, \tag{5.37}$$

we obtain

$$\begin{aligned}
\lim_{k\to\infty}(Ax(k)-b) &= \lim_{z\to 1}(z-1)\tfrac{A(zI-F)^{-1}G-b}{z-1} \\
&= \lim_{z\to 1}\left(A(zI-F)^{-1}G-b\right) \\
&= \lim_{z\to 1}\left(A(zI-F)^{-1}\tfrac{\Gamma\Gamma^T A^T A}{\alpha}\begin{bmatrix} x \\ 0 \end{bmatrix}\right) - A\begin{bmatrix} x \\ 0 \end{bmatrix} \\
&= \lim_{z\to 1} A\left((zI-F)^{-1}\tfrac{\Gamma\Gamma^T A^T A}{\alpha} - I\right)\begin{bmatrix} x \\ 0 \end{bmatrix} \\
&= \lim_{z\to 1} A(zI-F)^{-1}\left(\tfrac{\Gamma\Gamma^T A^T A}{\alpha} - I + F\right)\begin{bmatrix} x \\ 0 \end{bmatrix} \\
&= 0.
\end{aligned}$$

This analysis reveals two facts. First, should all eigenvalues of Υ be inside the unit circle then the formation is attained. Second, the deeper inside the unit circle these eigenvalues are, the faster the rate of convergence. In the sequel we tie the magnitude of these eigenvalues to the redundancy in the network. In particular, observe that the edges in the formation topology completely determine the matrix A, and hence Υ. For a formation topology described by the undirected graph $G = (V, E)$, we will define the corresponding A matrix as $A(G)$ and the B in (5.33) as $B(G)$. Then the following lemma is crucial.

Lemma 5.2.1 *Consider the formation topologies with associated undirected graphs* $G_1 = (V, E_1)$ *and* $G_2 = (V, E_2)$. *Suppose* $E_1 \subset E_2$. *Then*

$$B(G_1) \leq B(G_2). \tag{5.38}$$

Proof: Associate with an undirected edge between i and j the vector e_{ij} the $2N$-vector all but the i and jth elements of which are zero. One of the remaining elements is 1 and the other -1. Then,

$$A(G_2)^T A(G_2) = A(G_1)^T A(G_1) + \sum_{\{i,j\}\in E_2 - E_1} e_{ij} e_{ij}^T \tag{5.39}$$

Thus

$$A(G_2)^T A(G_2) \geq A(G_1)^T A(G_1). \tag{5.40}$$

Thus the result follows from the definition $B(G_i)$. ∎

Now observe that with $B = \text{diag}(b_i)$, within a symmetric perturbation one can express

$$\Upsilon = \bigoplus_{i=1}^{2N-2} \Upsilon_{ii} \tag{5.41}$$

where

$$\Upsilon_{ii} = \begin{bmatrix} 1-b_i & 1-b_i \\ -2b_i & 1-2b_i \end{bmatrix}. \tag{5.42}$$

The characteristic polynomial of each Υ_{ii} is

$$\lambda^2 - (2-3b_i)\lambda + (1-b_i). \tag{5.43}$$

Observe that as long as

$$0 < b_i < 8/9, \tag{5.44}$$

both the eigenvalues of Υ_{ii} are complex with magnitude $1-b_i$. Thus as long as (5.44) holds increasing b_i forces the eigenvalues further inside the unit circle. On the other hand in the range $b_i \in [8/9, 1)$, recall from (5.34) $0 < b_i < 1$, as b_i increases, one eigenvalue of Υ_{ii} approaches $\mathbf{0}$, while the other approaches $\mathbf{1}$. This leads us to the main result of this chapter.

Theorem 5.2.1 *Consider the two formation topologies with associated undirected graphs $G_1 = (V, E_1)$ and $G_2 = (V, E_2)$. Suppose $E_1 \subset E_2$. Suppose also that for each $i \in \{1, 2\}$,*

$$\alpha I - \frac{9A^T(G_i)A(G_i)}{8} \geq 0. \tag{5.45}$$

Then (3.4) converges for both topologies but at a faster rate for G_2.

Proof: Recall, through the construction of B, that B is a positive definite diagonal matrix whose diagonal elements contain the non-zero eigenvalues of $A_p^T A_p$ divided by α. Equation (5.45) can be rewritten:

$$\frac{8}{9} I \geq \frac{1}{\alpha} A^T(G_i)A(G_i)$$

Therefore $0 < \lambda(B(G_i)) \leq \frac{8}{9}$. Then result follows from Lemma 5.2.1 and (5.41) - (5.43). ∎

Therefore, depending on the value of α, a more redundant network will lead to

a faster convergence. The way to interpret the cutoff point of 8/9 is as follows. Too dense a network will cause the positive definiteness of Q to be violated. Thus given an α, the performance improves monotonically up to a clearly demarcated level of redundancy, but degrades thereafter.

5.3 Simulation Results

Here we show some simulations which verify the results of Theorem 5.2.1. The trajectories of the agents in a non-redundant formation, as in Figure 1.2, are shown in Figure 5.1. The agents initial positions are chosen randomly, but the same random initial positions are used in all of the presented figures. In Figure 5.2 the formation topology is completely connected.

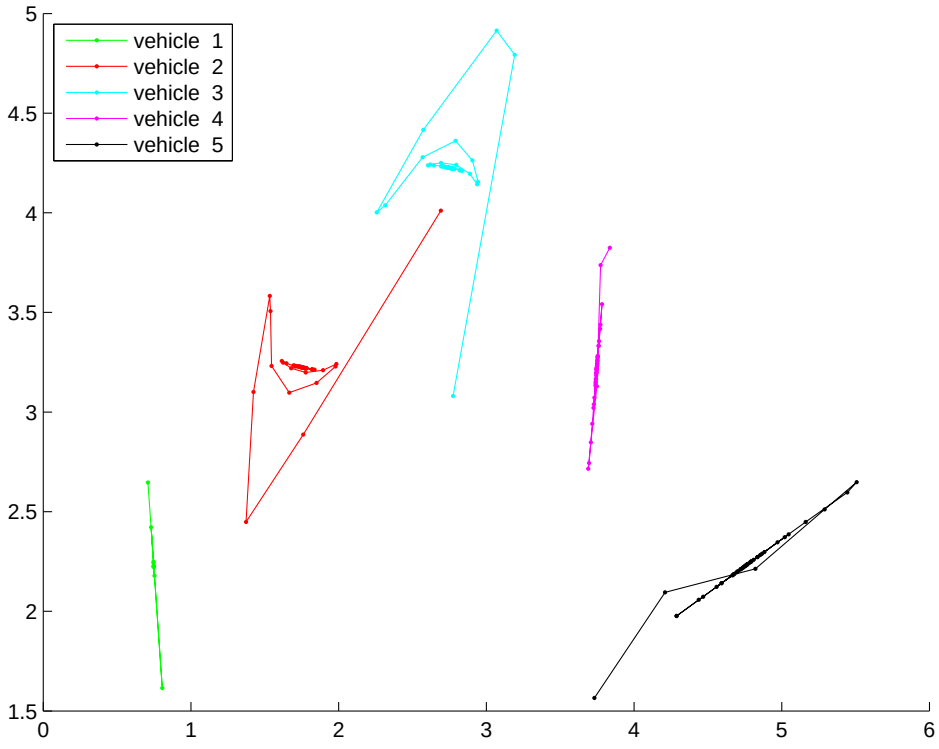

Figure 5.1: Non-Redundant Vehicle Trajectory

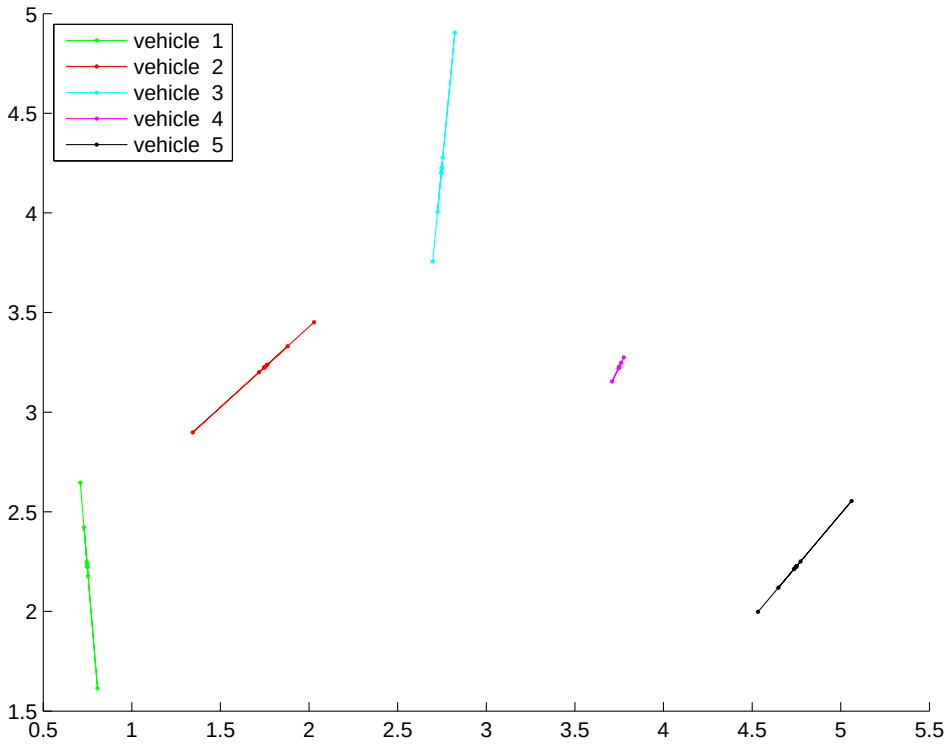

Figure 5.2: Fully Connected Vehicle Trajectory

The relative position errors, measured by $\|Ax(k) - b\|_2$, are shown in Figure 5.3. In this figure, simulation 1 represents a non-redundant formation. Redundancy is added as the simulations numbers increase until we reach the fully connected formation topology in simulation 6. As demonstrated, a more redundant network leads to a faster convergence.

5.4 Conclusion

We have examined the cooperative control of a fleet of autonomous agents that achieve arbitrary relative positions from random starting positions. We have revisited the control law (3.4) to show that not only does increased connectivity among the agents result in better robustness to loss of agents, but that up to a clearly

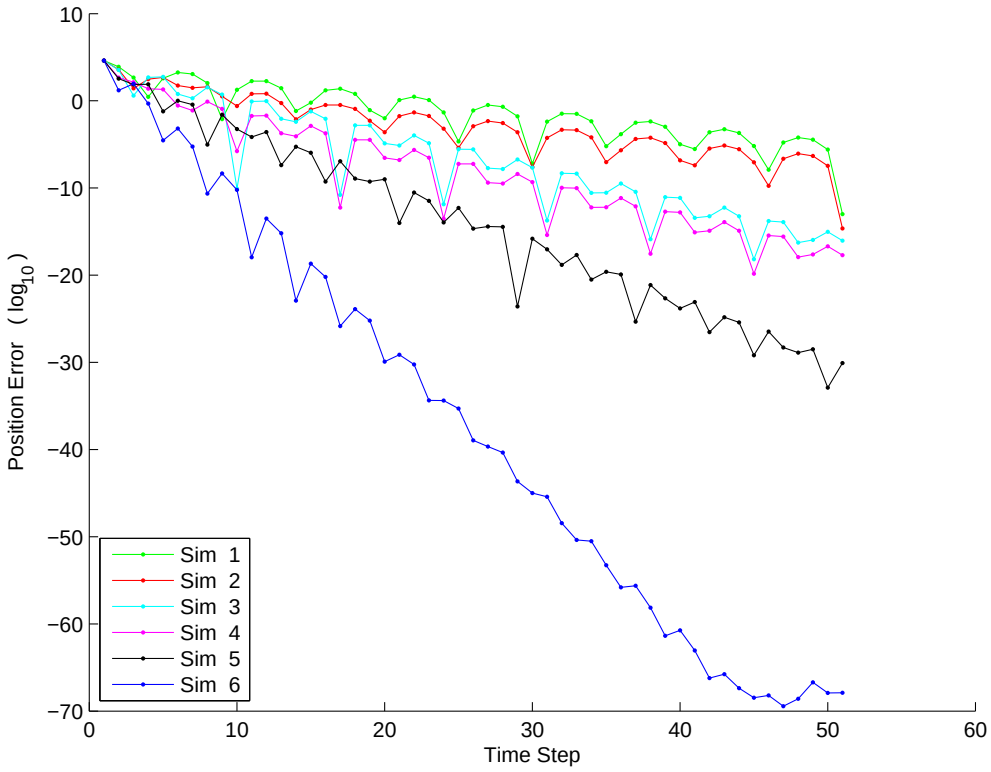

Figure 5.3: Convergence Rates

quantifiable point it also results in faster convergence to the desired formation.

CHAPTER 6
FORMATION CONTROL WITH ENHANCED SCALABILITY

In this chapter an alternate control law is presented which results in enhanced scalability and better overall performance. Recall, in Chapter 3, Λ was chosen as

$$\Lambda = \alpha I. \tag{6.1}$$

With this choice in Λ, it was shown that stability is guaranteed when Q is positive definite. Thus, α was chosen to exceed the largest eigenvalue of $\Gamma^T A^T A \Gamma$.

Definition 6.0.1 *Define e_{ij} as a vector with length N, with all elements equal to 0 except the ith and jth elements which are 1 and -1 respectively.*

Observe from Assumption 2.2.1 that

$$A_{ps}^T A_{ps} = \sum e_{ij} e_{ij}^T. \tag{6.2}$$

Consequently as the size of the network grows, in terms of either the number of nodes or the number of constraints, the largest eigenvalue of $\Gamma^T A^T A \Gamma$ grows correspondingly. Therefore, if one were to select (6.1) as done in Chapter 3, one would have to anticipate the largest network one is likely to confront. If, in the course of actual operation, the network undergoes large variation in size, then such a worst case design leads to poor performance since α penalizes the control input. Alternatively, α could be chosen dynamically by the agents in the formation, but this approach leads to the global exchange and thus poor scalability results.

6.1 Basic Control

A basic fixed velocity formation is considered. Thus the L_p position constraints will be specified by the $\left[\begin{array}{cc} A_p, & b_p \end{array} \right]$ pair as described in (2.9) and Assumption 2.2.1. Suppose we wish to assign the the fixed velocity to L_v agents and that the velocity in the x and y directions is v_x and v_y respectively. The L_v velocity constraints are defined by the $\left[\begin{array}{cc} A_v, & b_v \end{array} \right]$ pair as described in (2.10) and Assumption 6.1.1.

Assumption 6.1.1 *Consider a set of agents $\mathcal{V} \in \{1, \ldots, N\}$ with cardinality L_v.*

For each agent $i \in \mathcal{V}$ there will be a row in A_{vs} containing all zeros except the ith element which will contain a 1. A_v will defined as in (2.10) and the first L_v elements of b_v will contain the velocity in the x direction, v_x, while the last L_v elements of b_v will contain the velocity in the y direction, v_y.

6.2 Control Law and Communication Topology

Using the same cost function (3.1) and resulting control law (3.4) as in Section 3.1, we will modify the definition of Λ in Q (3.2) to account for the agent's individual velocity constraints and connectivity instead of the global solution, αI.

Suppose p_i is the number of connections for agent i. Then define:

$$\lambda_i = \epsilon + \beta p_i \tag{6.3}$$

with some $\epsilon > 0$ and $\beta \geq 2$. The individual contribution of the connectivity of agent i in $\Gamma^T A^T A \Gamma$ will be counteracted by λ_i. With:

$$\Lambda_{ps} = \text{diag}\,(\lambda_i) \tag{6.4}$$

and $\Lambda_p = \Lambda_{ps} \oplus \Lambda_{ps}$, Λ_p will represent the connectivity portion of Λ, while the velocity contribution will be represented by Λ_v, as shown below:

$$\Lambda = \Lambda_p + \Lambda_v \tag{6.5}$$

where, $\Lambda_v = \Lambda_{vs} \oplus \Lambda_{vs}$. With Assumption 6.1.1, the velocity contribution to Λ can be defined as follows:

$$\Lambda_{vs} = 4A_{vs}^T A_{vs}. \tag{6.6}$$

Lemma 6.2.1 *Under (6.3)-(6.6) and Assumptions 2.3.1 and 6.1.1,* $\Lambda - \Gamma^T A^T A \Gamma > 0$.

Proof: Note that:

$$\Lambda - \Gamma^T A^T A \Gamma = I_2 \otimes \left(\Lambda_{ps} - A_{ps}^T A_{ps}\right) \tag{6.7}$$

Therefore, it suffices to show that: $\Lambda_{ps} - A_{ps}^T A_{ps} > 0$. The proof follows from the fact that

$$(\beta + \epsilon) I - \begin{bmatrix} 1 \\ \\ -1 \end{bmatrix} \begin{bmatrix} 1, & -1 \end{bmatrix} > 0. \tag{6.8}$$

■

Now we will show that the communication topology resulting from (3.4) is identical to the geometric topology and further that only a local knowledge of the formation topology is required by each agent. Observe that the control inputs to agent i are u_i and u_{i+N}. We will now show that if agents i and j do not have an arc between them in the formation topology, then u_i and u_{i+N} do not depend on $\{\Phi x\}_j, \{\Phi x\}_{j+N}, \{\Phi x\}_{j+2N}$ and $\{\Phi x\}_{j+3N}$. Because of Fact 2.1.1, this in turn implies that u_i and u_{i+N} do not depend on x_j, x_{j+N}, x_{j+2N} and x_{j+3N}, establishing the structure of the communication topology. *Furthermore observe that agent i can select λ_i by knowing the number of constraints it is involved in.* As Theorem 6.2.1 shows and is evident from (3.4) and the fact that Λ is a diagonal matrix, λ_i is only needed by agent i to construct its input.

Fact 6.2.1 *Due to the construction of Λ in (6.3)-(6.6) and Assumption 6.1.1, Λ is a diagonal matrix.*

Observe that (3.4) becomes,

$$u(k) = \Lambda^{-1}\left(A_p^T b_p + 2A_v^T b_v - [A_p^T A_p, 2A_v^T A_v]\Phi x(k)\right) \tag{6.9}$$

Theorem 6.2.1 *Consider (6.9) under (2.3), (2.6), (2.7), and (2.13). Then the finding $u_i(k)$ and $u_{i+N}(k)$ requires:*

(i) The states of agent l only if there is an arc between agents l and i in the formation topology.

(ii) The l-th row of A only if for some $j \in \{i, i+N, i+2N, i+3N\}$ $a_{lj} \neq 0$.

(iii) The l-th element of b only if for some $j \in \{i, i+N, i+2N, i+3N\}$ $a_{lj} \neq 0$.

(iv) The gain λ_i if the agent has no velocity constraints, or the gain $\lambda_i + 4$ if the agent has velocity constraints.

Proof: Consider the determination of u_p, $p \in \{i, i+N\}$. Suppose this requires the knowledge of Φx_q, for some $q \in \{l, l+N\}$. Then from (6.9) and Fact 6.2.1,

$\left(A_p^T A_p\right)_{pq}$ is non zero. Then because of Lemma 3.1.1 for at least one m the m-th row of A_p must have nonzero entries in both the p-th and the q-th locations. Similarly if the determination of u_p, $p \in \{i, i+N\}$ requires the knowledge of Φx_q, for some $q \in \{l+2N, l+3N\}$, then for at least one m the m-th row of A_v has nonzero entries in both the p-th and the q-th locations. Then Facts 2.1.1, 2.2.1 and 6.2.1, together with (2.13) prove *(i)*.

Now, from (6.9) and Fact 6.2.1, the computation of u_p, $p \in \{i, i+N\}$ requires the computation of the p-th rows of $A_p^T A_p$ and $A_v^T A_v$ and the p-th elements of $A_p^T b_p$ and $A_v^T b_v$. Then from Lemma 3.1.1, for such a p, the computation of the p-th rows of $A_p^T A_p$ and $A_v^T A_v$ require respectively, the knowledge of the l-th rows of A_p and A_v only if the lp-th elements of respectively A_p and A_v are nonzero. Further the p-th elements of $A_p^T b_p$ and $A_v^T b_v$ require the knowledge of l-th rows of A_p and A_v and/or the l-th elements of b_p and b_v only if the lp-th elements of respectively A_p and A_v are nonzero. Then *(ii)* and *(iii)* follow from (2.3), (2.13) and Facts 2.1.1 and 6.2.1.

Finally, *(iv)* follows from Fact 6.2.1 and the construction of Λ in (6.3)-(6.6). ■

(i) shows that the communication topology is the same as the formation topology. *(ii)* and *(iii)* show that agent i need only know those rows of A and elements of b which define the arcs emanating from it. Thus agent i must only know its place in the formation topology. Therfore a described knowledge of the formation topology suffices.

If despite the loss of an agent, for example agent 4 in Figure 1.3, the formation topology remains viable, then this modified formation topology is described by an $\left[\begin{array}{cc} A, & b \end{array}\right]$ matrix that is a sub-matrix of its counterpart in the original formation topology, and obtained by removing the rows characterizing the two arcs impacting 4 and the four columns of A corresponding to the states of 4. As the elements of these columns in the rows of the original A matrix defining the arcs of 2 and 3 are zero, the inputs to agents 2 and 3 are unchanged. These agents do not need to reconfigure

their control laws and need not know about the loss. Similarly if communication between 1 and 5 be impaired or lost, then only 1 and 5 must know of this loss and adjust their control law.

Let us now turn to the significance of *(iv)* to scalability. Suppose a new agent arrives and attaches itself to a subset of the agents in the network. Then to ensure that $\Lambda - \Gamma^T A^T A \Gamma$ is positive definite, these agents simply need to adjust their corresponding λ_i to account for the new arcs created in the formation topology. The remaining agents need not adjust the λ_i they are responsible for and consequently need not adjust their control law. As importantly, the need to *a priori* choose α, as in Chapter 3, to accommodate the largest possible network is removed.

6.3 Proof of Stability

In this section we prove that the control law in (3.4) asymptotically attains all viable formation topologies as long as

$$I - \Lambda^{-1}\Gamma^T A^T A \Gamma > 0 \tag{6.10}$$

To this end observe that with

$$F = \Phi - \Gamma\Lambda^{-1}\Gamma^T A^T A \Phi \tag{6.11}$$

and

$$G = \Gamma\Lambda^{-1}\Gamma^T A^T b \tag{6.12}$$

the control law (3.4) results in the closed loop

$$x(k+1) = Fx(k) + G. \tag{6.13}$$

Define

$$y(k) = Ax(k) - b. \tag{6.14}$$

We need to find conditions under which $y(k)$ asymptotically approaches zero. To this end we first provide the following lemma.

Lemma 6.3.1 *Under (6.10), with F and G defined in (6.11), (6.12), (6.3)-(6.6), (2.6), (2.7) and A in (2.13), all poles of $A(zI - F)^{-1}$ are inside the unit circle.*

Proof: The detailed proof is in Appendix B.1 and is comprised of two parts. In the first we show that (6.10) ensures that the poles of F are either at 1 or inside the unit circle. The second part shows that the poles at 1 are unobservable through A.

■

This brings us to the main result of this section.

Theorem 6.3.1 *Suppose the formation topology is viable and $A_p \neq 0$. Then*

$$\lim_{k\to\infty} Ax(k) = b$$

Proof: We need to show that

$$R(z) = \frac{z-1}{z}\left[A(zI-F)^{-1}x(0) + A(zI-F)^{-1}G\frac{z}{z-1} - b\frac{z}{z-1}\right] \tag{6.15}$$

is analytic on or inside the unit circle and

$$\lim_{z\to 1} R(1) = 0 \tag{6.16}$$

Because of Lemma 6.3.1, $A(zI-F)^{-1}$ and hence $R(z)$ is analytic on or outside the unit circle. Thus it suffices to show that

$$\lim_{z\to 1}\left[A(zI-F)^{-1}G - b\right] = 0 \tag{6.17}$$

Since the formation topology is viable there exists an x as in (2.3) that satisfies the constraints imposed by Theorem 2.3.1. For such an x and all nonnegative integer l, from Theorem 2.3.1, we have

$$A\Phi^l\begin{bmatrix} x_v \\ 0 \end{bmatrix} = \begin{bmatrix} A_p & 0 \\ 0 & A_v \end{bmatrix}\begin{bmatrix} I & lI \\ 0 & I \end{bmatrix}\begin{bmatrix} x_v \\ 0 \end{bmatrix} = A_p x_v = 0 \tag{6.18}$$

Further for such an x an all nonnegative integer m, we have from (5.3) and (6.18) that

$$AF^m\begin{bmatrix} x_v \\ 0 \end{bmatrix} = AF^{m-1}\left[I - \Gamma\Lambda^{-1}\Gamma^T A^T A\right]\Phi\begin{bmatrix} x_v \\ 0 \end{bmatrix} = AF^{m-1}\Phi\begin{bmatrix} x_v \\ 0 \end{bmatrix} \tag{6.19}$$

Thus by induction and (6.18) for all nonnegative integer m

$$AF^m\begin{bmatrix} x_v \\ 0 \end{bmatrix} = A\Phi^m\begin{bmatrix} x_v \\ 0 \end{bmatrix} = 0. \tag{6.20}$$

Since $A\Phi^m x = b$ for all nonnegative integer m,

$$\lim_{z\to 1} A(zI-F)^{-1}G - b$$

$$= \lim_{z\to 1} A(zI-F)^{-1}G - Ax$$

$$= \lim_{z\to 1} \left[A(zI-F)^{-1}\{G-(zI-F)x\}\right]$$

$$= \lim_{z\to 1} \left[A(zI-F)^{-1}\{\Gamma\Lambda^{-1}\Gamma^T A^T b - zx + \Phi x - \Gamma\Lambda^{-1}\Gamma^T A^T A\Phi x\}\right]$$

$$= \lim_{z\to 1} \left[A(zI-F)^{-1}\left\{\Gamma\Lambda^{-1}\Gamma^T A^T Ax - x + \Phi x - \Gamma\Lambda^{-1}\Gamma^T A^T A\left(x + \begin{bmatrix} x_v \\ 0 \end{bmatrix}\right)\right\}\right] \tag{6.21}$$

$$= \lim_{z\to 1} \left[A(zI-F)^{-1}\{\Phi x - x\}\right]$$

$$= \lim_{z\to 1} \left[A(zI-F)^{-1}\begin{bmatrix} x_v \\ 0 \end{bmatrix}\right]$$

We will now show that in fact

$$A(zI-F)^{-1}\begin{bmatrix} x_v \\ 0 \end{bmatrix} = 0 \tag{6.22}$$

almost every where. Thus as it is rational it is zero everywhere including at $z = 1$.

Indeed in the region of convergence of $(zI - F)^{-1}$.

$$\begin{aligned} A(zI-F)^{-1}\begin{bmatrix} x_v \\ 0 \end{bmatrix} &= Az^{-1}(I-z^{-1}F)^{-1}\begin{bmatrix} x_v \\ 0 \end{bmatrix} \\ &= [Az^{-1} + z^{-1}\textstyle\sum_{i=1}^{\infty} z^{-i}AF^i]\begin{bmatrix} x_v \\ 0 \end{bmatrix} \\ &= z^{-1}\textstyle\sum_{i=1}^{\infty} z^{-i}AF^i\begin{bmatrix} x_v \\ 0 \end{bmatrix} \\ &= 0 \end{aligned} \tag{6.23}$$

where the last equality follows from (6.19). ■

Thus this distributed control law helps attain and maintain all viable formation topologies. Three implications of this result bear reiteration. First, the necessary conditions for viablity given in Theorem 2.3.1 are all that are invoked in the proof of Theorem 6.3.1. Thus these necessary conditions are also sufficient for viability. Second, it is easily seen from the proof of Theorem 6.3.1 that in fact

$$\lim_{k\to\infty} u(k) = 0.$$

In other words once the formation is attained it can be maintained with no control input. Finally, and more compellingly, the class of formation topology under consideration here has the attractive property that a distributed control law for its achievement exists, as long as a centralized law exists. Thus whatever can be done through global action can also be achieved through local action, and as importantly through local knowledge of the overall objective.

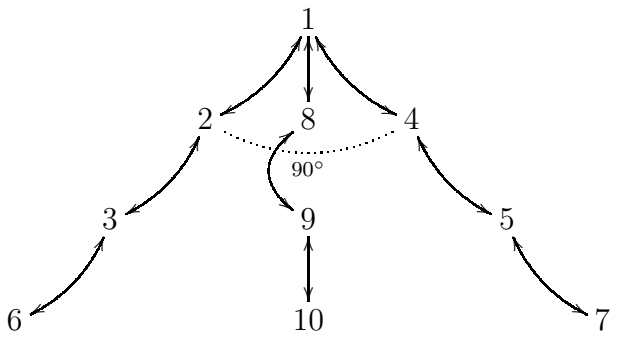

Figure 6.1: 10 Agent Formation Topology with no Redundancy

6.4 Simulation Results

The following simulations compare the convergence rates of the limited scalability approach presented in Chapter 3 to enhanced scalability approach presented in this chapter, when the size of the formation changes significantly during the simulation. All simulations assume a fully connected formation topology with velocity constraints on agents 1, 2 and 4.

In Figure 6.2 a fully connected 10 agent formation topology is considered. The basic shape of the formation is shown in Figure 6.1. This simulation was used to choose α in equation (3.3) and ϵ in equation (6.3) such that the formations are stable and the convergence rates for the limited scalability approach and the enhanced scalability are comparable. Notice that α was chosen such that the limited scalability approach slightly outperforms the enhanced scalability approach.

Figures 6.3-6.5 use the values for α and ϵ found in the simulation used create Figure 6.2. Additionally, vehicles 1-5 start with the same initial positions and velocities used in Figure 6.2. The simulations start using a 5-agent, fully connected formation topology with the basic shape shown in Figure 1.2. At time $k = 21$, agents 6-10 join the formation following the same basic shape shown in Figure 6.1. The initial positions for these agents are the same as those used in Figure 6.2, except shifted to compensate for the trajectories of the other agents during the first 20 time steps.

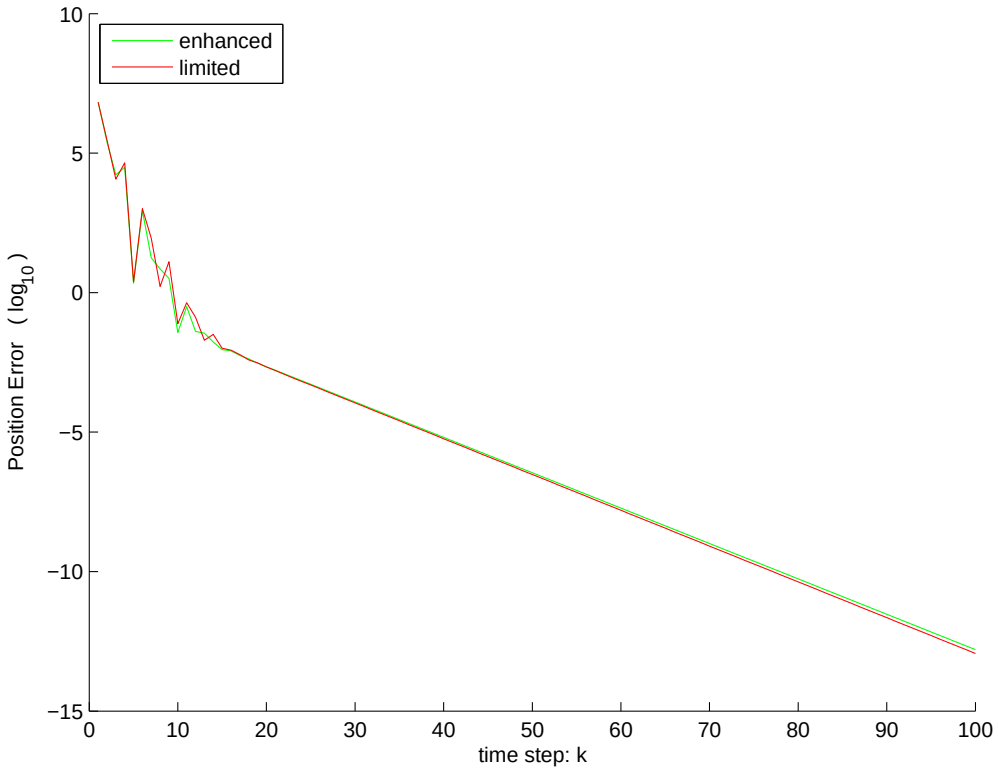

Figure 6.2: Synchronization of α and ϵ

In both approaches the agents were shifted equally.

As mentioned earlier, the largest eigenvalue of $\Gamma^T A^T A \Gamma$ increases with the number of agents and the number of connections. Because α was chosen to account for a fully connected 10-agent formation topology, the performance of the fully connected 5-agent formation topology suffers. Notice that the rates of convergence are much faster for the initial 5-agent topology with the enhanced approach, but the convergence rates virtually identical after agents 6-10 join. Figure 6.4 shows the trajectory of the agents using the limited scalability approach, while Figure 6.5 shows the trajectory of the agents using the enhanced scalability approach.

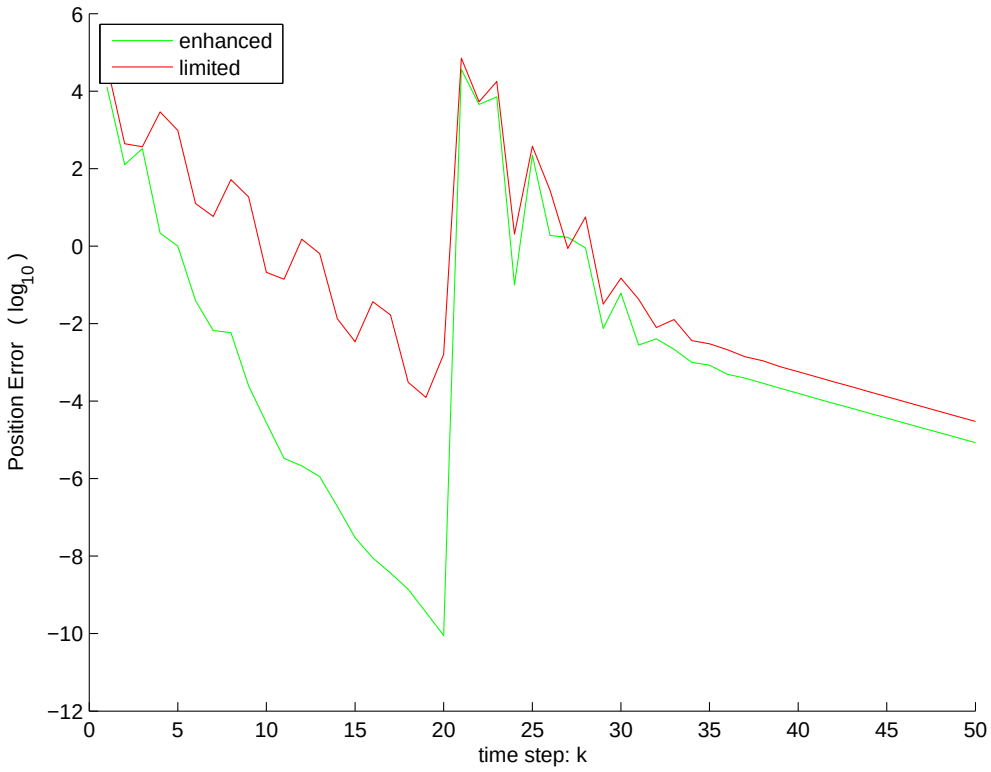

Figure 6.3: Comparison of Convergence Rates

6.5 Conclusion

A new control law was presented that results in distributed control, requiring a communication topology that mirrors exactly the formation topology. Additionally, this control law has enhanced scalability over the approach presented in Chapter 3. Specifically, to accommodate new agents that may arrive in the network, the approach presented in Chapter 3 requires an *a priori* knowledge of a hard bound on the maximum size of a network. This can lead to sluggish responses in networks that undergo large fluctuations in size, especially in epochs where the network is much smaller than the largest network. The new law removes this requirement and can accommodate new arrivals by requiring adjustment of control laws of only agents that the new agent attaches itself to.

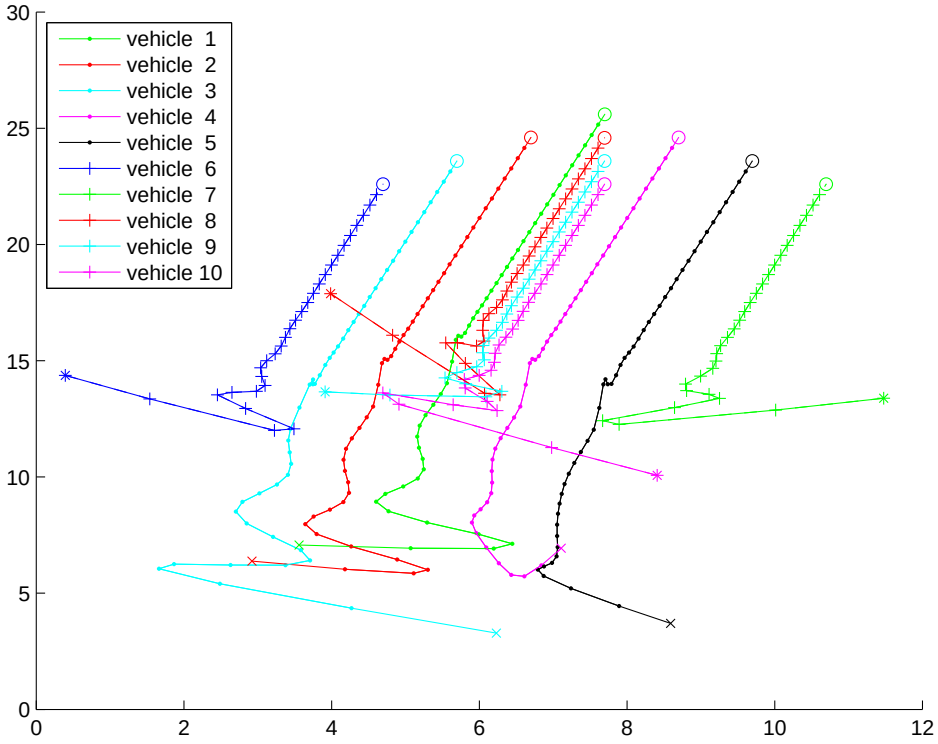

Figure 6.4: Trajectory of the Limited Scalability Approach

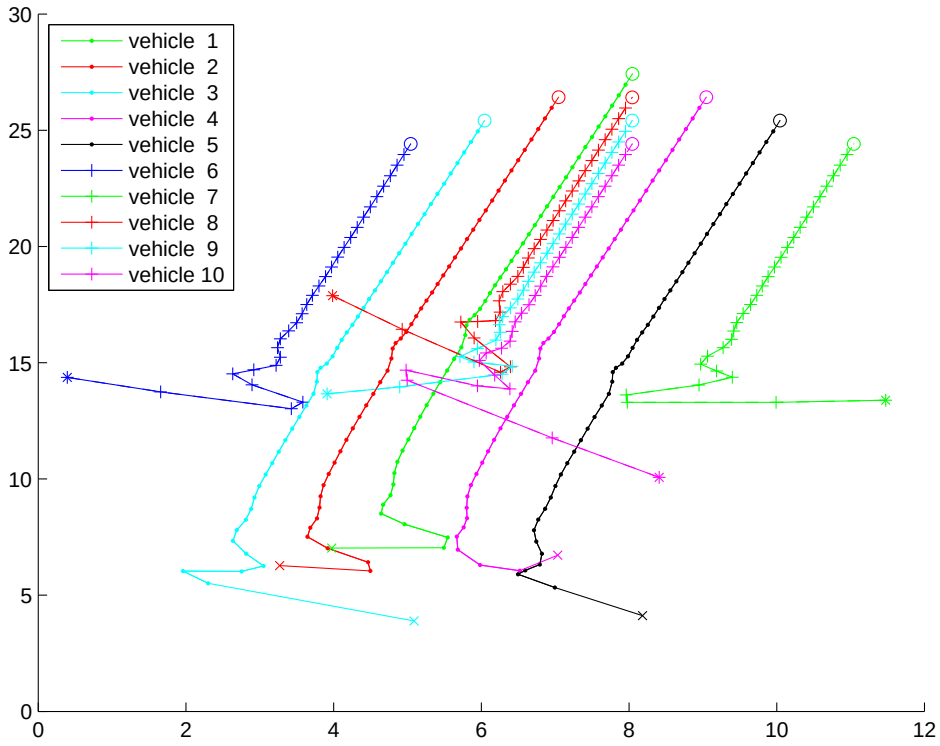

Figure 6.5: Trajectory of the Enhanced Scalability Approach

CHAPTER 7
THE IMPACT OF DYNAMIC CHANGES TO THE COMMUNICATION TOPOLOGY

In the previous chapters, we have shown that our control law is robust against loss of craft and/or communication channels. This analysis has been of a static nature and it does not address dynamic changes to the communication topology, specifically when a lost link may return. We now investigate the impact that dynamic changes to the communication topology can have upon stability. In particular we show that it is possible for such a dynamic network to be unstable.

7.1 A Periodic Sequence of Dynamic Communication Changes

We will consider an M-periodic sequence of dynamic communication changes. Recall from the previous chapters that the communication topologies mirror the formation topologies. Thus, if formation topologies are switched with each time step, we are in fact changing the communication topology. Therefore, we consider a set of $P \leq M$ formation topologies that switch periodically with the time step k. In particular, for $i \in \{1 \dots P\}$, the P formation topologies are specified by the the $\begin{bmatrix} A_i, & b_i \end{bmatrix}$ pair, where

$$A_i = \begin{bmatrix} A_{pi} & 0 \\ 0 & A_{vi} \end{bmatrix} \qquad \text{and} \qquad b_i = \begin{bmatrix} b_{pi} \\ b_{vi} \end{bmatrix}. \tag{7.1}$$

As in Chapter 2, A_{pi} is $2L_{pi} \times 2N$, b_{pi} is $2L_{pi} \times 1$, A_{vi} is $2L_{vi} \times 2N$, b_{vi} is $2L_{vi} \times 1$.

Consider a function $f(\cdot)$ that maps $\{0 \dots M-1\}$ to some $\{1 \dots P\}$. Then the M-periodic closed loop system can be written as:

$$\begin{aligned} \widehat{x}(k+1) &= \widehat{F}_{f(k \bmod M)}\widehat{x}(k) + \widehat{G}_{f(k \bmod M)} \\ y(k) &= \widehat{A}_{f(k \bmod M)}\widehat{x}(k) - b_{f(k \bmod M)} \end{aligned} \qquad f : X \to Y \tag{7.2}$$

A time-invariant representation of (7.2) can be obtained by "stacking" the inputs

and outputs over periods of M samples as shown below. With

$$\widetilde{x} = \begin{bmatrix} \widehat{x}(Mk) \\ \widehat{x}(Mk-1) \\ \vdots \\ \widehat{x}(Mk-M+1) \end{bmatrix} \tag{7.3}$$

the closed loop becomes,

$$\widetilde{x}(k+1) = \widetilde{F}\widetilde{x}(k) + \widetilde{G} \tag{7.4}$$

$$\widetilde{y}(k) = \widetilde{A}\widetilde{x}(k) + \widetilde{B} \tag{7.5}$$

where

$$\widetilde{F} = \begin{bmatrix} \prod_{i=1}^{M} \widehat{F}_{f(M-i)} & 0 & \dots & 0 \\ \prod_{i=2}^{M} \widehat{F}_{f(M-i)} & 0 & \dots & 0 \\ \vdots & \vdots & & \vdots \\ \widehat{F}_{f(0)} & 0 & \dots & 0 \end{bmatrix} \tag{7.6}$$

$$\widetilde{G} = \begin{bmatrix} \widehat{G}_{f(M-1)} + \sum_{i=1}^{M-1} \left(\prod_{j=1}^{i} \widehat{F}_{f(M-j)} \right) \widehat{G}_{f(M-1-i)} \\ \widehat{G}_{f(M-2)} + \sum_{i=2}^{M-1} \left(\prod_{j=2}^{i} \widehat{F}_{f(M-j)} \right) \widehat{G}_{f(M-1-i)} \\ \vdots \\ \widehat{G}_{f(1)} + \sum_{i=M-1}^{M-1} \left(\prod_{j=M-1}^{i} \widehat{F}_{f(M-j)} \right) \widehat{G}_{f(M-1-i)} \\ \widehat{G}_{f(0)} \end{bmatrix} \tag{7.7}$$

$$\widetilde{A} = \begin{bmatrix} \widehat{A}_{f(0)} & 0 & \dots & 0 \\ 0 & \widehat{A}_{f(1)} & & \vdots \\ \vdots & & \ddots & 0 \\ 0 & \dots & 0 & \widehat{A}_{f(M-1)} \end{bmatrix} \tag{7.8}$$

$$\widetilde{b} = \begin{bmatrix} b_{f(0)} \\ b_{f(1)} \\ \vdots \\ b_{f(M-1)} \end{bmatrix} \tag{7.9}$$

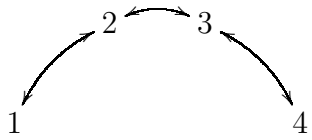

Figure 7.1: Formation Topology 1 (minimal system)

7.2 Observations for the Limited Scalability Approach

We have provided a set of equations which maps system of M-periodic dynamic communication topology changes to a non-time-varying system. A simulation environment was developed which uses a recursive algorithm to find the worst possible communication topology from a provided set of topologies at each time step. We used the simulations to check that stability for a variety of N agent formations.

First consider the 4 agent formation topologies shown in Figures 7.1 and 7.3. Using the simulation environment we were able to isolate a number of periodic sequences which switch between the two formation topologies and result in instability. The worst of these sequences was the 11-periodic sequence shown below:

$$\{3,1,3,1,3,1,3,1,3,1,1\}. \qquad \text{with eigenvalues at -43.9159} \tag{7.10}$$

We also isolated much simpler sequences that resulted in instability:

$$\{3,1,1\} \qquad \text{with eigenvalues at -2.6947}$$

$$\{3,1\}. \qquad \text{with eigenvalues at -2.0057}$$

In all of these simulations α was chosen to be 0.5 larger than the largest eigenvalue of $\Gamma^T A_3^T A_3 \Gamma$. Where A_3 corresponds to the formation topology shown in Figure 7.3.

Now consider the formation topologies shown in Figures 7.1 and 7.2. Again we were able to isolate sequences which resulted in instability, the worst of which is the 4-periodic sequence shown below:

$$\{2,1,1,1\} \qquad \text{with eigenvalues at -1.5038}$$

Additionally we were able to isolate the following unstable 5-periodic sequence:

$$\{2,1,1,1,1\} \qquad \text{with eigenvalues at -1.3136}$$

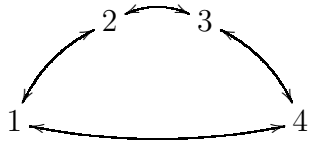

Figure 7.2: Formation Topology 2 (Minimal System Plus One Link)

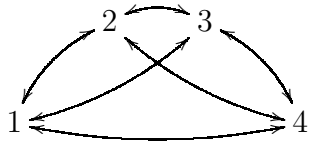

Figure 7.3: Formation Topology 3 (Maximal System)

An important observation was made while running the simulations. The choice of α does have an impact on the level of instability in the system, but not in a simple fashion. Depending on the initial choice of α, a small increase may push the unstable poles further outside the unit circle, but as α continues to increase the unstable poles will eventually move back within the unit circle and stability will result.

7.3 Observations for the Enhanced Scalability Approach

A simulation environment was developed which uses a recursive algorithm to find the worst possible communication topology from a provided set of topologies at each time step. We used the simulations to check that stability for a variety of N agent formations. We found that while the enhanced approach does become unstable with select dynamic communication topology changes, the number of periodic systems that result in instability is less when compared to the limited approach.

First consider the 4 agent formation topologies shown in Figures 7.1 and 7.3. Using the simulation environment we were able to isolate a couple of periodic sequences which switch between the two formation topologies and result in instability.

The worst of these sequences was the 3-periodic sequence shown below:

$$\{3, 1, 1\}. \qquad \text{with eigenvalues at -1.2627} \tag{7.11}$$

The only other sequence we were able to isolate is shown below:

$$\{3, 1, 1, 1\} \qquad \text{with eigenvalues at -1.0596}$$

In all of these simulations ϵ was chosen to be 0.5 and β was chosen to be 2 as defined in (6.3).

Now consider the formation topologies shown in Figures 7.1 and 7.2. Unlike in the limited scalability approach we were unable to isolate any sequences which switch between these topologies that result in instability.

An important observation was made while running the simulations. The choice of ϵ and β does have an impact on the level of instability in the system. As either ϵ or β increase the unstable poles move towards the unit circle. In fact, with $\beta = 2$, both time varying sequences become stable when ϵ is increased to 2. If $\epsilon = 0.5$ and β is increased to 2.45, then again, both time varying sequences become stable.

7.4 Conclusion

Clearly not all periodic sequences are stable; however, many are indeed stable. In fact, we ran thousands of simulations which randomly switch between the formation topologies and never encountered a system which did not reach the formation goal. Through experimentation we have found the unstable systems to be periodic. We hypothesize that sets of stable and unstable systems can be characterized. Additionally we believe it may be possible to create adaptive algorithms using these characterizations that can reject additional information that may result in instability; however, we leave these problems for future work. Additionally, the role that α plays in the limited scalability approach and the role β and ϵ play in the enhanced scalability approach should be further investigated; perhaps a condition exists on these terms which will ensure stability in the face of dynamic communication

topology changes.

CHAPTER 8
CONCLUSION

This thesis considered the coordinated control of autonomous agents. The agents were modeled as double integrators, one for each Cartesian dimension. With the goal, to force the agents' convergence to a formation specified by their desired relative positions, a pair of one-step-ahead optimization based control laws were developed.

The control algorithms produced a communication topology that mirrored the geometric formation topology due to the careful choice of the minimized cost functions. The equivalence provided an intuitive understanding of the relationship between the geometric formation topology and the communication infrastructure. It was shown that the control laws are stable and guarantee convergence for all viable formation topologies. Moreover, theorems were developed which allowed for the addition of fixed or arbitrary time-varying velocity constraints.

Both control algorithms only required local information exchange. With the arrival of additional agents, it was shown that only the agents with whom the new agents were dependent upon needed to adjust their control laws. Moreover, when redundancy was incorporated into the formation topology, it became possible for the system to survive loss of agents or communication channels. In the event that an agent dropped out of the formation, only the agents which had position interdependence on the lost agent needed to adjust their control laws. Finally, in the event of a lost communication channel, only the agents that shared the communication channel were required to adjust their control laws.

In Chapter 2 we provided an introduction to the core mathematical equations and concepts used throughout the paper. In Section 2.1 we introduced a set of equations that were used to represent our system of agents. Section 2.2 introduced the mathematical formulas that were used to represent the agent formations. Formations

were specified by a matrix, vector pair $\left[\begin{array}{cc} A, & b \end{array}\right]$. We established an assumption on the construction of the $\left[\begin{array}{cc} A, & b \end{array}\right]$ pair that allowed the user to create formations specified by relative inter-agent distances. It was then shown how additional redundancy and static velocity constraints could be incorporated into the formation specification. We then formally showed the relation between relative position constraints and the individual elements of A. Finally, we described how additional redundancy, loss of an agent or the loss of a communication channel impacts the $\left[\begin{array}{cc} A, & b \end{array}\right]$ pair. In Section 2.3, a set of conditions were developed to address the feasibility of a formation. We first assigned some basic assumptions to the communication topology, namely that the sub-matrices of A, which specify the position constraints in each Cartesian direction, had a rank of $N-1$ for an N agent formation and that b was in the range space of A. The first assumption ensured that the formation was *connected* while the second ensured that the formation was well defined. We then provided a basic definition for formation viability. It was then proven that for all viable formations, a solution exists for the formation topology and that once the formation is achieved, it could be maintained without any additional input into the system.

Chapter 3 presented a distributed approach to the formation control problem. This approach required either an *a priori* knowledge of the largest possible formation size or the global information exchange of the current formation size. As such, this approach was not as scalable as some would desire; however, it did have some interesting properties. We provided a one-step-ahead optimal control law which guaranteed a fleet of autonomous agents could attain any fixed velocity, viable formation. We showed that the formation topology was in fact equivalent to the communication topology and, assuming the use of *a priori* knowledge, only local information exchange. In other words, each agent only required knowledge of its neighbors, as specified by the formation topology. In the face of a lost agent, only neighbors of the lost agent were required adjust their control laws. If a communication channel

was lost, only the agents that shared the communication channel were required to adjust their control laws. Finally, the arrival of a new agent only impacted the agents against which the arriving agent's relative position constraints were defined.

In Chapter 4, we extended the work presented in Chapter 3 to allow the agents to track arbitrary velocities. Using the presented control law, all of the attractive properties presented in Chapter 3 applied, aside from the fact that the agents were required to apply an input force to maintain the dynamic velocity changes. It is important to note; however, that the input force was not used to maintain the relative positions amongst the agents once the formation was attained.

In Chapter 5, we analyzed the impact that redundancy had upon the rate of convergence. It was shown that each time additional redundancy was added, the rate of convergence to the desired formation improved.

Chapter 6 presented a fully decentralized approach to multi-agent formation control that results in enhanced scalability. It did not require *a priori* knowledge or global information exchange. An alternate one step ahead optimal control law was presented that guaranteed that a fleet of autonomous agents could attain any fixed velocity viable formation with the additional benefit of enhanced scalability and in most cases better performance. We proceeded to show, like the distributed approach presented in Chapter 3, the fully decentralized approach also only requires local information exchange.

Finally, in Chapter 7 we investigated how dynamic changes to the communication topology can influence system stability. A number of unstable systems were presented for both the limited scalability approach and the enhanced scalability approach. We found that while both approaches are susceptible to dynamically changing communication topologies, the enhanced approach appears to be robust against a larger set.

Research in the area of the coordinated control of autonomous agents has been growing rapidly. Many of the basic problems have been solved. Of particular interest are the provably correct algorithms and those which do not require the global exchange of information.

We have shown our system is not robust against all dynamic changes to the communication topology. We have however seen that our system is in fact robust against certain dynamic changes to the communication topology. We aim to characterize this set of stable dynamic communication systems.

An important aspect of this research includes the impact that information flow can have upon stability and the rate of convergence. A problem exists with respect to the amount and type of information flow and its influence on stability and rate of convergence. It is obvious that additional information exchange will enhance the robustness of the system; however the amount of information that can be achieved is limited by the communication channels. As the number of agents in the network increases the amount of bandwidth available to each agent decreases. These problems are compounded with multi-hop communication. The optimization of the communication network with respect to the formation geometry is an area that still needs significant attention.

APPENDIX A
SELECTED PROOFS - LIMITED SCALABILITY

A.1 Basic Control: Proof of Lemma 3.2.1

We first complete through the lemma below the first part of the proof of Lemma 3.2.1.

Lemma A.1.1 *Under (2.13) (3.7)-(3.9), (2.6), and (2.7) the poles of* $A(zI-F)^{-1}$ *are either inside the unit circle or at 1.*

Proof: Choose:

$$T = \begin{bmatrix} I & -I/2 \\ 0 & I \end{bmatrix} \text{ and hence } T^{-1} = \begin{bmatrix} I & I/2 \\ 0 & I \end{bmatrix}.$$

Call

$$\Sigma_i = A_i^T A_i \geq 0 \qquad \text{with } i \in \{p, v\}$$

Because of (2.6), (2.7) and (3.7)

$$0 \leq \frac{\Sigma_p + 4\Sigma_v}{\alpha} < 1. \tag{A.1}$$

Then

$$\begin{aligned} TFT^{-1} &= \Phi - \frac{1}{\alpha}\begin{bmatrix} 0 \\ 2I \end{bmatrix}\begin{bmatrix} \Sigma_p & 2\Sigma_v \end{bmatrix}\begin{bmatrix} I & \frac{3}{2}I \\ 0 & I \end{bmatrix} \\ &= \Phi - \frac{1}{\alpha}\begin{bmatrix} 0 \\ 2I \end{bmatrix}\begin{bmatrix} \Sigma_p & \frac{3}{2}\Sigma_p + 2\Sigma_v \end{bmatrix} \\ &= \begin{bmatrix} I & I \\ -\frac{2\Sigma_p}{\alpha} & I - \frac{3\Sigma_p + 4\Sigma_v}{\alpha} \end{bmatrix}. \end{aligned}$$

Then

$$\begin{aligned} &\det(zI - TFT^{-1}) \\ &= \det\left[(z-1)^2 I + (z-1)\tfrac{3\Sigma_p + 4\Sigma_v}{\alpha} + \tfrac{2\Sigma_p}{\alpha}\right] \\ &= \det\left[z^2 I + \left(\tfrac{3\Sigma_p + 4\Sigma_v}{\alpha} - 2I\right) z - \left(\tfrac{\Sigma_p + 4\Sigma_v}{\alpha} - I\right)\right] \end{aligned}$$

Then if z is an eigenvalue of F, there exists a unit η such that

$$z^2 + (3\sigma_1^2 + 4\sigma_2^2 - 2)z - (\sigma_1^2 + 4\sigma_2^2 - 1) = 0 \tag{A.2}$$

where

$$\sigma_i^2 = \frac{\eta^T \Sigma_i \eta}{\alpha}.$$

From (A.1)

$$0 \leq \sigma_1^2 + 4\sigma_2^2 < 1, \tag{A.3}$$

and therefore

$$0 \leq 3\sigma_1^2 + 4\sigma_2^2 < 1 + 2\sigma_1^2, \tag{A.4}$$

First observe that if (A.2) has a complex root ρ then from (A.3)

$$|\rho|^2 = 1 - \sigma_1^2 - 4\sigma_2^2 \leq 1, \tag{A.5}$$

with equality holding *iff* $\sigma_1 = \sigma_2 = 0$, which in turn leads to

$$\rho = 1. \tag{A.6}$$

If on the other hand the roots are real then they are

$$\rho_1 = \frac{2 - 3\sigma_1^2 - 4\sigma_2^2 + \sqrt{(3\sigma_1^2 + 4\sigma_2^2)^2 - 8\sigma_1^2}}{2} \tag{A.7}$$

and

$$\rho_2 = \frac{2 - 3\sigma_1^2 - 4\sigma_2^2 - \sqrt{(3\sigma_1^2 + 4\sigma_2^2)^2 - 8\sigma_1^2}}{2} \tag{A.8}$$

Clearly $\rho_1 \leq 1$, and because of (A.4) $\rho_1 > -\frac{1}{2}$ as shown below

$$\rho_1 \geq \frac{2 - (3\sigma_1^2 + 4\sigma_2^2)}{2} > \frac{1}{2} - \sigma_1^2 \geq -\frac{1}{2}.$$

Further $\rho_2 \leq 1$. Now assume

$$\begin{aligned} \rho_2 &\leq -1 \\ \Leftrightarrow 4 - (3\sigma_1^2 + 4\sigma_2^2) &\leq \sqrt{(3\sigma_1^2 + 4\sigma_2^2)^2 - 8\sigma_1^2} \\ \Leftrightarrow 16 - 8(3\sigma_1^2 + 4\sigma_2^2) &\leq -8\sigma_1^2 \\ \Leftrightarrow 1 &\leq \sigma_1^2 + 2\sigma_2^2 \end{aligned}$$

But by (A.4), $1 > \sigma_1^2 + 4\sigma_2^2$, leading to a contradiction. ∎

We next need to show that the eigenvalues of F that are at 1, are in fact unobservable from A. To this end we consider a singular value decomposition (SVD) of A_p, that is, with U_p, $2L_p \times 2L_p$, V_p, $n \times n$ unitary matrices

$$A_p = U_p D_p V_p \tag{A.9}$$

where

$$D_p = \begin{bmatrix} \Delta_p & 0 \\ 0 & 0 \end{bmatrix} \tag{A.10}$$

and Δ_p is diagonal, $n_p \times n_p$, positive definite.

Partition the $2L_v \times n$ matrix $A_v V_p^H$ as

$$A_v V_p^H = \begin{bmatrix} \overline{A}_{v1} & \overline{A}_{v2} \end{bmatrix} \tag{A.11}$$

where $\overline{A}_{v2}$ is $2L_v \times (n - n_p)$.

Consider next the SVD of $\overline{A}_{v2}$, that is, with U_v, $2L_v \times 2L_v$ and V_v, $(n - n_p) \times (n - n_p)$ and both unitary

$$\overline{A}_{v2} = U_v D_v V_v \tag{A.12}$$

where

$$D_v = \begin{bmatrix} \Delta_v & 0 \\ 0 & 0 \end{bmatrix} \tag{A.13}$$

with Δ_v, $n_v \times n_v$, positive definite.

Define

$$W = V_p^H \begin{bmatrix} I_{n_1} & 0 \\ 0 & V_v^H \end{bmatrix} \tag{A.14}$$

In the sequel $\oplus$ will denote the direct sum, for example $A = A_p \oplus A_v$. Consider next a system equivalent to (3.10).

Lemma A.1.2 *With Φ, Γ, A, b, F, G, U_i, V_i and D_i with $i \in \{p, v\}$ and $\overline{A}_{v2}$ defined in (2.6), (2.7), (2.13), (3.8), (3.9) and (A.9-A.14) define*

$$\widehat{F} = \Phi - \frac{\Gamma\Gamma^T \widehat{A}^T \widehat{A}\Phi}{\alpha} \tag{A.15}$$

$$\widehat{A} = (U_p D_p) \oplus \left[\overline{A}_{v1}, U_v D_v\right] \tag{A.16}$$

$$\widehat{G} = \frac{\Gamma\Gamma^T \widehat{A}^T b}{\alpha} \tag{A.17}$$

$$\widehat{x}(k) = (W^H \oplus W^H) x(k). \tag{A.18}$$

Then one has that

$$\widehat{x}(k+1) = \widehat{F}\widehat{x}(k) + \widehat{G} \tag{A.19}$$

$$y(k) = \widehat{A}\widehat{x}(k) - b \tag{A.20}$$

Proof: First note that

$$\begin{aligned} A(W \oplus W) &= \begin{bmatrix} A_p V_p^H & 0 \\ 0 & A_v V_p^H \end{bmatrix} \begin{bmatrix} I & 0 & 0 & 0 \\ 0 & V_v^H & 0 & 0 \\ 0 & 0 & I & 0 \\ 0 & 0 & 0 & V_v^H \end{bmatrix} \\ &= \begin{bmatrix} U_p \begin{bmatrix} \Delta_p & 0 \\ 0 & 0 \end{bmatrix} \end{bmatrix} \oplus \left[\overline{A}_{v1}, U_v D_v \right] \\ &= \widehat{A}. \end{aligned} \tag{A.21}$$

Further

$$\begin{aligned} &\left(W^H \oplus W^H\right) F(W \oplus W) = \\ &= \begin{pmatrix} W^H & 0 \\ 0 & W^H \end{pmatrix} \left(I - \tfrac{1}{\alpha} \Gamma \Gamma^T A^T A\right) \begin{bmatrix} I & I \\ 0 & I \end{bmatrix} \begin{bmatrix} W & 0 \\ 0 & W \end{bmatrix} \\ &= \begin{pmatrix} W^H & 0 \\ 0 & W^H \end{pmatrix} \left(I - \tfrac{1}{\alpha} \begin{bmatrix} I & 2I \\ 2I & 4I \end{bmatrix} A^T A\right) \begin{bmatrix} W & 0 \\ 0 & W \end{bmatrix} \Phi \\ &= \left(I - \tfrac{1}{\alpha} \Gamma \Gamma^T \begin{pmatrix} W^H & 0 \\ 0 & W^H \end{pmatrix} A^T A \begin{bmatrix} W & 0 \\ 0 & W \end{bmatrix}\right) \Phi \\ &= \widehat{F} \end{aligned}$$

because of (2.13). Similarly, because of (2.13), (2.7) and (3.9)

$$\widehat{G} = \left(W^H \oplus W^H\right) G. \tag{A.22}$$

Thus the lemma holds. ∎

We next show that a condition comparable to (3.7) holds.

Lemma A.1.3

$$I - \frac{\Gamma^T \widehat{A}^T \widehat{A} \Gamma}{\alpha} > 0 \tag{A.23}$$

Proof: Follows from (A.21), the fact that

$$W^H W = I$$

and that

$$\Gamma W = (W \oplus W)\Gamma$$

■

Denoting 0_q to be the $q \times q$, 0 matrix, we observe from (A.10), (A.13) and (A.16):

$$\widehat{A}^T\widehat{A} = \begin{bmatrix} D_p^H U_p^H & 0 \\ 0 & \overline{A}_{v1}^T \\ 0 & D_v^H U_v^H \end{bmatrix} \begin{bmatrix} U_p D_p & 0 & 0 \\ 0 & \overline{A}_{v1} & U_v D_v \end{bmatrix}$$

$$= \begin{bmatrix} \Delta_p^2 & 0 & 0 & 0 & 0 \\ 0 & 0_{n-n_p} & 0 & 0 & 0 \\ 0 & 0 & \overline{A}_{v1}^T\overline{A}_{v1} & B & 0 \\ 0 & 0 & B^H & \Delta_v^2 & 0 \\ 0 & 0 & 0 & 0 & 0_{n-n_p-n_v} \end{bmatrix}, \tag{A.24}$$

where

$$B = \overline{A}_{v1}^T U_v \begin{bmatrix} \Delta_v \\ 0 \end{bmatrix}. \tag{A.25}$$

Further,

$$\Gamma^T\widehat{A}^T\widehat{A} = \tag{A.26}$$
$$\begin{bmatrix} \Delta_p^2 & 0 & 0 & 2\overline{A}_{v1}^T\overline{A}_{v1} & 2B & 0 \\ 0 & 0_{n_v} & 0 & 2B^H & 2\Delta_v^2 & 0 \\ 0 & 0 & 0_{n-n_p-n_v} & 0 & 0 & 0_{n-n_p-n_v} \end{bmatrix}$$

and

$$\Gamma^T\widehat{A}^T\widehat{A}\Phi = \tag{A.27}$$
$$\begin{bmatrix} \Delta_p^2 & 0 & 0 & \Delta_p^2 + 2\overline{A}_{v1}^T\overline{A}_{v1} & 2B & 0 \\ 0 & 0 & 0 & 2B^H & 2\Delta_v^2 & 0 \\ 0 & 0 & 0 & 0 & 0 & 0_{n-n_p-n_v} \end{bmatrix}.$$

Then

$$\widehat{F} = \begin{bmatrix} \widehat{F}_{11} & \widehat{F}_{12} \\ \widehat{F}_{21} & \widehat{F}_{22} \end{bmatrix} \tag{A.28}$$

Where:

$$\widehat{F}_{11} = \begin{bmatrix} I_{n_p} - \frac{\Delta_p^2}{\alpha} & 0 & 0 \\ 0 & I_{n_v} & 0 \\ 0 & 0 & I_{n-n_p-n_v} \end{bmatrix}$$

$$\widehat{F}_{12} = \begin{bmatrix} I_{n_p} - \frac{\Delta_p^2 + 2\bar{A}_{v1}^T \bar{A}_{v1}}{\alpha} & -\frac{2B}{\alpha} & 0 \\ -\frac{2B^H}{\alpha} & I_{n_v} - \frac{2\Delta_v^2}{\alpha} & 0 \\ 0 & & I_{n-n_p-n_v} \end{bmatrix} \tag{A.29}$$

$$\widehat{F}_{21} = \begin{bmatrix} -\frac{2\Delta_v^2}{\alpha} & 0 & 0 \\ 0 & 0 & 0 \\ 0 & 0 & 0 \end{bmatrix}$$

$$\widehat{F}_{22} = \begin{bmatrix} I_{n_1} - \frac{\Delta_p^2 + 4\bar{A}_{v1}^T \bar{A}_{v1}}{\alpha} & -\frac{4B}{\alpha} & 0 \\ -\frac{4B^H}{\alpha} & I_{n_v} - \frac{4\Delta_v^2}{\alpha} & 0 \\ 0 & 0 & I_{n-n_p-n_v} \end{bmatrix}$$

Notice (A.23) and (A.1) imply

$$\frac{4\Delta_v^2}{\alpha} < I. \tag{A.30}$$

Then the following lemma goes toward a Kalman like decomposition.

Lemma A.1.4 *Under (A.9-A.16). with $L = L_p + L_v$ as defined in Section 2.2.*

$$\widehat{A}\left(zI - \widehat{F}\right)^{-1} = \begin{bmatrix} H(z) & 0_{2L\times(2n-2n_p-n_v)} \end{bmatrix} \Pi \tag{A.31}$$

where

$$H(z) = C(zI - \Upsilon)^{-1},$$

$$\Upsilon = \begin{bmatrix} I - \frac{\Delta_p^2}{\alpha} & I - \frac{\Delta_p^2 + 2\overline{A}_{v1}^T \overline{A}_{v1}}{\alpha} & -\frac{2B}{\alpha} \\ -\frac{2\Delta_p^2}{\alpha} & I - \frac{2\Delta_p^2 + 4\overline{A}_{v1}^T \overline{A}_{v1}}{\alpha} & -\frac{4B}{\alpha} \\ 0 & -\frac{4B^H}{\alpha} & I - \frac{4\Delta_v^2}{\alpha} \end{bmatrix},$$

$$C = \left(U_p \begin{bmatrix} \Delta_p \\ 0 \end{bmatrix} \right) \oplus \left(\begin{bmatrix} \overline{A}_{v1} & U_v \begin{bmatrix} \Delta_v \\ 0 \end{bmatrix} \end{bmatrix} \right) \tag{A.32}$$

and

$$\Pi = \begin{bmatrix} I_{n_p} & 0 & 0 & 0 \\ 0 & 0 & I_{n_p+n_v} & 0 \\ 0 & I_{n-n_v} & 0 & 0 \\ 0 & 0 & 0 & I_{n-(n_p+n_v)} \end{bmatrix}. \tag{A.33}$$

Proof: Note

$$\Pi^T \Pi = I. \tag{A.34}$$

Hence

$$\widehat{A}(zI - \widehat{F})^{-1} = \widehat{A}\Pi^T \left[zI - \Pi \widehat{F} \Pi^T \right]^{-1} \Pi.$$

Now,

$$\begin{aligned} \widehat{A}\Pi^T &= \begin{bmatrix} U_p \begin{bmatrix} \Delta_p \\ 0 \end{bmatrix} & 0 & 0 & 0 & 0 \\ 0 & 0_{n-n_p} & \overline{A}_{v1} & U_v \begin{bmatrix} \Delta_v \\ 0 \end{bmatrix} & 0 \end{bmatrix} \times \\ &\quad \times \begin{bmatrix} I_{n_p} & 0 & 0 & 0 \\ 0 & 0 & I_{n-n_p} & 0 \\ 0 & I_{n_p+n_v} & 0 & 0 \\ 0 & 0 & 0 & I_{n-(n_p+n_v)} \end{bmatrix} \\ &= \begin{bmatrix} C & 0_{2L \times (2n-2n_p-n_v)} \end{bmatrix} \end{aligned}$$

Further, from (A.28)

$$\Pi \widehat{F} \Pi^T = \begin{bmatrix} I - \widehat{\Upsilon} & 0 \\ \times_1 & \times_2 \end{bmatrix}$$

where $\begin{bmatrix} \times_1 & \times_2 \end{bmatrix}$ has $2(n-n_p)-n_v$ rows and

$$\widehat{\Upsilon} = \begin{bmatrix} \frac{\Delta_p^2}{\alpha} & -I_{n_p} + \frac{\Delta_p^2 + 2\overline{A}_{v1}^T \overline{A}_{v1}}{\alpha} & \frac{2B}{\alpha} \\ \frac{2\Delta_p^2}{\alpha} & \frac{2\Delta_p^2 + 4\overline{A}_{v1}^T \overline{A}_{v1}}{\alpha} & \frac{4B}{\alpha} \\ 0 & \frac{4B^H}{\alpha} & \frac{4\Delta_v^2}{\alpha} \end{bmatrix} \tag{A.35}$$

Then the result follows. ■

Lemma A.1.5 *Under the conditions of Lemma A.1.1, $A(zI-F)^{-1}$ has no poles at 1.*

Proof: Because of Lemmas A.1.2 and A.1.4, It suffices to show that Υ defined in Lemma A.1.4 has no eigenvalues at 1. Choose

$$T = \begin{bmatrix} I_{n_p} & -I_{n_p}/2 & 0 \\ 0 & I_{n_p} & 0 \\ 0 & 0 & I_{n_v} \end{bmatrix}$$

and note that

$$T^{-1} = \begin{bmatrix} I_{n_p} & I_{n_p}/2 & 0 \\ 0 & I_{n_p} & 0 \\ 0 & 0 & I_{n_v} \end{bmatrix}.$$

Then

$$\begin{aligned} T\Upsilon T^{-1} = & \\ = & \begin{bmatrix} I_{n_p} & I_{n_p}/2 & 0 \\ -\frac{2\Delta_p^2}{\alpha} & I_{n_1} - \frac{2\Delta_p^2 + 4\overline{A}_{v1}^T \overline{A}_{v1}}{\alpha} & -\frac{4B}{\alpha} \\ 0 & -\frac{4B^H}{\alpha} & I - \frac{4\Delta_v^2}{\alpha} \end{bmatrix} T^{-1} \\ = & \begin{bmatrix} I_{n_p} & I_{n_p} & 0 \\ -\frac{2\Delta_p^2}{\alpha} & I_{n_p} - \frac{3\Delta_p^2 + 4\overline{A}_{v1}^T \overline{A}_{v1}}{\alpha} & -4B \\ 0 & -4B^H & I - \frac{4\Delta_v^2}{\alpha} \end{bmatrix}. \end{aligned}$$

Now, $T\Upsilon T^{-1}$ has an eigenvalue at 1 iff there exists

$$\eta = \begin{bmatrix} \eta_1 \\ \eta_2 \\ \eta_3 \end{bmatrix} \neq 0$$

such that

$$\begin{bmatrix} 0 & -I_{n_1} & 0 \\ \frac{2\Lambda_1^2}{\alpha} & \frac{3\Lambda_1^2+4\overline{A}_{21}^T\overline{A}_{21}}{\alpha} & \frac{4B}{\alpha} \\ 0 & \frac{4B^H}{\alpha} & I-\frac{4\Lambda_2^2}{\alpha} \end{bmatrix} \begin{bmatrix} \eta_1 \\ \eta_2 \\ \eta_3 \end{bmatrix} = 0.$$

Now the first block equation implies $\eta_2 = 0$. Further because of (A.30), the third block equation gives $\eta_3 = 0$. Thus as $\Delta_p > 0$, the second block equation assures that $\eta_1 = 0$, leading to a contradiction. ■

Thus Lemma 3.2.1 follows from Lemmas A.1.1 and A.1.5.

APPENDIX B
SELECTED PROOFS - ENHANCED SCALABILITY

B.1 Proof of Lemma 6.3.1

We first complete through the lemma below the first part of the proof of Lemma 6.3.1.

Lemma B.1.1 *Under (2.13) (6.10), (6.11), (2.6), and (2.7) the poles of* $A(zI-F)^{-1}$ *are either inside the unit circle or at 1.*

Proof: Choose:

$$T = \begin{bmatrix} \Lambda^{\frac{1}{2}} & -\frac{1}{2}\Lambda^{\frac{1}{2}} \\ 0 & \Lambda^{\frac{1}{2}} \end{bmatrix} \text{ and hence } T^{-1} = \begin{bmatrix} \Lambda^{-\frac{1}{2}} & \frac{1}{2}\Lambda^{-\frac{1}{2}} \\ 0 & \Lambda^{-\frac{1}{2}} \end{bmatrix}.$$

Call

$$\Sigma_i = A_i^T A_i \geq 0 \qquad \text{with } i \in \{p, v\}$$

Because of (2.6), (2.7) and (6.10)

$$0 \leq \Lambda^{-1}\left(\Sigma_p + 4\Sigma_v\right) < 1. \tag{B.36}$$

Then

$$\begin{aligned} TFT^{-1} &= \Phi - \begin{bmatrix} 0 \\ 2\Lambda^{-\frac{1}{2}} \end{bmatrix} \begin{bmatrix} \Sigma_p & 2\Sigma_v \end{bmatrix} \begin{bmatrix} \Lambda^{-\frac{1}{2}} & \frac{3}{2}\Lambda^{-\frac{1}{2}} \\ 0 & \Lambda^{-\frac{1}{2}} \end{bmatrix} \\ &= \Phi - \begin{bmatrix} 0 \\ 2\Lambda^{-\frac{1}{2}} \end{bmatrix} \begin{bmatrix} \Sigma_p\Lambda^{-\frac{1}{2}} & \frac{3}{2}\left(\Sigma_p + 2\Sigma_v\right)\Lambda^{-\frac{1}{2}} \end{bmatrix} \\ &= \begin{bmatrix} I & I \\ -2\Lambda^{-\frac{1}{2}}\Sigma_p\Lambda^{-\frac{1}{2}} & I - \Lambda^{-\frac{1}{2}}\left(3\Sigma_p + 4\Sigma_v\right)\Lambda^{-\frac{1}{2}} \end{bmatrix}. \end{aligned}$$

Then

$$\begin{aligned} &\det(zI - TFT^{-1}) \\ &= \det\left[(z-1)^2 I + (z-1)\Lambda^{-\frac{1}{2}}\left(3\Sigma_p + 4\Sigma_v\right)\Lambda^{-\frac{1}{2}} + 2\Lambda^{-\frac{1}{2}}\Sigma_p\Lambda^{-\frac{1}{2}}\right] \\ &= \det\left[z^2 I + \left(\Lambda^{-\frac{1}{2}}\left(3\Sigma_p + 4\Sigma_v\right)\Lambda^{-\frac{1}{2}} - 2I\right)z - \left(\Lambda^{-\frac{1}{2}}\left(\Sigma_p + 4\Sigma_v\right)\Lambda^{-\frac{1}{2}} - I\right)\right] \end{aligned}$$

Then if z is an eigenvalue of F, there exists a unit η such that

$$z^2 + (3\sigma_1^2 + 4\sigma_2^2 - 2)z - (\sigma_1^2 + 4\sigma_2^2 - 1) = 0 \tag{B.37}$$

where

$$\sigma_i^2 = \eta^T \Lambda^{-\frac{1}{2}} \Sigma_i \Lambda^{-\frac{1}{2}} \eta.$$

From (B.36)

$$0 \leq \sigma_1^2 + 4\sigma_2^2 < 1, \tag{B.38}$$

and therefore

$$0 \leq 3\sigma_1^2 + 4\sigma_2^2 < 1 + 2\sigma_1^2, \tag{B.39}$$

First observe that if (B.37) has a complex root ρ then from (B.38)

$$|\rho|^2 = 1 - \sigma_1^2 - 4\sigma_2^2 \leq 1, \tag{B.40}$$

with equality holding *iff* $\sigma_1 = \sigma_2 = 0$, which in turn leads to

$$\rho = 1. \tag{B.41}$$

If on the other hand the roots are real then they are

$$\rho_1 = \frac{2 - 3\sigma_1^2 - 4\sigma_2^2 + \sqrt{(3\sigma_1^2 + 4\sigma_2^2)^2 - 8\sigma_1^2}}{2} \tag{B.42}$$

and

$$\rho_2 = \frac{2 - 3\sigma_1^2 - 4\sigma_2^2 - \sqrt{(3\sigma_1^2 + 4\sigma_2^2)^2 - 8\sigma_1^2}}{2} \tag{B.43}$$

Clearly $\rho_1 \leq 1$, and because of (B.39) $\rho_1 > -\frac{1}{2}$ as shown below

$$\rho_1 \geq \frac{2 - (3\sigma_1^2 + 4\sigma_2^2)}{2} > \frac{1}{2} - \sigma_1^2 \geq -\frac{1}{2}.$$

Further $\rho_2 \leq 1$. Now assume

$$\begin{aligned} \rho_2 &\leq -1 \\ \Leftrightarrow 4 - (3\sigma_1^2 + 4\sigma_2^2) &\leq \sqrt{(3\sigma_1^2 + 4\sigma_2^2)^2 - 8\sigma_1^2} \\ \Leftrightarrow 16 - 8(3\sigma_1^2 + 4\sigma_2^2) &\leq -8\sigma_1^2 \\ \Leftrightarrow 1 &\leq \sigma_1^2 + 2\sigma_2^2 \end{aligned}$$

But by (B.39), $1 > \sigma_1^2 + 4\sigma_2^2$, leading to a contradiction. ∎

We must now show that the eigenvalues of F that are at 1, are in fact unobservable from A. Now consider a singular value decomposition (SVD) of $A_p \Lambda^{-\frac{1}{2}}$.

$$A_p \Lambda^{-\frac{1}{2}} = U_p D_p V_p \tag{B.44}$$

Where U_p is an $2L_p \times 2L_p$ unitary matrix, V_p is an $n \times n$ unitary matrix and D_p is as defined below:

$$D_p = \begin{bmatrix} \Delta_p & 0 \\ 0 & 0 \end{bmatrix} \tag{B.45}$$

and Δ_p diagonal, $n_p \times n_p$, positive definite.

Partition the $2L_v \times n$ matrix $A_v \Lambda^{-\frac{1}{2}} V_p^H$ as

$$A_v \Lambda^{-\frac{1}{2}} V_p^H = \begin{bmatrix} \overline{A}_{v1} & \overline{A}_{v2} \end{bmatrix} \tag{B.46}$$

where $\overline{A}_{v2}$ is $2L_v \times (n - n_p)$.

Consider next the SVD of $\overline{A}_{v2}$, that is, with U_v, $2L_v \times 2L_v$ and V_v, $(n - n_p) \times (n - n_p)$ and both unitary

$$\overline{A}_{v2} = U_v D_v V_v \tag{B.47}$$

where

$$D_v = \begin{bmatrix} \Delta_v & 0 \\ 0 & 0 \end{bmatrix} \tag{B.48}$$

with Δ_v, $n_v \times n_v$, positive definite.

Define

$$S = \Lambda^{-\frac{1}{2}} V_p^H \begin{bmatrix} I_{n_p} & 0 \\ 0 & V_v^H \end{bmatrix} \tag{B.49}$$

In the sequel $\oplus$ will denote the direct sum, for example $A = A_p \oplus A_v$. Consider next a system equivalent to (6.13).

Lemma B.1.2 *With Φ, Γ, A, b, F, G, U_i, V_i and D_i with $i \in \{p, v\}$ and S defined in (2.6), (2.7), (2.13), (6.11), (6.12), and (B.44 - B.49) define:*

$$\widehat{F} = \Phi - \Gamma \Gamma^T \widehat{A}^T \widehat{A} \Phi \tag{B.50}$$

$$\widehat{A} = (U_p D_p) \oplus \left[\overline{A}_{v1}, U_v D_v\right] \tag{B.51}$$

$$\widehat{G} = \Gamma \Gamma^T \widehat{A}^T b \tag{B.52}$$

$$\widehat{x}(k) = (S^{-1} \oplus S^{-1}) x(k). \tag{B.53}$$

Then one has that

$$\widehat{x}(k+1) = \widehat{F} \widehat{x}(k) + \widehat{G} \tag{B.54}$$

$$y(k) = \widehat{A} \widehat{x}(k) - b \tag{B.55}$$

Proof: First note that

$$\begin{aligned} A(S \oplus S) &= \begin{bmatrix} A_p \Lambda^{-\frac{1}{2}} V_p^H & 0 \\ 0 & A_v \Lambda^{-\frac{1}{2}} V_p^H \end{bmatrix} \begin{bmatrix} I_{n_p} & 0 & 0 & 0 \\ 0 & V_v^H & 0 & 0 \\ 0 & 0 & I_{n_p} & 0 \\ 0 & 0 & 0 & V_v^H \end{bmatrix} \\ &= \left[U_p \begin{bmatrix} \Delta_p & 0 \\ 0 & 0 \end{bmatrix} \right] \oplus \left[\overline{A}_{v1}, U_v D_v \right] \\ &= \widehat{A}. \end{aligned} \tag{B.56}$$

Further

$$\begin{aligned} &(S^{-1} \oplus S^{-1})\, F(S \oplus S) = \\ &= \begin{pmatrix} S^{-1} & 0 \\ 0 & S^{-1} \end{pmatrix} \left(I - \Gamma \Lambda^{-1} \Gamma^T A^T A \right) \begin{bmatrix} I & I \\ 0 & I \end{bmatrix} \begin{bmatrix} S & 0 \\ 0 & S \end{bmatrix} \\ &= \begin{pmatrix} S^{-1} & 0 \\ 0 & S^{-1} \end{pmatrix} \left(I - \begin{bmatrix} \Lambda^{-1} & 2\Lambda^{-1} \\ 2\Lambda^{-1} & 4\Lambda^{-1} \end{bmatrix} A^T A \right) \begin{bmatrix} S & 0 \\ 0 & S \end{bmatrix} \Phi \\ &= \left(I - \Gamma \Gamma^T \begin{pmatrix} S^{-1} & 0 \\ 0 & S^{-1} \end{pmatrix} \begin{bmatrix} \Lambda^{-1} & 0 \\ 0 & \Lambda^{-1} \end{bmatrix} A^T A \begin{bmatrix} S & 0 \\ 0 & S \end{bmatrix} \right) \Phi \\ &= \widehat{F} \end{aligned}$$

because of (2.13). Similarly, because of (2.13), (2.7) and (6.12)

$$\widehat{G} = \left(S^H \oplus S^H \right) G.$$

Thus the lemma holds. ∎

Lemma B.1.3 *We now show that a condition comparable to (3.7) holds.*

$$I - \Gamma^T \widehat{A}^T \widehat{A} \Gamma > 0 \tag{B.57}$$

Proof: Follows from (B.56), the fact that

$$S^{-1} S = I$$

and that

$$\Gamma S = (S \oplus S)\Gamma$$

■

Denoting 0_q to be the $q \times q$, 0 matrix, we observe from (B.45), (B.48) and (B.51):

$$\widehat{A}^T \widehat{A} = \begin{bmatrix} D_p^H U_p^H & 0 \\ 0 & \overline{A}_{v1}^T \\ 0 & D_v^H U_v^H \end{bmatrix} \begin{bmatrix} U_p D_p & 0 & 0 \\ 0 & \overline{A}_{v1} & U_v D_v \end{bmatrix} \tag{B.58}$$

(B.59)

$$= \begin{bmatrix} \Delta_p^2 & 0 & 0 & 0 & 0 \\ 0 & 0_{n-n_p} & 0 & 0 & 0 \\ 0 & 0 & \overline{A}_{v1}^T \overline{A}_{v1} & B & 0 \\ 0 & 0 & B^H & \Delta_v^2 & 0 \\ 0 & 0 & 0 & 0 & 0_{n-n_p-n_v} \end{bmatrix}, \tag{B.60}$$

where

$$B = \overline{A}_{v1}^T U_v \begin{bmatrix} \Delta_v \\ 0 \end{bmatrix}. \tag{B.61}$$

Further,

$$\Gamma^T \widehat{A}^T \widehat{A} = \tag{B.62}$$

$$\begin{bmatrix} \Delta_p^2 & 0 & 0 & 2\overline{A}_{v1}^T \overline{A}_{v1} & 2B & 0 \\ 0 & 0_{n_v} & 0 & 2B^H & 2\Delta_v^2 & 0 \\ 0 & 0 & 0_{n-n_p-n_v} & 0 & 0 & 0_{n-n_p-n_v} \end{bmatrix}$$

and

$$\Gamma^T \widehat{A}^T \widehat{A} \Phi = \tag{B.63}$$

$$\begin{bmatrix} \Delta_p^2 & 0 & 0 & \Delta_p^2 + 2\overline{A}_{v1}^T \overline{A}_{v1} & 2B & 0 \\ 0 & 0 & 0 & 2B^H & 2\Delta_v^2 & 0 \\ 0 & 0 & 0 & 0 & 0 & 0_{n-n_p-n_v} \end{bmatrix}.$$

Then

$$\widehat{F} = \begin{bmatrix} \widehat{F}_{11} & \widehat{F}_{12} \\ \widehat{F}_{21} & \widehat{F}_{22} \end{bmatrix} \tag{B.64}$$

Where:

$$\widehat{F}_{11} = \begin{bmatrix} I_{n_p} - \Delta_p^2 & 0 & 0 \\ 0 & I_{n_v} & 0 \\ 0 & 0 & I_{n-n_p-n_v} \end{bmatrix}$$

$$\widehat{F}_{12} = \begin{bmatrix} I_{n_p} - \Delta_p^2 + 2\bar{A}_{v1}^T \bar{A}_{v1} & -2B & 0 \\ -2B^H & I_{n_v} - 2\Delta_v^2 & 0 \\ 0 & & I_{n-n_p-n_v} \end{bmatrix} \tag{B.65}$$

$$\widehat{F}_{21} = \begin{bmatrix} -2\Delta_v^2 & 0 & 0 \\ 0 & 0 & 0 \\ 0 & 0 & 0 \end{bmatrix}$$

$$\widehat{F}_{22} = \begin{bmatrix} I_{n_1} - \Delta_p^2 + 4\bar{A}_{v1}^T \bar{A}_{v1} & -4B & 0 \\ -4B^H & I_{n_v} - 4\Delta_v^2 & 0 \\ 0 & 0 & I_{n-n_p-n_v} \end{bmatrix}$$

Notice (B.57) and (B.58) imply

$$4\Delta_v^2 < I. \tag{B.66}$$

Then the following lemma goes toward a Kalman like decomposition.

Lemma B.1.4 *Under (B.44-B.51). with $L = L_p + L_v$ as defined in Section 2.2.*

$$\widehat{A}\left(zI - \widehat{F}\right)^{-1} = \begin{bmatrix} H(z) & 0_{2L\times(2n-2n_p-n_v)} \end{bmatrix} \Pi \tag{B.67}$$

where

$$H(z) = C(zI - \Upsilon)^{-1},$$

$$\Upsilon = \begin{bmatrix} I - \frac{\Delta_p^2}{\alpha} & I - \frac{\Delta_p^2 + 2\overline{A}_{v1}^T \overline{A}_{v1}}{\alpha} & -\frac{2B}{\alpha} \\ -\frac{2\Delta_p^2}{\alpha} & I - \frac{2\Delta_p^2 + 4\overline{A}_{v1}^T \overline{A}_{v1}}{\alpha} & -\frac{4B}{\alpha} \\ 0 & -\frac{4B^H}{\alpha} & I - \frac{4\Delta_v^2}{\alpha} \end{bmatrix},$$

$$C = \left(U_p \begin{bmatrix} \Delta_p \\ 0 \end{bmatrix} \right) \oplus \left(\begin{bmatrix} \overline{A}_{v1} & U_v \begin{bmatrix} \Delta_v \\ 0 \end{bmatrix} \end{bmatrix} \right) \tag{B.68}$$

and

$$\Pi = \begin{bmatrix} I_{n_p} & 0 & 0 & 0 \\ 0 & 0 & I_{n_p+n_v} & 0 \\ 0 & I_{n-n_v} & 0 & 0 \\ 0 & 0 & 0 & I_{n-(n_p+n_v)} \end{bmatrix}. \tag{B.69}$$

Proof: Note

$$\Pi^T \Pi = I. \tag{B.70}$$

Hence

$$\widehat{A}(zI - \widehat{F})^{-1} = \widehat{A}\Pi^T \left[zI - \Pi \widehat{F} \Pi^T \right]^{-1} \Pi.$$

Now,

$$\begin{aligned} \widehat{A}\Pi^T &= \begin{bmatrix} U_p \begin{bmatrix} \Delta_p \\ 0 \end{bmatrix} & 0 & 0 & 0 & 0 \\ 0 & 0_{n-n_p} & \overline{A}_{v1} & U_v \begin{bmatrix} \Delta_v \\ 0 \end{bmatrix} & 0 \end{bmatrix} \times \\ &\quad \times \begin{bmatrix} I_{n_p} & 0 & 0 & 0 \\ 0 & 0 & I_{n-n_p} & 0 \\ 0 & I_{n_p+n_v} & 0 & 0 \\ 0 & 0 & 0 & I_{n-(n_p+n_v)} \end{bmatrix} \\ &= \begin{bmatrix} C & 0_{2L \times (2n-2n_p-n_v)} \end{bmatrix} \end{aligned}$$

Further, from (B.64)

$$\Pi \widehat{F} \Pi^T = \begin{bmatrix} I - \widehat{\Upsilon} & 0 \\ \times_1 & \times_2 \end{bmatrix}$$

where $\begin{bmatrix} \times_1 & \times_2 \end{bmatrix}$ has $2(n-n_p)-n_v$ rows and

$$\widehat{\Upsilon} = \begin{bmatrix} \Delta_p^2 & -I_{n_p} + \Delta_p^2 + 2\overline{A}_{v1}^T \overline{A}_{v1} & 2B \\ 2\Delta_p^2 & 2\Delta_p^2 + 4\overline{A}_{v1}^T \overline{A}_{v1} & 4B \\ 0 & 4B^H & 4\Delta_v^2 \end{bmatrix} \tag{B.71}$$

Then the result follows. ■

Lemma B.1.5 *Under the conditions of Lemma B.1.1, $A(zI-F)^{-1}$ has no poles at 1.*

Proof: Because of Lemmas B.1.1 and B.1.4, It suffices to show that Υ defined in Lemma B.1.4 has no eigenvalues at 1. Choose

$$T = \begin{bmatrix} I_{n_p} & -I_{n_p}/2 & 0 \\ 0 & I_{n_p} & 0 \\ 0 & 0 & I_{n_v} \end{bmatrix}$$

and note that

$$T^{-1} = \begin{bmatrix} I_{n_p} & I_{n_p}/2 & 0 \\ 0 & I_{n_p} & 0 \\ 0 & 0 & I_{n_v} \end{bmatrix}.$$

Then

$$\begin{aligned} T\Upsilon T^{-1} = & \\ = & \begin{bmatrix} I_{n_p} & I_{n_p}/2 & 0 \\ -2\Delta_p^2 & I_{n_1} - 2\Delta_p^2 + 4\overline{A}_{v1}^T \overline{A}_{v1} & -4B \\ 0 & -4B^H & I - 4\Delta_v^2 \end{bmatrix} T^{-1} \\ = & \begin{bmatrix} I_{n_p} & I_{n_p} & 0 \\ -2\Delta_p^2 & I_{n_p} - 3\Delta_p^2 + 4\overline{A}_{v1}^T \overline{A}_{v1} & -4B \\ 0 & -4B^H & I - 4\Delta_v^2 \end{bmatrix}. \end{aligned}$$

Now, $T\Upsilon T^{-1}$ has an eigenvalue at 1 iff there exists

$$\eta = \begin{bmatrix} \eta_1 \\ \eta_2 \\ \eta_3 \end{bmatrix} \neq 0$$

such that

$$\begin{bmatrix} 0 & -I_{n_1} & 0 \\ 2\Lambda_1^2 & 3\Lambda_1^2 + 4\overline{A}_{21}^T\overline{A}_{21} & 4B \\ 0 & 4B^H & I - 4\Lambda_2^2 \end{bmatrix} \begin{bmatrix} \eta_1 \\ \eta_2 \\ \eta_3 \end{bmatrix} = 0.$$

Now the first block equation implies $\eta_2 = 0$. Further because of (A.30), the third block equation gives $\eta_3 = 0$. Thus as $\Delta_p > 0$, the second block equation assures that $\eta_1 = 0$, leading to a contradiction. ■

Thus Lemma 6.3.1 follows from Lemmas B.1.1 and B.1.5.

REFERENCES

[1] C. W. Reynolds, "Flocks, herds, and schools: A distributed behavioral model," *Computer Graphics*, July 1987, pp. 25–34.

[2] T. Vicsek, A. Czirok, E. Ben-Jacob, I. Cohen, and O. Shochet, "Novel type of phase transition in a system of self-driven particles," *The American Physical Society*, vol. 75, no. 6, August 1995, vol. 75, no. 6, pp. 1226–1229.

[3] T. Balch and R. C. Arkin, "Behavior-based formation control for multirobot teams," *IEEE Transactions on Robotics and Automation*, vol. 14, no. 6, December 1998, vol. 14, no. 6, p. 926.

[4] S. S. Ge and C.-H. Fua, "Multi-robot formations: Queues and artificial trenches potential," in *Proceedings of the IEEE International Conference on Robotics and Automation*, 2004.

[5] ——, "Queues and artificial potential trenches for multirobot formations," *IEEE Transactions on Robotics*, vol. 21, no. 4, August 2005, vol. 21, no. 4, pp. 646–656.

[6] D. Swaroop and J. K. Hedrick, "String stability of interconnected systems," *IEEE Transactions on Automatic Control*, vol. 41, no. 3, March 1996, vol. 41, no. 3, pp. 349–357.

[7] J. K. H. Darbha Swaroop and S. B. Choi, "Direct adaptive longitudinal control of vehicle platoons," *150 IEEE TRANSACTIONS ON VEHICULAR TECHNOLOGY,*, vol. 50, no. 1, January 2001, vol. 50, no. 1, pp. 150–161.

[8] D. Swaroop and J. K. Hedrick, "Direct adaptive longitudinal control of vehicle platoons," in *Conference on Decision and Control*, 1994.

[9] ——, "Constant spacing strategies for platooning in automated highway systems," *ASME Journal of Dynamic Systems, Measurement, and Control*, vol. 121, no. 3, September 1999, vol. 121, no. 3, pp. 462–470.

[10] M. E. Khatir and E. J. Davison, "Decentralized control of a large platoon of vehicles using non-identical controllers," in *American Control Conference*, 2004.

[11] ——, "A nearest neighbourhood decentralized controllers for controlling a platoon of vehicles," in *12th Mediterranean Conference*, 2004.

[12] X. Liu, A. Goldsmith, S. Mahal, and J. Hedrick, "Effects of communication delay on string stability in vehicle platoons," *Intelligent Transportation Systems, 2001. Proceedings. 2001 IEEE*, 2001, pp. 625–630.

[13] M. E. Khatir and E. J. Davison, "Bounded stability and eventual string stability of a large platoon of vehicles using non-identical controllers," in *IEEE Conference on Decision and Control*, December 2004.

[14] P. S. Aniruddha Pant and K. Hedrick, "Mesh stability of look-ahead interconnected systems," *IEEE Transactions on Automatic Control*, vol. 47, no. 2, February 2002, vol. 47, no. 2, pp. 403–407.

[15] Z. Jin and R. M. Murray, "Stability and performance analysis with double-graph model of vehicle formations," in *American Control Conference*, 2003.

[16] H. Ando, Y. Oasa, I. Suzuki, and M. Yamashita, "Distributed memoryless point convergence algorithm for mobile robots with limited visibility," *IEEE Transactions on Robotics and Automation*, vol. 15, no. 5, October 1999, vol. 15, no. 5, pp. 818–828.

[17] J. Lin, A. S. Morse, and B. D. Anderson, "The multi-agent rendezvous problem," in *Proceedings of the 42nd IEEE Conference on Decision and Control*, 2003.

[18] ——, "The multi-agent rendezvous problem -part 1: The synchronous case," *SIAM Journel on Control and Optimization*, to appear 2006.

[19] L. Moreau, "Stability of multiagent systems with time-dependent communication links," *IEEE Transactions on Automatic Control*, vol. 50, no. 2, February 2005, vol. 50, no. 2, pp. 169–182.

[20] A. Jadbabaie, J. Lin, and A. S. Morse, "Coordination of groups of mobile autonomous agents using nearest neighbor rules," *IEEE Transactions on Automatic Control*, vol. 48, no. 6, June 2003, vol. 48, no. 6, pp. 988–1001.

[21] J. A. Fax and R. M. Murray, "Graph laplacians and stabilization of vehicle formations," in *Proceedings of 15th IFAC World Congress*, July 2002.

[22] ——, "Information flow and cooperative control of vehicle formations," in *IFAC World Congress*, 2002.

[23] ——, "Information flow and cooperative control of vehicle formations," *Transactions on Automatic Control*, pp. 1465–1476, September 2004.

[24] S. GlavaSki, M. Chaves, R. Day, P. Nag, A. Williams, and W. Zhang, "Vehicle networks: Achieving regular formation," in *American Control Conference*, June 2003.

[25] A. Williams, S. Glavaski, and T. Samad, "Formations of formations: Hierarchy and stability," in *American Control Conference*, June 2004.

[26] R. O. Abel, S. Dasgupta, and J. G. Kuhl, "Coordinated fault-tolerant control of autonomous agents: geometry and communications architecture," in *Preprints of IFAC World Congress*, 2005.

[27] ——, "Fault tolerant, reconfigurable, scalable and distributed multiagent formation control," in *International Symposium on Mathematical Theory of Networks and Systems*, July 24-28 2006.

[28] ——, "One step ahead quadratic receding horizon distributed control of multiagent formations," in *IEEE International Conference on Control Applications*, no. 569-574, October 1-3 2007.

[29] ——, "Distributed multiagent formation control with enhanced scalability," in *European Control Conference*, July 2-5 2007.

[30] ——, "Fault tolerant scalable coordinated control of agent formations with arbitrary trajectories," *Control and Automation, 2007. ICCA 2007. IEEE International Conference on*, pp. 1559–1564, May 2007.

[31] ——, "The relation between redundancy and convergence rate in distributed multi-agent formation control," in *Decision and Control, 2008. CDC 2008. 47th IEEE Conference on*, December 9-11 2008, pp. 3977–3982.

[32] ——, "Coordinated fault tolerant optimal control of autonomous agents: geometry and communications architecture," *Communications in Information and Systems*, to appear 2011.